Brigham Young University
BYU ScholarsArchive

All Theses and Dissertations

2009-02-10

Redox, Pressure and Mass Transfer Effects on Syngas Fermentation

Allyson White Frankman
Brigham Young University - Provo

Follow this and additional works at: https://scholarsarchive.byu.edu/etd

 Part of the Chemical Engineering Commons

BYU ScholarsArchive Citation

Frankman, Allyson White, "Redox, Pressure and Mass Transfer Effects on Syngas Fermentation" (2009). *All Theses and Dissertations*. 1986.
https://scholarsarchive.byu.edu/etd/1986

This Thesis is brought to you for free and open access by BYU ScholarsArchive. It has been accepted for inclusion in All Theses and Dissertations by an authorized administrator of BYU ScholarsArchive. For more information, please contact scholarsarchive@byu.edu, ellen_amatangelo@byu.edu.

REDOX, PRESSURE AND MASS TRANSFER EFFECTS ON SYNGAS FERMENTATION

by

Allyson W. Frankman

A dissertation/thesis submitted to the faculty of

Brigham Young University

in partial fulfillment of the requirements for the degree of

Master of Science

Department of Chemical Engineering

Brigham Young University

April 2009

BRIGHAM YOUNG UNIVERSITY

GRADUATE COMMITTEE APPROVAL

of a thesis submitted by

Allyson W. Frankman

This thesis has been read by each member of the following graduate committee and by majority vote has been found to be satisfactory.

Date	Randy S. Lewis, Chair
Date	William R. McCleary
Date	Larry L. Baxter

BRIGHAM YOUNG UNIVERSITY

As chair of the candidate's graduate committee, I have read the thesis of Allyson W. Frankman in its final form and have found that (1) its format, citations, and bibliographical style are consistent and acceptable and fulfill university and department style requirements; (2) its illustrative materials including figures, tables, and charts are in place; and (3) the final manuscript is satisfactory to the graduate committee and is ready for submission to the university library.

Date

Randy S. Lewis
Chair, Graduate Committee

Accepted for the Department

Richard L. Rowley
Graduate Coordinator

Accepted for the College

Alan R. Parkinson
Dean, Ira A. Fulton College of Engineering and Technology

ABSTRACT

REDOX, PRESSURE AND MASS TRANSFER EFFECTS ON SYNGAS FERMENTATION

Allyson W. Frankman

Department of Chemical Engineering

Master of Science

The fermentation of syngas (a mixture of CO, CO_2 and H_2) to produce ethanol is of interest as an alternative fuel. *Clostridium carboxidivorans*, has been found to produce higher than average amounts of ethanol and butanol from CO-rich mixtures. This project sought to determine the effects of the redox level in the solution, partial pressures in the headspace and mass transfer limitations on the products obtained through fermentation of syngas. It was determined that cysteine sulfide has a greater effect on the redox level of the media used to grow bacteria, than does the gas composition. Therefore, changing gas composition during the process will have little effect on the redox. However, addition of cysteine sulfide may vary the redox level. When cells were first inoculated, the redox level dropped and leveled at -200 mV SHE for optimal growth. In addition, cells switch from acetic acid to ethanol production after a drop of 40-70 mV in the redox level.

Different sizes of reactors were used, including 1 liter reactors (non-pressurized), 50 mL bottles (20 psig) and 100 mL bottles (20 psig). The 50 mL bottles have more than double the growth rate than the 100 mL bottles (0.57 day^{-1} compared to 0.20 day^{-1}). Partial pressures were measured in these two sizes to determine the different consumptions and the effect of partial pressure on both growth and production of acetic acid/ethanol. It is clear that re-gassing the bottles every 12 hours to keep the pressure higher in the 100 mL bottles makes a significant difference in the growth, making them very similar to the 50 mL bottles. Both the 50 mL and 100 mL bottle were found to have essentially the same mass transfer rate (0.227 L/hr vs. 0.255 L/hr). However, because of headspace differences, there was more CO available for the 50 mL bottles (on a per liter basis) as compared to the 100 mL bottles. Mass transfer analysis proved useful in pointing out that all three reactors likely experienced mass transfer limitations such that mass transfer effects are critical to address when performing studies involving syngas fermentation.

ACKNOWLEDGMENTS

I am very grateful for the opportunity to work with Dr. Randy Lewis. I have appreciated his guidance and direction, patience and encouragement, and willingness to listen. He has been a great support to me not only in my research, but also in other engineering interests such as Engineers Without Borders. I'm also grateful to a wonderful advisory committee, Dr. William McCleary and Dr. Larry Baxter for their assistance and advice. I have enjoyed the company of many other great students in the lab, who have increased the quality of my research through their probing questions, and willingness to work hard. A special thanks to my wonderful husband, Dave, without whom, the completion of this work would not have been possible.

Table of Contents

Table of Contents vii
List of Tables ix
List of Figures xi
Chapter 1 - Introduction 1
Formation of Acetyl-CoA 4
Products of acetyl-CoA 9
Objectives 12
Objective 1. Effects of gas composition on redox potential 12
Objective 2. Optimum redox level for production of ethanol and acetate 13
Objective 3. Effects of pressure and mass transfer 13
Chapter 2 - Review of Recent Research 15
Acetogenesis to Solventogenesis Switch 15
Redox Potential 17
Pressure Effects on Growth and Ethanol Production 21
Chapter 3 – Effects of Gas Composition on Redox Potential 25
Methods/Equipment 26
Bioreactor media 26
500 mL Bioreactor 26
Independent Gas Runs 29
Conclusions 37
Chapter 4 – Optimum Redox Level for Production of Ethanol and Acetate 39
Methods 39

Microorganism 39
1 Liter Bioreactor 40
Inoculum 42
Analytical procedures 43
Results and Discussion 44
Redox Levels 44
Acetogenesis to Solventogenesis Switch 49
Conclusions & Future Work 58
Chapter 5 – Pressure and Mass Transfer Effects 61
Methods 63
Bottle Studies 63
Gas Composition 63
Gas Pressure 64
Results and Discussion 64
Growth in 50 mL vs. 100 mL bottles 64
Partial Pressure 67
Pressure experiment with regassing 78
Effect of CO Partial Pressure on Ethanol Production 80
Mass Transfer 82
Mass Transfer in 1 Liter Reactor 84
Mass Transfer in Bottles 88
Conclusions and Future Work 95
Chapter 6 – Conclusions and Future Work 99
Conclusions 99
Future Work 101
References 103

List of Tables

Table 1. Summary of chemicals used to control the culture redox level 19

Table 2. Summary of raw pure gas redox levels in media at 37^{o}C from 500 mL bioreactors referenced to a standard hydrogen electrode (SHE) 33

Table 3. Growth Rate Constants for experiments AFRED2-8 47

Table 4. Bacterial growth rate for 50 mL vs. 100 mL septum bottles 66

Table 5. Growth rates for 50 mL vs. 100 mL experiment while monitoring gas pressure and composition 68

Table 6. Summary of Mass Transfer Coefficients for oxygen in the 1 Liter Reactors 85

Table 7. Empirical ratio compared to a correlation for mass transfer coefficient ratio ... 86

Table 8. Summary of k_La (L/hr) at 175 rpm and 100 sccm for O_2, CO and CO_2 for 1 Liter reactor 86

Table 9. Mass transfer coefficients of O_2, CO, CO_2 and H_2 for 1 Liter reactor, 50 mL bottles and 100 mL bottles 89

List of Figures

Figure 1. Fossil Energy Ratio (FER) is a term that relates the energy in fuel to the fossil energy input. Cellulosic ethanol (Cell. EtOH) has a much higher ratio than corn ethanol (Wang 2005)..... 2

Figure 2. The Wood-Ljungdahl pathway of autotrophic CO and CO_2 fixation. CODH, CO dehydrogenase; ACS, acetyl-CoA synthase; MeTr, methyltransferase; CFeSP, Corrinoid iron-sulfur protein. PFOR, pyruvate ferredoxin oxidoreductase. Reactions leading to the formation of the methyl group of acetyl-CoA are colored red, while those leading to the carbonyl group are colored blue (Ragsdale 2004).....5

Figure 3. A detailed description of the methyl branch pathway beginning with a CO_2 molecule, and ending with 5-MethylTHF..... 6

Figure 4. Carbon monoxide dehydrogenase (CODH) is shown at the top which converts CO_2 into CO. CODH works in tangent with Hydrogenase (shown below). Hydrogenase makes the necessary electrons available for CODH. 7

Figure 5. The combination of the methyl branch and carbonyl branch to yield Acetyl-CoA over the enzyme Acetyl-CoA Synthase (ACS). 8

Figure 6. Structure of Acetyl-CoA with acetyl group highlighted on the right (Wikipedia 2006) 8

Figure 7. A diagram of the conversion of Acetyl-CoA to either ethanol (solventogenesis) or acetate (acetogenesis). 9

Figure 8. Cell concentration, pH, and product profiles from days 0 to 8.5 using clean bottled gas. Liquid was in the batch mode from days 0 to 6.5 and in the continuous mode from days 6.5 to 8.5. The liquid feed rate during the continuous mode was 1.5 mL/min. Gas was always continuous at an inlet flow rate of 180 ccm at 3.5 psig (Datar, Shenkman et al. 2004) 10

Figure 9. Cell concentration, pH, and product profiles from days 8.5 to 11.5 using biomass-generated producer gas. Both gas and liquid were in the continuous mode. The inlet gas flow rate was 180 ccm at 3.5 psig and the liquid feed and withdrawal rate was 1.5 mL/min (Datar, Shenkman et al. 2004) 11

Figure 10. Comparison of ethanol production under various partial pressures of CO (Hurst 2005)..... 22

Figure 11. 500 mL bioreactor used in Objective #1 experiments..... 27

Figure 12. Top view of 500 mL bioreactor 28

Figure 13. Liquid recycle line for 500 mL reactors to measure redox (with ORP probe) and take liquid samples. 28

Figure 14. Hydrogen in water at 25^{o}C in the 500 mL bioreactor using an Ag/AgCl redox reference electrode 30

Figure 15. Pure H_2 bubbled through media at 37^{o}C in 500 mL bioreactor while measuring redox 31

Figure 16. Pure CO_2 bubbled through media at 37^{o}C in 500 mL bioreactor while measuring redox 32

Figure 17. Pure CO bubbled through media at 37^{o}C in 500 mL bioreactor while measuring redox 32

Figure 18. Redox potential (SHE) in cell-free media with syngas and cysteine sulfide 35

Figure 19. Redox potential (SHE) in cell-free media with nitrogen and cysteine sulfide 35

Figure 20. 1-Liter working volume BioFlo 110 Benchtop Fermentors used in redox experiments 40

Figure 21. Close-up picture of 1 Liter bioreactor 41

Figure 22. Representative pre-inoculation redox history (from AFRED 8). 45

Figure 23. Redox levels for AFRED2, AFRED3, AFRED4, AFRED5, AFRED6, AFRED7 & AFRED8 46

Figure 24. Optical Density profiles for AFRED experiments 46

Figure 25. Redox comparison of a no lag-time run (AFRED 2) with that of a 1 day lag-time run (AFRED4) 48

Figure 26. Acetic acid concentrations in comparison to the redox levels for all runs 49

Figure 27. Ethanol concentrations in comparison to the redox levels for all runs 50

Figure 28. Redox comparison between the earlier onset of ethanol production profiles (AFRED3 and AFRED7) along with their acid and solvent concentrations 51

Figure 29. Redox comparison between the earlier onset of ethanol production profiles (AFRED3 and AFRED7) along with their pH 51

Figure 30. Redox comparison between the later onset of ethanol production profiles (AFRED2, AFRED6 and AFRED8) along with their acid and solvent concentrations ... 52

Figure 31. Redox comparison between the later onset of ethanol production profiles (AFRED2, AFRED6 and AFRED8) along with their pH 53

Figure 32. Redox for AFRED4 which exhibited no large redox level drop and ethanol production hadn't kicked in before run was stopped due to syngas tank running out 53

Figure 33. Redox for AFRED5 which exhibited no large redox level drop however, ethanol production did kick in, run was stopped due to technical failure of controller 54

Figure 34. The change in ethanol from the beginning of ethanol production vs. time 55

Figure 35. The change in redox level from the beginning of ethanol production vs. time 55

Figure 36. Relative redox levels with various liquid concentrations at the beginning of a run (increasing acetic acid, increasing ethanol) 57

Figure 37. AFRED2 redox history 59

Figure 38. Growth comparison between 50 mL bottle, 100 mL bottle, and 1 Liter bioreactor 62

Figure 39. Optical Density summary for 50 mL vs. 100 mL bottles in a normal run 65

Figure 40. Liquid concentrations for 50 mL vs. 100 mL cultures 66

Figure 41. Growth profile for 50 mL vs. 100 mL experiment while monitoring headspace gas pressure and composition 68

Figure 42. Liquid concentrations for 50 mL vs. 100 mL experiment while monitoring headspace gas pressure and composition 69

Figure 43. Total pressure profile for 50 mL vs. 100 mL experiment while monitoring headspace gas pressure and composition 70

Figure 44. Total pressure and acetic acid concentrations for the 50 mL vs. 100 mL experiment while monitoring headspace gas pressure and composition 71

Figure 45. Moles of CO in the headspace for the 50 mL vs. 100 mL experiment while monitoring headspace gas pressure and composition 72

Figure 46. Moles of H_2 in the headspace for the 50 mL vs. 100 mL experiment while monitoring headspace gas pressure and composition 73

Figure 47. Moles of CO_2 in the headspace for the 50 mL vs. 100 mL experiment while monitoring headspace gas pressure and composition 74

Figure 48. Moles of CO_2 with average liquid concentrations 75

Figure 49. Moles of CO per gram of bacteria in the headspace for the 50 mL vs. 100 mL experiment while monitoring headspace gas pressure and composition..... 75

Figure 50. Moles of H_2 per gram of bacteria in the headspace for the 50 mL vs. 100 mL experiment while monitoring headspace gas pressure and composition..... 76

Figure 51. Moles of CO_2 per gram of bacteria in the headspace for the 50 mL vs. 100 mL experiment while monitoring headspace gas pressure and composition..... 77

Figure 52. A plot of the pressure vs. time in the pressure re-gassing experiment with the error bars showing the standard deviation 78

Figure 53. The growth comparison between the 50 mL bottle regassing every two days, the 100 mL bottle regassing every two days, and the 50 mL bottle regassing every six hours, error bars represent standard deviation..... 79

Figure 54. Cell growth (OD) data from CO experiment where bottles were switched to different CO levels halfway through the experiment..... 81

Figure 55. Ethanol production for CO experiment in which CO partial pressure was changed around day 20. High CO was 60% CO, 30% H_2, 10% CO_2, Regular CO was 30% H_2, 30% CO_2 and 40% CO and Low CO was 20% CO, 30% H_2, and 50% CO_2..... 82

Figure 56. Mass transfer graphs for 175 rpm and 100 sccm. a). dissolved oxygen % as a function of time b). negative log of concentration difference where C* is saturated oxygen % and C is the dissolved oxygen %..... 83

Figure 57. Cumulative carbon (grams/Liter) used in the reactor in the formation of cells, acetic acid and ethanol..... 87

Figure 58. Average moles of CO consumption assuming mass transfer limited vs. actual moles of CO consumed, with error bars representing standard deviation between three bottles..... 91

Figure 59. Average moles of H_2 consumption assuming mass transfer limitations vs. actual H_2 consumption, with error bars representing standard deviation 92

Figure 60. Cumulative carbon used (gram carbon) for 50 mL and 100 mL bottles 95

Chapter 1 - Introduction

The availability of future energy is of constant interest in the United States. Around 40% of the United States energy demand is being supplied by petroleum in the form of liquid fuels. The transportation industry in particular is dependent on liquid fuels (Forsberg 2005) and there is an ever pressing need to find replacement fuels for petroleum for both political and economical reasons. One alternative to petroleum is the utilization of ethanol obtained from renewable energy sources such as corn, grasses, wood, etc. Ethanol is renewable and greenhouse-gas friendly and relieves some reliance on foreign countries for fuel. Ethanol is currently being blended with gasoline at 10% (E10) and 85% (E85). Car manufacturers are producing more engines able to run off higher ethanol concentrations.

There are many ways to create ethanol. The most popular method currently used in the US is the fermentation of the simple sugars in corn to create ethanol. However, this production process has a very low Fossil Energy Ratio (FER), a term that relates the energy available in the fuel to the fossil energy input for production (see Figure 1 below). A higher FER means a higher energy efficiency in the production of that particular fuel. For example, more fossil energy (via growing and harvesting the corn) goes into the corn-to-ethanol process than into the cellulose-to-ethanol process, such that the FER is lower for the corn process.

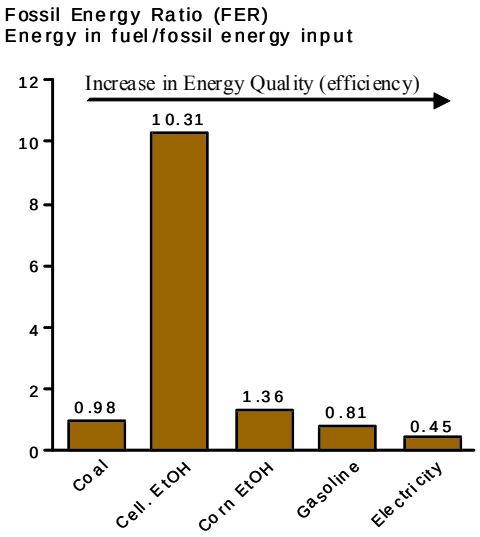

Figure 1. Fossil Energy Ratio (FER) is a term that relates the energy in fuel to the fossil energy input. Cellulosic ethanol (Cell. EtOH) has a much higher ratio than corn ethanol (Wang 2005).

Due to its high available fuel energy relative to the fossil energy input, ethanol obtained using a cellulosic feedstock appears to be most applicable from an energy standpoint. The most prevalent cellulosic feedstock processes that are being researched include: syngas fermentation (cellulose is gasified to syngas, composed of CO, CO_2, and H_2, and then fermented to ethanol using bacteria), Fisher Tropsch synthesis (cellulose is gasified to syngas and then converted to ethanol using metal catalysts), and cellulosic fermentation (cellulose is converted to simple sugars using enzymes and then converted to ethanol using yeast). This prospectus will focus on the research involving syngas fermentation. Fermentation is an anaerobic metabolic process for bacteria, where chemical compounds are biochemically modified for biosynthesis and energy.. This process is accomplished through the use of enzymes. Electrons from an oxidized energy source are placed in a metabolic intermediate to balance the overall redox state of the cell

Different types of bacteria include different enzymes that in turn affect their metabolic pathways.

With regards to syngas fermentation, biomass (grasses, woods, agricultural residues, etc.) can be gasified to yield a "syngas" made up of carbon monoxide (CO), carbon dioxide (CO_2), and hydrogen (H_2), with small amounts of impurities. The overall stoichiometry for the fermentation of syngas to form ethanol is:

$$6CO + 3H_2O \rightarrow C_2H_5OH + 4CO_2 \quad (1)$$

$$2CO_2 + 6H_2 \rightarrow C_2H_5OH + 3H_2O \quad (2)$$

One of the main advantages of syngas fermentation is the wide variety of raw materials that can be utilized as a feedstock; such as prairie grasses, wood chips, solid municipal wastes and paper wastes. This process is also well-suited to raw materials such as softwoods that are normally difficult to handle (Dayton and Spath 2003). A second main advantage is that gasification can break down cellulosic, hemicellulosic and lignin bonds that are difficult to break down using fermentative or enzymatic reactions. This provides a greater conversion efficiency of biomass to energy (McKendry 2002). *Clostridium ljungdahlii (Phillips, Clausen et al. 1994)*, *Butyribacterium methylotrophicum (Bredwell, Srivastava et al. 1999)* and *Clostridium autoethanogenum* (Abrini, Naveau et al. 1994) are known examples of bacteria that have been shown to produce ethanol from syngas. *Clostridium carboxidivorans* (carbon dioxide devouring), a bacteria isolated in an agricultural settling lagoon in Stillwater, Oklahoma, has been

found to produce higher than average rates of ethanol and butanol from CO-rich mixtures (Liou and Balkwill 2005).

Clostridium carboxidivorans can grow through the fermentation of a myriad of substrates including: CO, H_2/CO_2, glucose, galactose, fructose, xylose, mannose, cellobiose, trehalose, cellulose, starch pectin, citrate, glycerol, ethanol, propanol, 2-propanol, butanol, glutamate, aspartate, alanine, histidine, asparagines, serine, betaine, choline and syringate (Liou and Balkwill 2005). The focus of this research, however, is on the fermentation of CO and H_2/CO_2 that incorporates either acetogenesis (production of acetate during growth) or solventogenesis (production of ethanol when growth is minimized).

During the lagoon sampling, there were several species of *Clostridium* that were harvested at the same time that exhibited ethanol-producing characteristics. *Clostridium carboxidivorans* (formerly known as P7, "pick 7") is the only one that is currently named. However, this research will use P11 ("pick 11") which is currently unnamed. P11 was found to exhibit slightly better ethanol production capabilities as compared to *Clostridium carboxidivorans*.

Formation of Acetyl-CoA

During acetogenesis and solventogenesis, acetyl-CoA is formed as an intermediate of the metabolic pathway. The acetyl-CoA pathway differs from other CO_2 fixation pathways as it is linear as opposed to cyclic like the Calvin cycle and the reductive tri-carboxylic acid cycle. There are a variety of paths through which acetyl-CoA can be produced. However, the traditional example of this (and the one discussed in

this prospectus) is the "Wood-Ljungdahl" pathway shown in Figure 2, in which two molecules of CO_2 are reduced to acetyl-CoA (Drake and Daniel 2004).

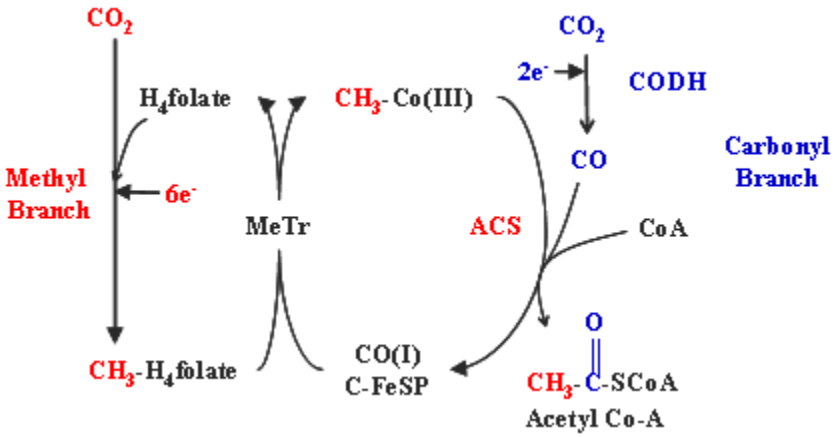

Figure 2. The Wood-Ljungdahl pathway of autotrophic CO and CO_2 fixation. CODH, CO dehydrogenase; ACS, acetyl-CoA synthase; MeTr, methyltransferase; CFeSP, Corrinoid iron-sulfur protein. PFOR, pyruvate ferredoxin oxidoreductase. Reactions leading to the formation of the methyl group of acetyl-CoA are colored red, while those leading to the carbonyl group are colored blue (Ragsdale 2004)

Although the Wood-Ljungdahl pathway begins with two CO_2 molecules, one of the CO_2 molecules (in the carbonyl branch) is immediately reduced to CO through the enzyme Carbon Monoxide Dehydrogenase (CODH); therefore the carbon source can come from either CO_2 or CO. In addition, the CODH can work the other direction, i.e. CO can be converted to CO_2 and used in the methyl branch pathway. The red CO_2 on the left leads to the methyl branch of acetyl-CoA, and the blue CO_2 on the right leads to the carbonyl branch of acetyl-CoA. The electrons that are added in this process come either from a) oxidizing the H_2 in the syngas; b) oxidizing the CO to CO_2; or c) other reducing agents in the media solution.

A more detailed description of the methyl branch conversion is shown in Figure 3. Beginning with the methyl branch, CO_2 is combined with H_4folate and 6 electrons to yield CH_3-H_4folate. There are a number of enzymes involved in this process. First, Formate Dehydrogenase adds two electrons through NADH (Nicotinamide adenine dinucleotide) to form formate.

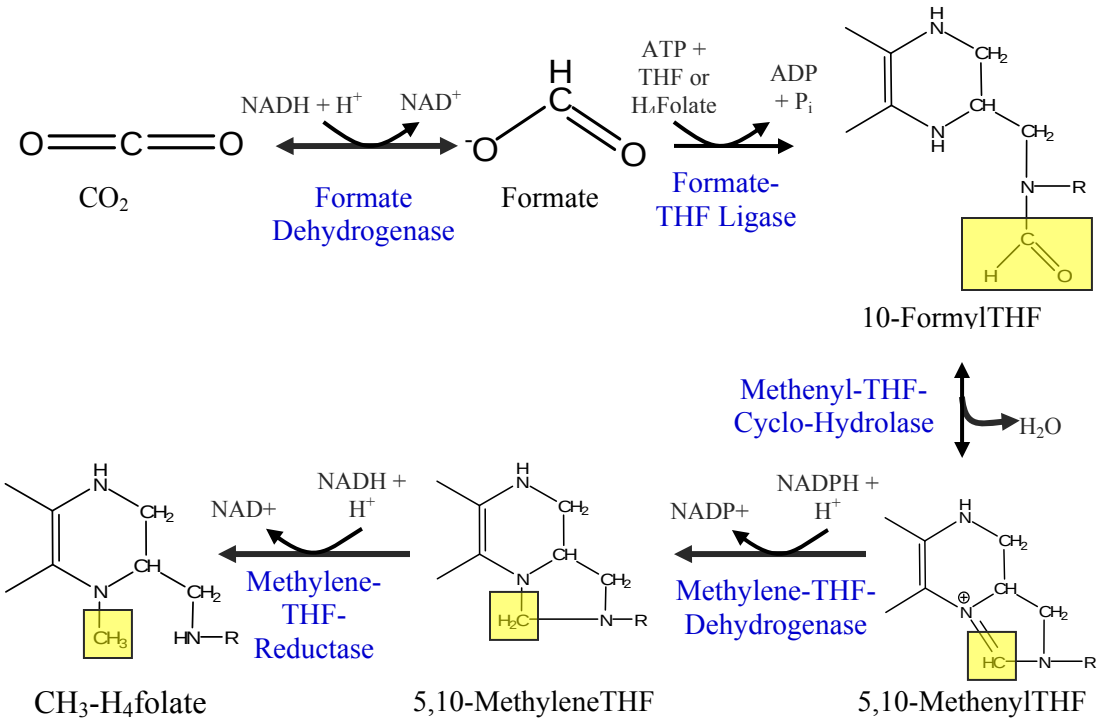

Figure 3. A detailed description of the methyl branch pathway beginning with a CO_2 molecule, and ending with 5-MethylTHF.

Formate is then combined with H_4folate (THF) by the enzyme Formate-THF Ligase. 10-FormylTHF becomes 5,10 MethenylTHF with the loss of a water molecule over the enzyme MethenylTHF Cyclo-Hydrolase. The next two electrons are added through NADPH (Nicotinamide adenine dinucleotide phosphate) by the enzyme Methylene-THF-Dehydrogenase to form 5,10 Methylene-THF. The enzyme Methylene-

THF Reductase adds the final two electrons through NADH. This final enzyme is up-regulated by methionine and GTP, and it is down-regulated by ATP, ITP, SAM, Guanosine, and Inosine.

The carbonyl branch also begins with a CO_2 molecule (see Figure 4).

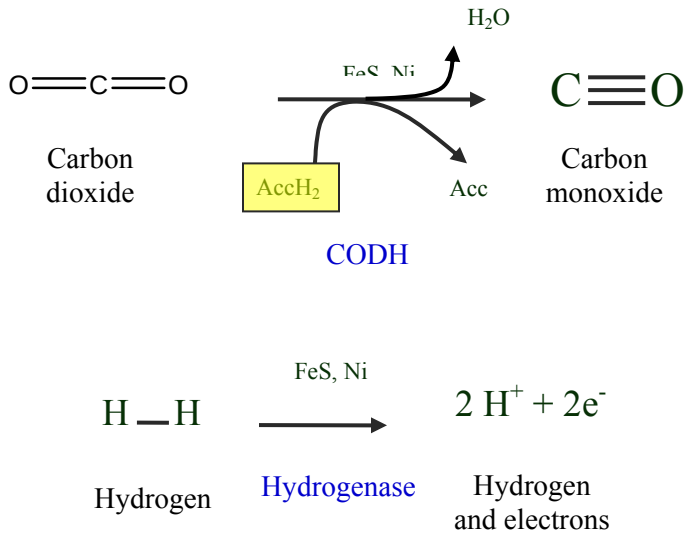

Figure 4. Carbon monoxide dehydrogenase (CODH) is shown at the top which converts CO_2 into CO. CODH works in tangent with Hydrogenase (shown below). Hydrogenase makes the necessary electrons available for CODH.

This CO_2 molecule is converted to CO by the addition of 2 electrons using the enzyme CODH. CODH works in tangent with Hydrogenase as Hydrogenase provides the necessary electrons available for CODH.

The final steps to the formation of acetyl-CoA are shown in Figure 5. Using the enzyme methyltransferase (MeTr), the methyl group is transferred from the H_4 folate group to CH_3-Co(III), an organometallic methylcobamide (a derivative of vitamin B12). This species is found on a corrinoid iron-sulfur protein (C-FeSP). The CO from the carbonyl branch is then combined with the organometallic methylcobamide (CH_3-

Co(III)) on the enzyme Acetyl-CoA Synthase (ACS) to yield acetyl-CoA. The structure of acetyl-CoA is shown in Figure 6, with the CoA group on the left and the acetyl group highlighted on the right.

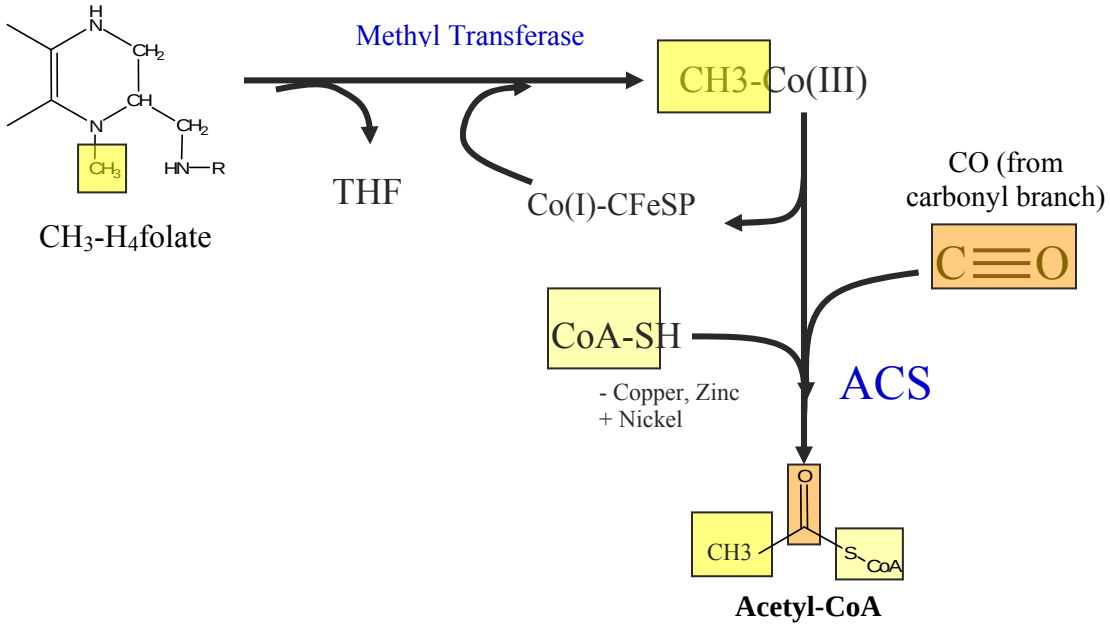

Figure 5. The combination of the methyl branch and carbonyl branch to yield Acetyl-CoA over the enzyme Acetyl-CoA Synthase (ACS).

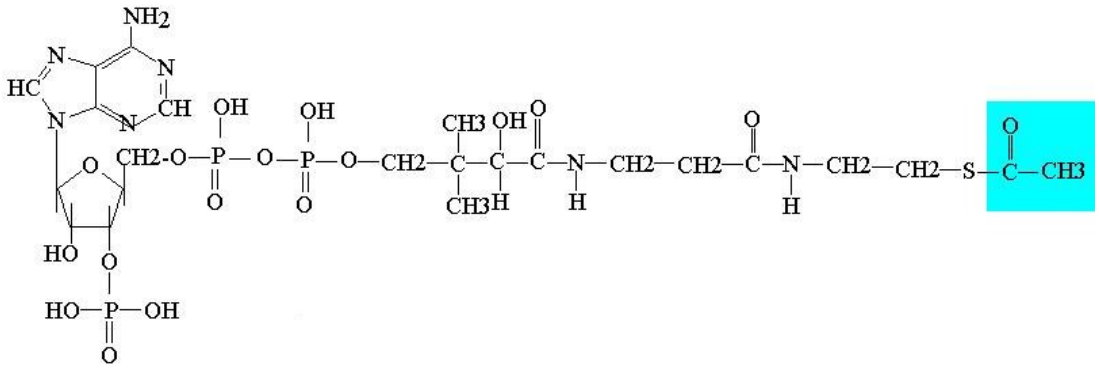

Figure 6. Structure of Acetyl-CoA with acetyl group highlighted on the right (Wikipedia 2006)

Products of Acetyl-CoA

Once acetyl-CoA is formed, acetyl-CoA can then be used in a variety of ways: building block for cell material, generation of ATP (the cells energy source) through acetate production, or to create liquid fuels such as ethanol and butanol. The two predominant paths discussed in this paper are the formation of acetate (also known as acetogenesis) and the formation of ethanol (also known as solventogenesis). The enzymatic pathway for the conversion of Acetyl-CoA to products is shown in Figure 7.

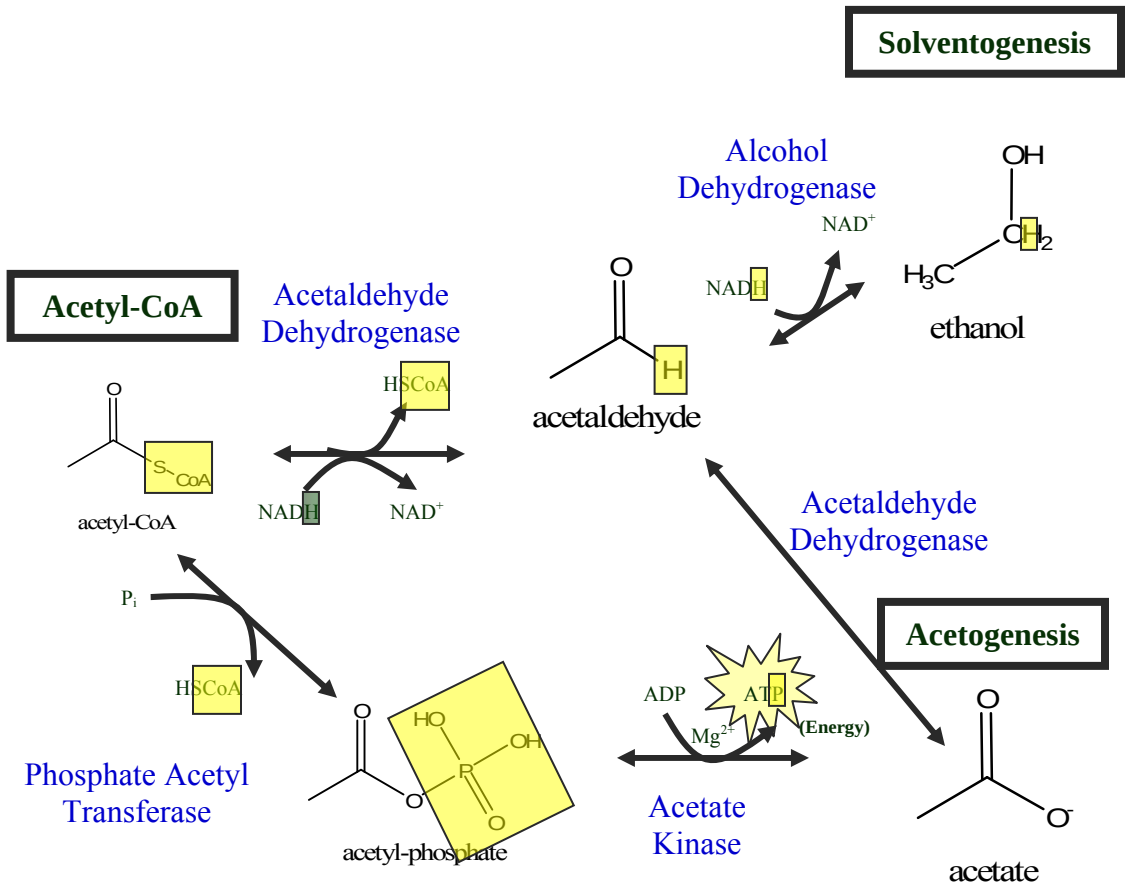

Figure 7. A diagram of the conversion of Acetyl-CoA to either ethanol (solventogenesis) or acetate (acetogenesis).

Although during acetogenesis the *Clostridium* bacteria primarily produce acetate, butyrate is also produced at times in smaller quantities. Similarly, butanol can be produced during solventogenesis, although ethanol is the primary product. The production of butyrate and butanol is seen more in *Clostridium carboxidivorans* than in P11.

An example of the results of an experiment using *Clostridium carboxidivorans* is shown below. Continuous clean bottled gasses were initially used, meaning the gas did not actually come from a gasifier, but is the same composition as a typical gasifier run. From Day 0 to 6.5, the liquid is in batch mode following which the liquid is switched to the continuous mode to replenish any needed nutrients. During the growth phase of the bacteria, the CO/CO_2 is converted to biomass carbon and needed ATP (through the production of acetate) as shown in Figure 8.

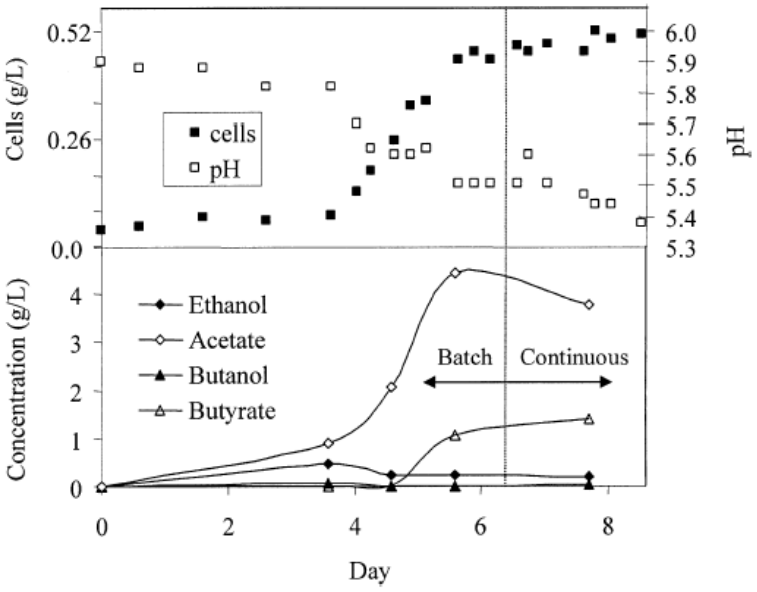

Figure 8. Cell concentration, pH, and product profiles from days 0 to 8.5 using clean bottled gas. Liquid was in the batch mode from days 0 to 6.5 and in the continuous mode from days 6.5 to 8.5. The liquid feed rate during the continuous mode was 1.5 mL/min. Gas was always continuous at an inlet flow rate of 180 ccm at 3.5 psig (Datar, Shenkman et al. 2004)

However, once the bacteria have reached a stationary phase and growth has leveled off, the pH level increases and the main product is ethanol with some butanol (see Figure 9) as the production of acetate and butyrate drop to essentially zero (Datar, Shenkman et al. 2004). During this phase of the experiment, syngas from switchgrass was used.

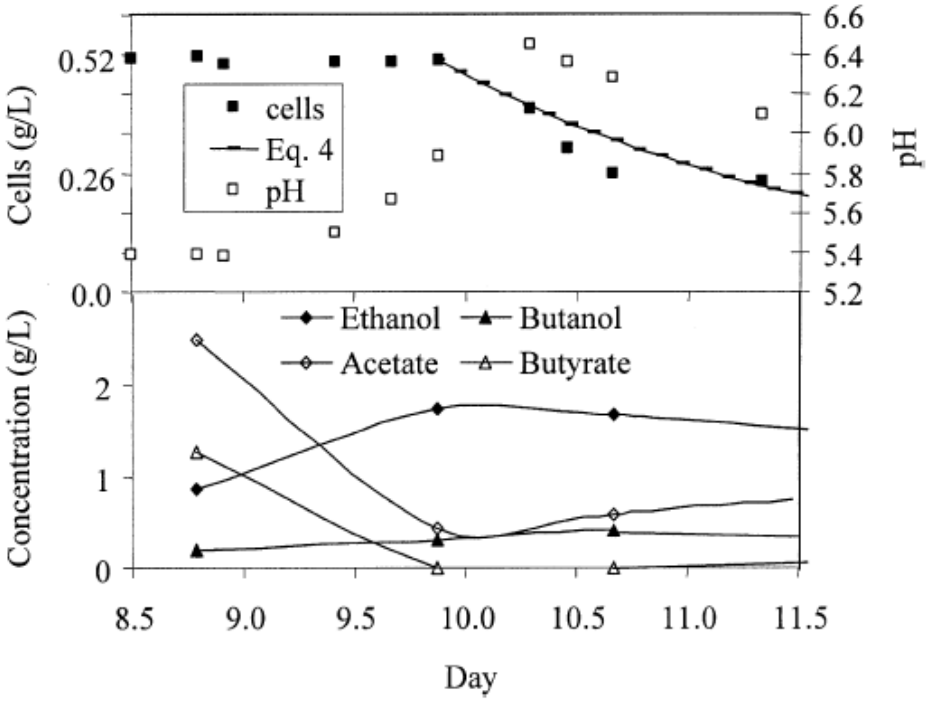

Figure 9. Cell concentration, pH, and product profiles from days 8.5 to 11.5 using biomass-generated producer gas. Both gas and liquid were in the continuous mode. The inlet gas flow rate was 180 ccm at 3.5 psig and the liquid feed and withdrawal rate was 1.5 mL/min (Datar, Shenkman et al. 2004)

The simplest path for ethanol to be produced is by converting acetyl-CoA to acetaldehyde and then to ethanol (see Figure 7). This is done by the donation of four electrons (see Equations 3 & 4).

$$Acetyl - CoA + NADH \rightarrow Acetaldehyde + HSCoA + NAD^{+} \qquad (3)$$

Butanol is made by combining two molecules of Acetyl-CoA to form acetoacetyl-CoA. With the addition of four more electrons, butanol is formed; however this is not a favored byproduct (see Equation 4).

$$\begin{aligned} &Acetyl-CoA \rightarrow Acetoacetyl-CoA \rightarrow 3-Hydroxybutyryl-CoA \rightarrow \\ &Crotonyl-CoA \rightarrow Butyrl-CoA \rightarrow Butyraldehyde \rightarrow \text{Butanol} \end{aligned} \quad (4)$$

Objectives

Although gasification of biomass and subsequent fermentation of the syngas has been demonstrated, there are still hurdles that need to be cleared before the process is commercialized. Further research needs to be conducted on increasing the feasibility of such a process, including higher cell growth yields as well as the ability to control metabolic pathways to achieve higher concentrations of desired products (ethanol). It is known that electron flow pathways have a significant influence on the product distribution of fermentative cultures, to the point of inducing solvent (ethanol) production (Rao, Ward et al. 1987). This project will focus on 1) understanding the effects of syngas composition on the culture redox potential for possible future metabolic pathway control, 2) determining the redox potential(s) that may play a role during acetogenesis (acetate production) and solventogenesis (ethanol production), and 3) understanding the effects of pressure and mass transfer on growth and ethanol production.

Objective 1. Effects of gas composition on redox potential

Redox levels are indicative of the reducing potential (how many electrons are available) in a solution. Because the production of ethanol requires the donation of

electrons, this is an important metric to understand. The hypothesis is that different gas compositions of CO, H_2 and CO_2 will affect the redox potential of the media. Assessing compositional effects on the redox level may be important since the gas compositions can change during syngas fermentation as a result of consumption and production processes resulting from cellular activity. The information from this work will be used to understand whether or not the feed gas compositions play a significant role in the redox levels determined in Objective #2. No substantial work has been done on syngas fermentative processes and redox potential associated with gas composition.

Objective 2. Optimum redox level for production of ethanol and acetate

The hypothesis is that there will be a range of culture redox potentials at which the bacteria optimally produce ethanol (the desired end-product), and a range at which they optimally produce acetate (and therefore ATP, aiding in cell growth). These ranges will be determined. This information can be valuable for future redox control applications although this is outside the scope of this research.

Objective 3. Effects of pressure and mass transfer

The hypothesis is that partial pressure (related to head space volume in closed bottle studies) and/or mass transfer issues cause the observational differences in growth and ethanol production. Thus, pressure (including CO partial pressure) will be explored in the bottle experiments and mass transfer effects on growth and ethanol production will be explored in both bottle and 1-liter reactors. Understanding pressure and mass transfer effects on growth and/or ethanol production will provide a basis for designing reactor systems.

Chapter 2 - Review of Recent Research

Acetogenesis to Solventogenesis Switch

The ability to predict and control the onset of solventogenesis is very valuable, and as such, much research has been performed in this area, although no research has been done for *Clostridium carboxidivorans* or P11. In clostridia cultures, researchers have identified many factors that effect solventogenesis, such as: pH, ATP levels, sporulation, availability of reducing energy (redox level) and iron-limitation among others (Gottschal and Morris 1981; Meyer, Roos et al. 1986; Adler and Crow 1987; Durre, Fischer et al. 1995; Girbal, Croux et al. 1995; Girbal, Vasconcelos et al. 1995; Guedon, Payot et al. 1999; Durre and Hollergschwandner 2004). To this point in the research group, pH does not induce solventogenesis in *Clostridium carboxidivorans* or P11.

Perhaps the governing of electron flow is the key to the switch from acetogenesis to solventogenesis in *Clostridium carboxidivorans* and P11. Many enzymatic reactions in P11 are oxidation-reduction reactions (the transfer of electrons from one substance to another) where one substance is oxidized to reduce another substance. It is therefore important to understand the reduction potential to determine the ability of the bacteria to perform the oxidation/reduction reactions. A colleague, Asma Ahmed, studied the effect of neutral red (a reducing agent) on the metabolic pathways of *Clostridium*

carboxidivorans. She found that adding neutral red increased the output of ethanol while decreasing the production of acetic acid (Ahmed 2005).

As pH control has not led to the ability to control product distribution in P11 cultures, redox potential appears to be a viable option and warrants further inspection. The work proposed here will give a starting place to determine if the governing of electron flow will control the switch from acetogenesis to solventogenesis. Although, redox control is outside of the scope of this research, this research will provide a foundation upon which control can be attempted by discovering the redox potential levels of the P11 cultures associated with acetate and ethanol production, as well as assessing the effects of gas composition on redox levels.

In many cultures, oscillating behavior between acetogenesis and solventogenesis has been observed. One study showed the effect of dilution rates on the culture parameters of a bioreactor cultivating *Clostridium acetobutylicum* grown on lactose (Kim, Bajapai et al. 1988). At a lower dilution rate, higher concentrations of solvents were observed, however *all* parameters showed oscillatory behavior (concentration of solvents increases, and then decreases in a cyclic fashion). These oscillations disappeared at higher dilution rates; however, solvent concentration was much lower. This oscillating state was attributed to the formation of toxic products in the system. However, when glucose was fermented, no oscillatory states were reported and when lactose was fermented, oscillations were observed. Therefore, the alcohol levels were toxic to the pathways of lactose metabolism, although they weren't toxic to glucose metabolism.

Another study of *Clostridium acetobutylicum* (Clarke, Hansford et al. 1988) concluded that the switch from acetogenesis to solventogenesis is analogous to the switch

from primary to secondary metabolism and results in a net decrease of ATP. Current biochemical evidence indicates that acid-producing and solvent-producing pathways are unlikely to operate simultaneously in the same cell, so when simultaneous production occurs in a culture, there are two populations of cells present, those in the solventogenesis stage and those in the acetogenesis stage. Clark and Hansford propose the following sequence of events (including changes in cell morphology) for these oscillations: 1. Higher specific growth rate of acid-producing cells leads to selective retention of these cells and an increase in cell numbers and the yield of acid end products. 2. Increase in cell density and the concentration of acids then results in an increase in the number of cells that undergo a shift to solvent production, causing a decrease in the yield of acid end products and an increase in the yield of solvents. 3. Decreased specific growth rate and/or rate of cell division associated with solvent-producing cells results in a reduction in the total biomass due to the washout of the elongated solvent producing cells. 4. The washout of solvent producing cells is accompanied by a decrease in solvent yield and an increase in glucose concentration which then favors the onset of a new cycle of cell division and an increase in the yield of acid end products (Clarke, Hansford et al. 1988).

Redox Potential

The redox potential is a measure of the affinity of a chemical solution for electrons compared with hydrogen. Substances with a positive redox potential are more capable of oxidizing hydrogen. Substances with a negative redox potential are more capable of reducing hydrogen. In an aqueous solution, the reduction potential is the tendency of the solution to gain or lose electrons when a new species is introduced. The

transfer of electrons between chemical species determines the reduction potential. Reduction potential can be measured in volts (V), millivolts (mv), or Eh (1 Eh = 1 mv).

In several studies, the culture redox potential (E_H) has been shown to correlate with product distributions. In *Clostridium acetobutylicum*, the redox potential was observed through the course of a reactor and it was found that between -225 and -275 mV, butyric acid reached a peak concentration whereas, butanol reached a peak concentration between -300 and -350 mV (Kim, Bajapai et al. 1988; Kim and Kim 1988). Thus, a more negative redox potential favored alcohol production, which is consistent with the fact that alcohols are more reduced as compared to acids.

Other studies have controlled the culture at certain redox potentials and measured the product distributions. In *Clostridium thermosuccinogenes*, it was found that at *controlled* culture redox potential levels, the fermentative product distribution varied such that higher values of culture redox potential (-225 to -250 mV) favored formation of hydrogen and ethanol, while lower values (-275 to-310 mV—more negative) nearly halted formation of these products and correlated with an increase in cell growth (Sridhar and Eiteman 2001). If cell growth correlated with acid production, such as with P11, then these findings suggest that a more negative redox potential correlates with acid production, which is contrary to the *Clostridium acetobutylicum* findings. Although the above studies did not use syngas as the feedstock, these apparent controversies demonstrate the need to study redox levels during syngas fermentation.

Research has shown that electron donors can cause the onset of solventogenesis. Methyl viologen (an electron donor) has also been added to solutions to shift the carbon balance in fermentation. In a study involving *Thermoanaeroabacter ethanolicus* and

Clostridium acetobutylicum, methyl viologen *induced* solvent production when added to a solution (Rao, Ward et al. 1987). Although the effect on redox potential was not quantified, the correlation between the reducing agent, methyl viologen, and the culture redox potential is shown in Peguinn and Soiucalle (1994).

Various compounds can be used to control the culture redox level in solution: sodium sulfide (Rao, Ward et al. 1987; Sridhar and Eiteman 2001) sodium thioglycolate, cysteine, ascorbic acid, methyl viologen (Rao, Ward et al. 1987), and hydrogen sulfide (Jee, Nishio et al. 1987). A summary with compound concentrations is given in Table 1.

Table 1. Summary of chemicals used to control the culture redox level

Chemical	Concentration	Reference	Notes
$Na_2S*10\ H_2O$	35 g/L	(Sridhar and Eiteman 2001)	By hand or with peristaltic pump
Titanium (III)-citrate	60 mM	(Jee, Nishio et al. 1987)	Peristaltic pump (on/off switch)
Potassium ferricyanide	0.1M	(Jee, Nishio et al. 1987)	Peristaltic pump (on/off switch)
Hydrogen Sulfide	10-3,200 ppm	(Jee, Nishio et al. 1987)	Complicated Configuration
Sodium thioglycolate	0.025-0.5 g/L	(Rao, Ward et al. 1987)	Represents final concentration in solution
Cysteine	0.025-0.5 g/L	(Rao, Ward et al. 1987)	Represents final concentration in solution
Ascorbic Acid	0.025-0.5 g/L	(Rao, Ward et al. 1987)	Represents final concentration in solution
Sodium sulfide	0.025 – 0.5 g/L	(Rao, Ward et al. 1987)	Represents final concentration in solution
Methyl viologen	0.01-0.1 g/L	(Rao, Ward et al. 1987)	Represents final concentration in solution

Because the extra-cellular redox potential readings are a function of the intracellular redox environment (Nakashimada, Rachman et al. 2002), the culture redox potential has also been indicative of cellular processes such as lag phases, switches to secondary metabolism, etc. (Kwong, Randers et al. 1992; Peguin, Goma et al. 1994). In solventogenesis, the bacteria utilize the reducing potential available in the form of NADH

to first form acetaldehyde by the enzyme acetaldehyde dehydrogenase, and then to form ethanol by the enzyme alcohol dehydrogenase. If NAD^+ is unable to be regenerated to NADH because of a lack of electrons, then the solventogenesis pathway is halted.

Although the work cited above involved non-gaseous feedstocks, little work involving gaseous feedstocks has occurred in understanding the effects of redox levels on cell growth and product formation. Some work has been done on gaseous feedstocks, (Jee, Nishio et al. 1987) using *Methanobacterium thermoautotrophicum* and studying the biomethanation from H_2 and CO_2. Once again it was determined cultural redox potential had an effect on product distribution. An optimum methane production rate was found in the range of -370 to -500 mV. In a study involving *Clostridium carboxidivorans* in the presence of syngas, neutral red (another electron donor) increased the production of ethanol, while the addition of NADH had no effect on the culture (Ahmed 2005). However, this latter study did not assess the redox levels.

As noted above, many of the redox levels associated with optimal cell growth and/or product formation vary significantly among different cell types and/or substrate type (gaseous versus non-gaseous). Therefore, to develop a viable commercial process for syngas fermentation to ethanol, it is important to understand redox levels associated with gas composition (H_2, CO_2, CO), acetate formation (acetogenesis), and ethanol formation (solventogenesis) using the organism of interest. The gas composition has the potential to affect the redox level of the media by dissolving into solution, and can further affect the media when cellular enzymatic activity oxidizes the gasses to potentially increase the reducing potential of the solution. Determining naturally occurring redox

levels in solution when acetate (and therefore ATP to aid cell growth) and ethanol is produced is beneficial for optimizing growth and ethanol production separately.

Pressure Effects on Growth and Ethanol Production

One study showed that increasing the CO partial pressure inhibits growth for *Clostridium acetobutylicum (Kim, Bellows et al. 1984).* This study was done in a culture medium that contained 30-60 g/L of glucose, and therefore CO was not utilized as the primary source of carbon for bacterial growth. An increase in CO concentration from 0-6% in the headspace in this same study was found to increase ethanol production by 14%.

A further study of *Clostridium acetobutylicum* (also using glucose as the primary substrate) showed that in the case of continuous fermentation, H_2 was essential for good solvent production (Mollah and Stuckey 1992). It was also shown that fermentations carried out at atmospheric pressure that contained both H_2 and CO_2 in the sparging gas had a higher butanol/acetone ratio than when the CO_2 was absent. An additional study of *Clostridium acetobutylicum* indicated that the presence of increased pressure when H_2 was in the headspace increased solvent production, as more dissolved H_2 gas was in the medium (Doremus, Linden et al. 1985). Agitation rate also had the same affect in an atmospheric reactor (once again dissolving more H_2 in the media), although in a pressurized reactor, agitation had no additional affect. This same effect of increased ethanol yield (13%) with increased hydrogen partial pressure when *Clostridium acetobutylicum* was grown up on glucose was found in a study from McGill University (Yerushalmi, Volesky et al. 1985).

Clostridium carboxidivorans and P11 utilize CO to produce acetate (and the building blocks for new cell mass) and ethanol. Therefore, it seems to follow that increasing the CO would increase the growth and/or production of ethanol.

Kendall Hurst, a recent graduate in this research group determined that CO partial pressure did indeed have a positive affect on the cell growth rate (Hurst 2005). Cell optical density and growth rate increased with increasing CO partial pressure. The growth of *Clostridium carboxidivorans* was shown to follow the Monod kinetic model for growth (utilized a single limiting substrate) indicating that CO limits the growth of the bacteria.

In Hurst's study, CO partial pressure was also revealed to have a positive effect on the production of ethanol (grams per gram of cell mass) as shown in Figure 10.

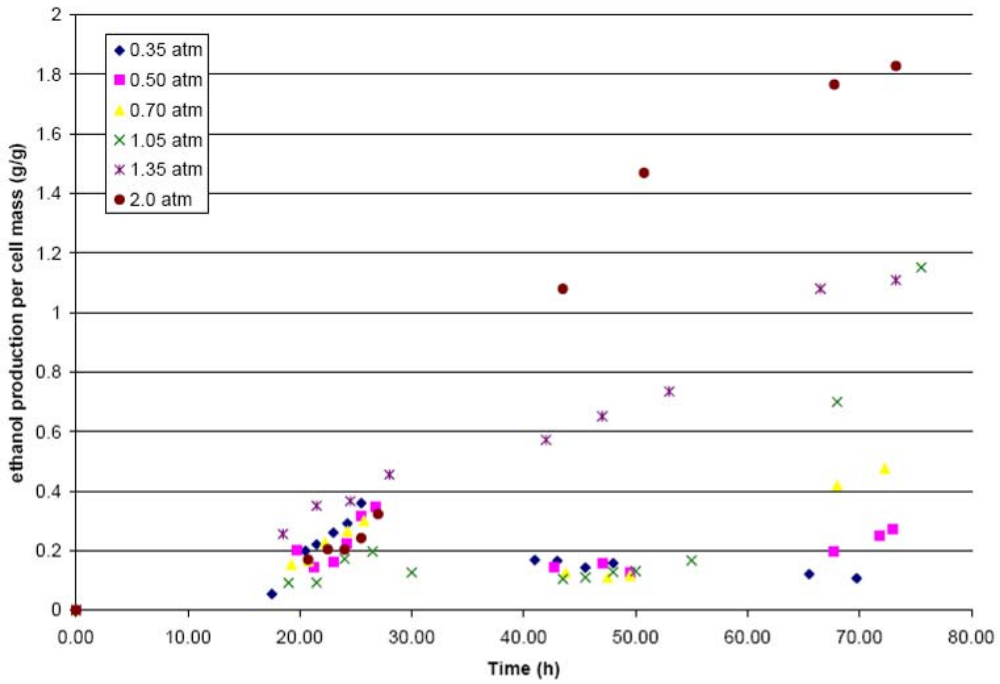

Figure 10. Comparison of ethanol production under various partial pressures of CO (Hurst 2005)

Although, Hurst's work showed a connection between CO partial pressure and cell growth, as well as ethanol production, there were still some unanswered questions. For instance, if cells begin producing ethanol at one rate, can this rate *then* be increased by increasing the partial pressure of CO? Does the partial pressure (not only of CO, but of H_2 and CO_2) explain the difference in growth when the liquid volume is adjusted (50 mL vs. 100 mL) in similar bottles studies? These questions will be further studied in the scope of this research.

Chapter 3 – Effects of Gas Composition on Redox Potential

Redox levels are indicative of the how many electrons are available in a solution (also called redox potential or reducing potential). Because the production of ethanol requires the donation of electrons, this is an important metric to understand. The hypothesis is that different gas compositions of CO, H_2 and CO_2 affect the redox potential of the media. When applying syngas to a bioreactor, gas compositions can change during syngas fermentation as a result of consumption and production processes resulting from cellular activity. Results from assessing the hypothesis help understand whether or not the gas compositions in media are significant for understanding redox levels observed in Objective #2.

Experiments from Objective 1 were performed in a 500 mL culture flask bioreactor. The redox potential with H_2 was first measured in distilled water to ensure the redox probes were accurately reading the redox level of a solution. Following the H_2 experiment, the pure gas components of CO, CO_2, or H_2 were bubbled through the culture media and the associated redox levels were measured once the media was saturated with the respective gas.

Methods/Equipment

Bioreactor media

The media contained three stock solutions (see below for composition): 10 ml metals solution, 25 ml mineral stock solution, 10 ml vitamin solution, 950 ml distilled water, 0.5 g DIFCO yeast extract and 20 g MES buffer. The solution was then pH titrated to 6.0 using 5N NaOH. Resazurin was added to the media as an oxygen indicator.

The trace metals stock solution contained (per liter) 0.2 g cobalt chloride, 0.02 g cupric chloride, 0.8 gm ferrous ammonium sulfate, 1 g manganese sulfate, 0.2 g nickel chloride, 2 gm nitrilotriacetic acid, 0.02 g sodium molybdate, 0.1 g sodium selenate, 0.2 g sodium tungstate, and 1 g zinc sulfate. The mineral stock solution contained (per liter) 4 g calcium chloride, 20 g hydrated magnesium sulfate, 10 g potassium chloride, 10 gm phosphate Mono, and 80 g sodium chloride. The vitamin stock solution contained (per liter) 0.005 g aminobenzoic acid, 0.002 g D-Biotin, 0.005 g pantothenic acid, 0.002 g folic acid, 0.01 g MESNA, 0.005 g nicotinic acid, 0.01 g pyridoxin, 0.005 g riboflavin, 0.005 g thiamine, 0.005 g thioctic acid, and 0.005 g vitamin B-12.

500 mL bioreactor

The bioreactors used in the experiments are shown in Figure 11 and Figure 12. The bioreactors are glass culture flasks (1000 mL total volume, with 500 mL liquid volume and 500 mL gas volume) with plastic lids that screw on and are sealed with an o-ring. Each reactor has two arms, each also sealed with plastic lids that screw on and seal tight with an O-ring. One arm was used as a gas outlet and the other arm was left sealed. Holes were tapped into the lid (in order for fittings to screw in tightly and be sealed with plumbers tape) for all the remaining needs such as gas inlet, liquid outlet, liquid inlet, and

temperature probe. Any additional holes were sealed with a plug. Initially, 500 ml of media were added to the bioreactor and sealed with a lid. A temperature probe and heating blanket maintained the temperature of the media at 37^{o}C. A magnetic stir rod (suspended from the lid) kept the media well mixed.

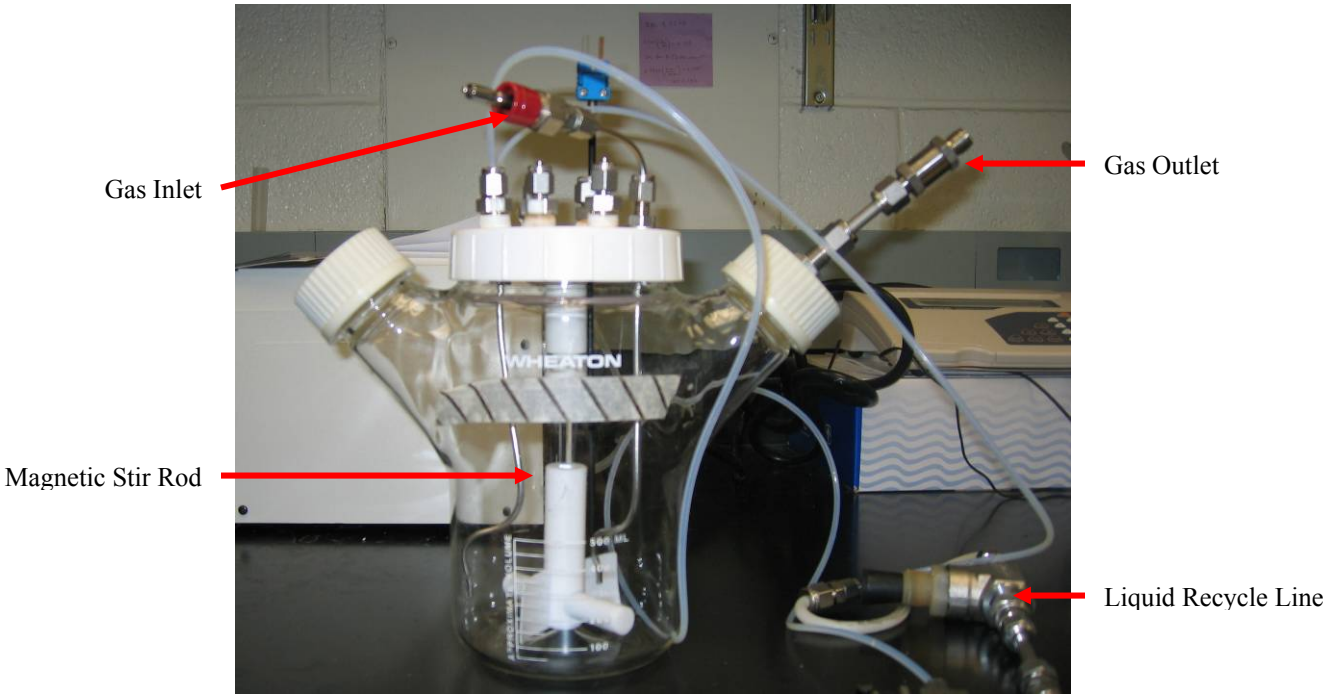

Figure 11. 500 mL bioreactor used in Objective #1 experiments

Two reactors were used in the experiments. The reactors were kept at near atmospheric pressure and continual gas feed was bubbled through the solution of each reactor by splitting a source gas supply between the two reactors. For each reactor, media was circulated through an external line (inner diameter 1.6 mm) using a peristaltic pump at 60 mL/min. The external line contained the redox probe to allow for redox measurements and liquid samples (see Figure 13).

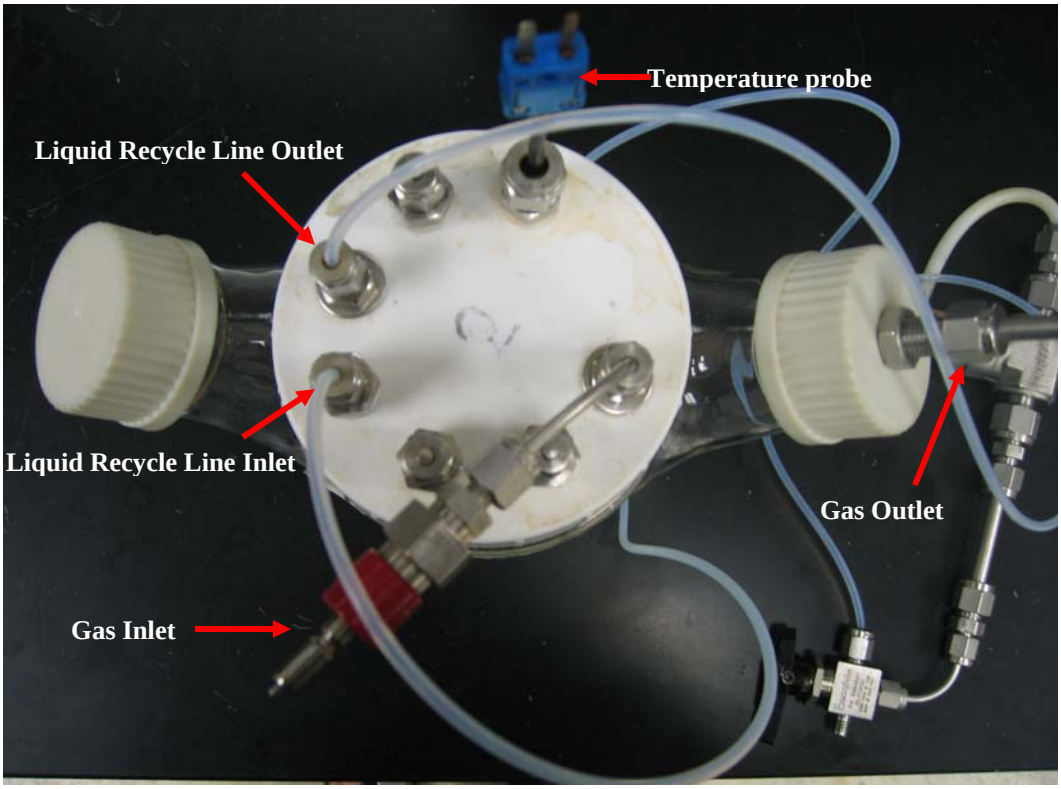

Figure 12. Top view of 500 mL bioreactor

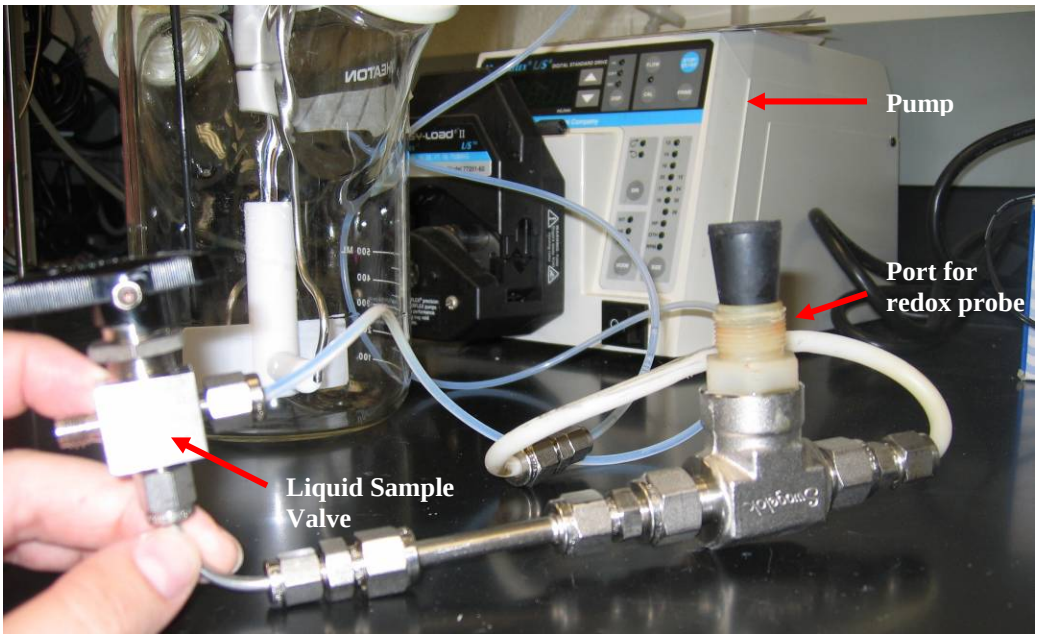

Figure 13. Liquid recycle line for 500 mL reactors to measure redox (with ORP probe) and take liquid samples.

Redox potential was measured using an ORP probe with an Ag/AgCl reference electrode (Cole Parmer, #C-27009-30). The redox potential in the 500 mL bioreactor was measured using an alpha-pH1000 pH/ORP Controller from Eutech Instruments (Cole Parmer #EW56717-30). The reading itself is almost instantaneous (roughly 250 milliseconds to update the display). Labview was used with an NI USB DAQ (National Instruments USB port data acquisition system) to convert the output from the ORP probe to mV so that it could be recorded on the computer.

All redox values were converted from the Ag/AgCl reference to the standard hydrogen electrode reference (SHE) assuming that the electrode potential for Ag/AgCl is E^0 = +222.4 mV using the SHE electrode and E^0 = 0 mV using the Ag/AgCl reference electrode (Doctors 2007). Therefore, if the Ag/AgCl reference gave a redox value of +200 mV, +222.4 mV was added to the value to adjust it to the SHE reference, making the reported value +422.4 mV. The probe was calibrated before each run using Light's Solution – Redox Standard Solution from the Ricca Chemical Company at a standard redox level of + 439 mV.

Independent Gas Runs

First, water at 25^{o}C was purged with H_2 to ensure that the redox level according to the standard hydrogen electrode (SHE) was 0 mV. The experiment showed a redox level of -230 mV using an Ag/AgCl redox reference electrode (see Figure 14 below).

The correction factor as explained earlier for an Ag/AgCl electrode to the standard hydrogen electrode (SHE) is +222.4 mV. Taking the measured value of -230 mV and adding the correction factor of 222.4 mV, the value according to a standard hydrogen electrode (SHE) would be -7.6 mV. This is very close to the true value of zero.

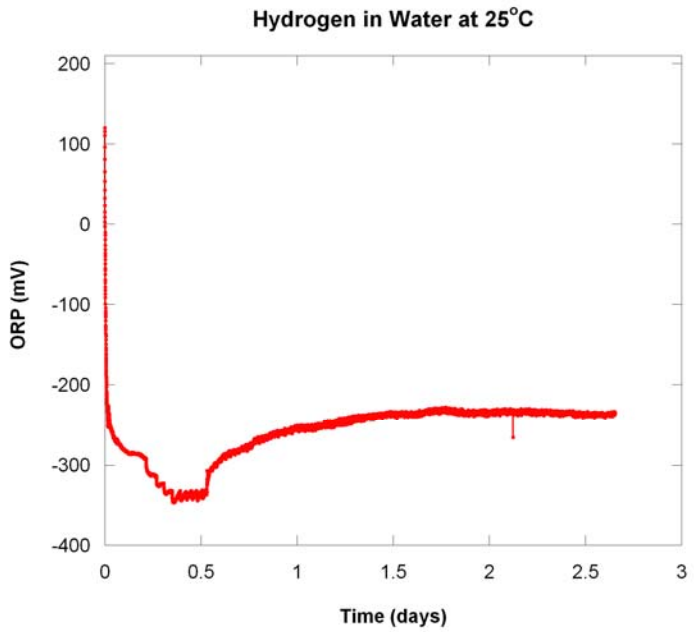

Figure 14. Hydrogen in water at 25°C in the 500 mL bioreactor using an Ag/AgCl redox reference electrode

Therefore it was determined that the redox electrodes accurately determined the redox level of the solution.

The approach of the gas to a steady level is curious, as it leveled off, then dropped down lower, and finally came back to the same value that it had previously leveled off at. This was seen in several of the gas experiments in the 500 mL reactors.

An additional issue with the 500 mL reactors was splitting the gas between the two reactors evenly. Because the reactors were not manufactured in a precision machining lab, there were slight differences that caused differences in pressure. Furthermore, it was very difficult to keep the reactors from leaking. At first, holes were drilled and the fittings were sealed with silicone. After the autoclave, the silicone would not seal as tightly and the fittings would leak. The lids were re-ordered and this time tapped so that the fittings could be screwed into the lid. The reactors were checked in a

water bath before the media was added and autoclaved and found to hold pressure up to 5 psi. However, after the autoclave, the fittings loosened in transport etc. and could not hold pressure at all. Although having a pressurized system is not important for this study, if any further studies are done on the gas compositions, it is recommended that they be completed in commercially built small reactors rather than the home-made reactors.

After assessing the redox level of H_2 in water, the redox levels of pure component gas compositions for CO, CO_2, or H_2, were assessed in actual media instead of water and at 37°C instead of 25°C. Each gas was run in two reactors to ensure both were leveling off to the same redox level. Figure 15 shows the redox data for H_2, Figure 16 shows the redox data for CO_2, and Figure 17 shows the redox data for CO.

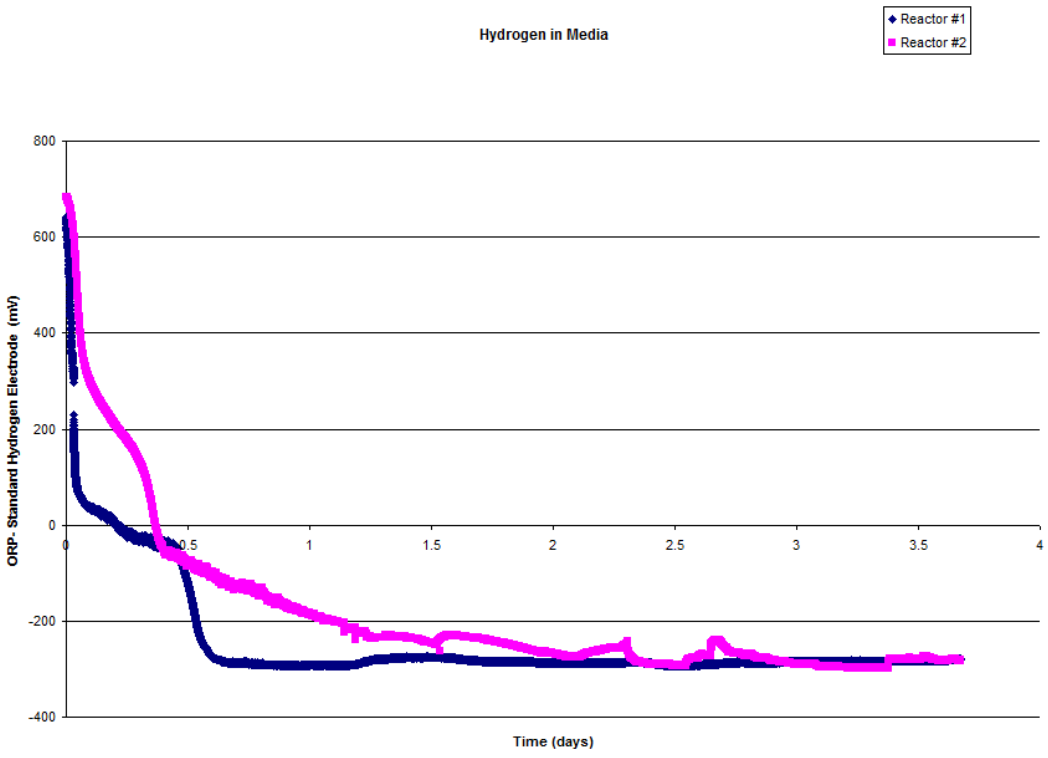

Figure 15. Pure H_2 bubbled through media at 37°C in 500 mL bioreactor while measuring redox

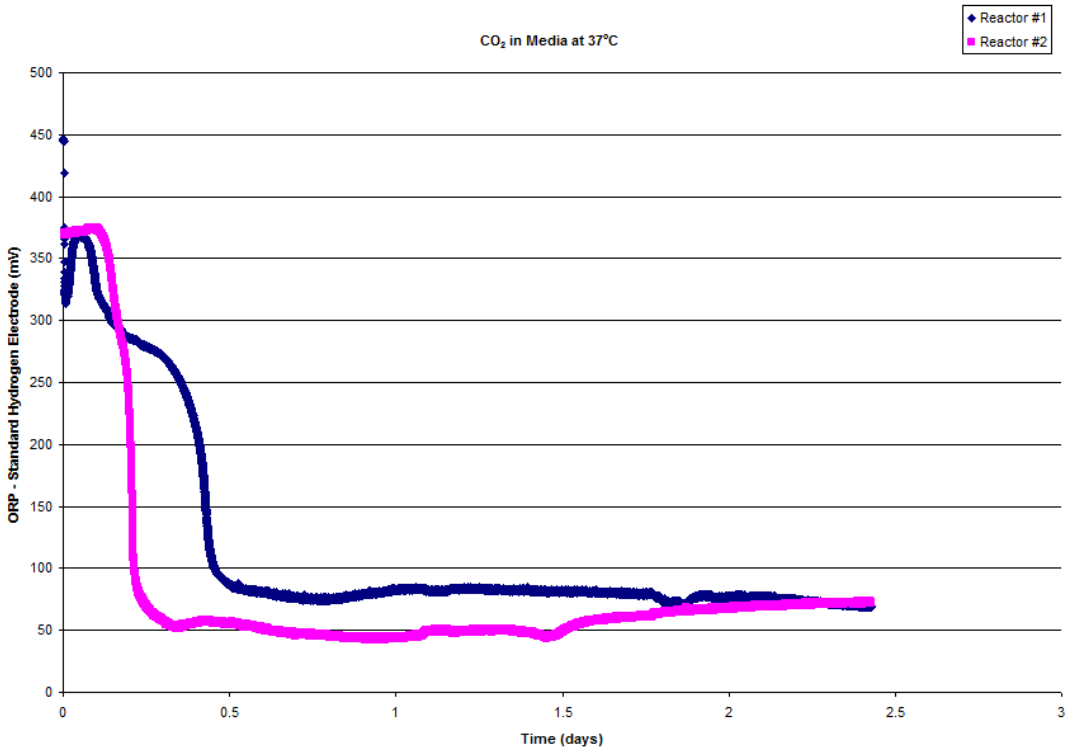

Figure 16. Pure CO_2 bubbled through media at 37°C in 500 mL bioreactor while measuring redox

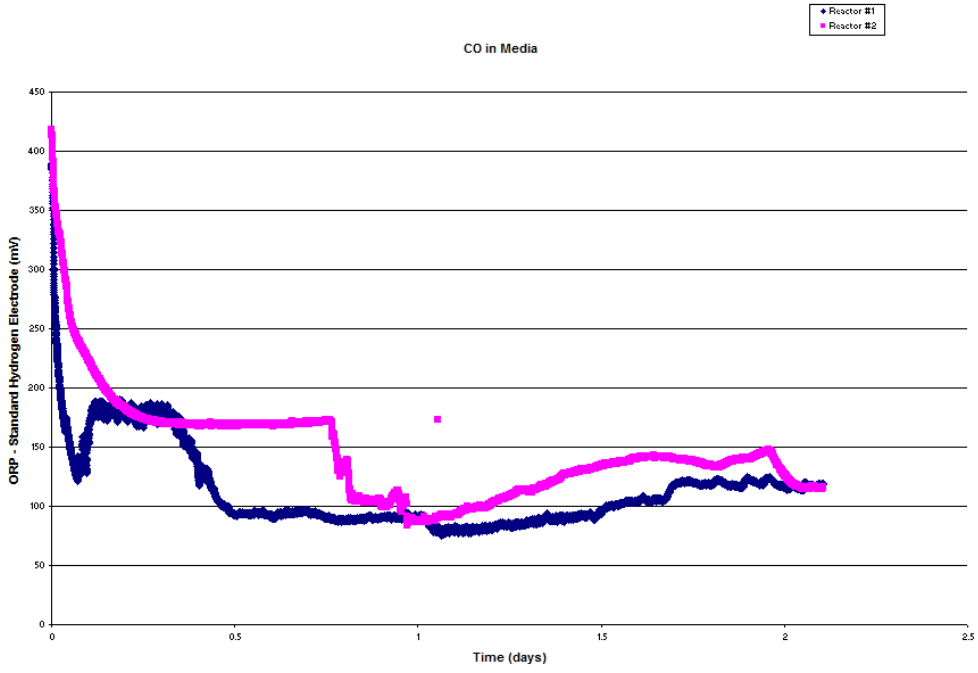

Figure 17. Pure CO bubbled through media at 37°C in 500 mL bioreactor while measuring redox

All runs leveled off at a repeatable redox level although the leveling off took up to two days. The prolonged time it took to level off could be a result of the fittings loosening and uneven gas flow between the two reactors. At times when the reactors were checked, one reactor would have no gas flow and the other reactor would have the entire gas flow. When this occurred, the fittings were adjusted and the gas flow rate was checked again. Initially, the gas flow rate would be uneven but eventually the reactors were able to reach the same gas flow rate and the redox leveled off to the same value for both reactors. The resulting redox levels (the level at which both reactors eventually leveled off at) for each gas are shown in Table 2 below.

Table 2. Summary of raw pure gas redox levels in media at 37°C from 500 mL bioreactors referenced to a standard hydrogen electrode (SHE)

Gas	Redox level (SHE)
CO_2	+72 mV
CO	+122 mV
H_2	-277 mV

As expected, H_2 has the most negative redox level, because it has the most reducing potential. In addition, the H_2 level in media at 37°C is different than the H_2 level in water at 25°C due to the temperature difference and the fact that species in the media are contributing to the reducing potential of the media. As noted in the Table, CO and CO_2 have similar reducing potentials that are much more positive than H_2, as expected. Although redox levels eventually leveled off such that the contribution of pure gases on the redox level could be assessed, it was decided that further studies noted below would be completed in commercially built 1-liter reactors rather than the home-made reactors.

The pure gas runs using the culture media omitted cysteine sulfide from the media since cysteine sulfide is a reducing agent that is primarily used to remove residual oxygen. In the P11 bacterial fermentation processes performed to date, cysteine sulfide is added as an oxygen scavenger. Therefore, several experiments were also performed in a 1-liter (liquid volume) reactor (see methods in Chapter 4 for reactor description) to determine whether cysteine sulfide played a more dominant role, as compared to gas compositions, on the redox level.

As shown in Figure 18 after purging 1 liter of media for 0.7 days using syngas (30% H_2, 30% CO_2, 40% CO at 100 sccm), the redox level was observed to be +100 mV SHE. If one were to estimate the redox level from the pure gas components, assuming each one contributed to the redox level according to the fraction of the syngas that they comprise, the redox level would be around -18 mV SHE. However, because of the complex redox/oxidation reactions between the gasses and the 30+ media components, it is inaccurate to estimate the redox level and therefore it must be determined experimentally. Therefore, the standard syngas mixture in media at 37^{o}C was determined to have a redox level of + 100 mV SHE. Afterwards, cysteine sulfide (0.4 gm/l) was added and the redox level decreased immediately to -140 mV SHE and then began rising again, leveling off at ~ -15 mV SHE.

Another experiment was performed in which the media was initially purged with N_2, rather than syngas (100 sccm), for 0.6 days. As shown in Figure 17, the redox level stabilized at approximately +200 mV. This redox level is more positive than the syngas (less reducing potential) as N_2 is an inert gas whereas syngas has H_2 and CO. When the

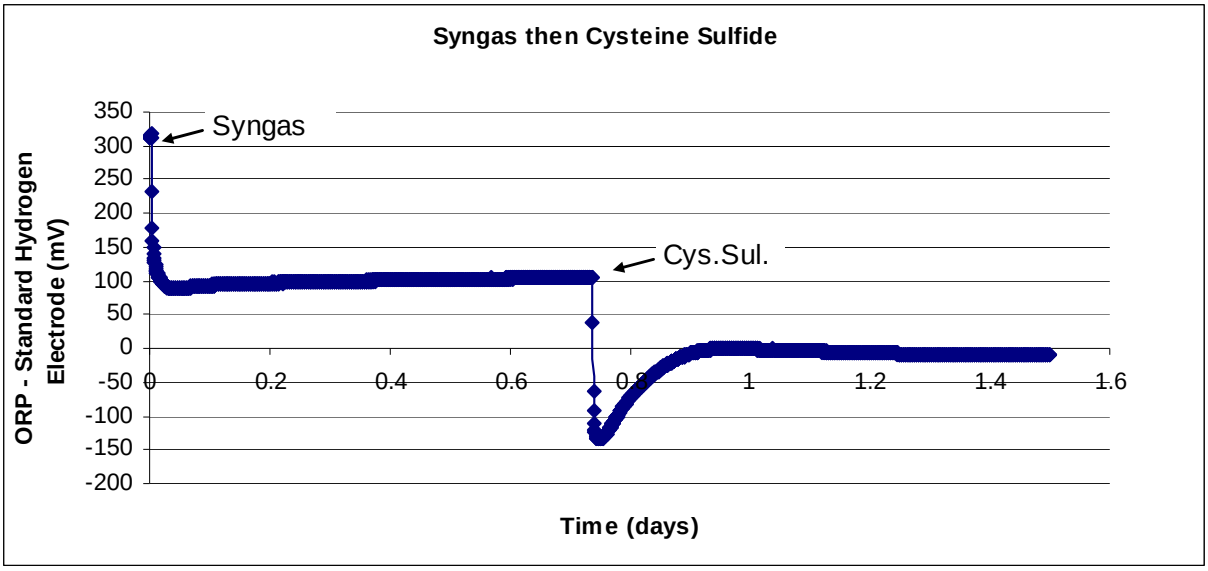

Figure 18. Redox potential (SHE) in cell-free media with syngas and cysteine sulfide.

cysteine sulfide (0.4 gm/l) was added, the solution redox level decreased immediately to -120 mV SHE and then began rising, again leveling off at ~ -15 mV SHE (see Figure 19).

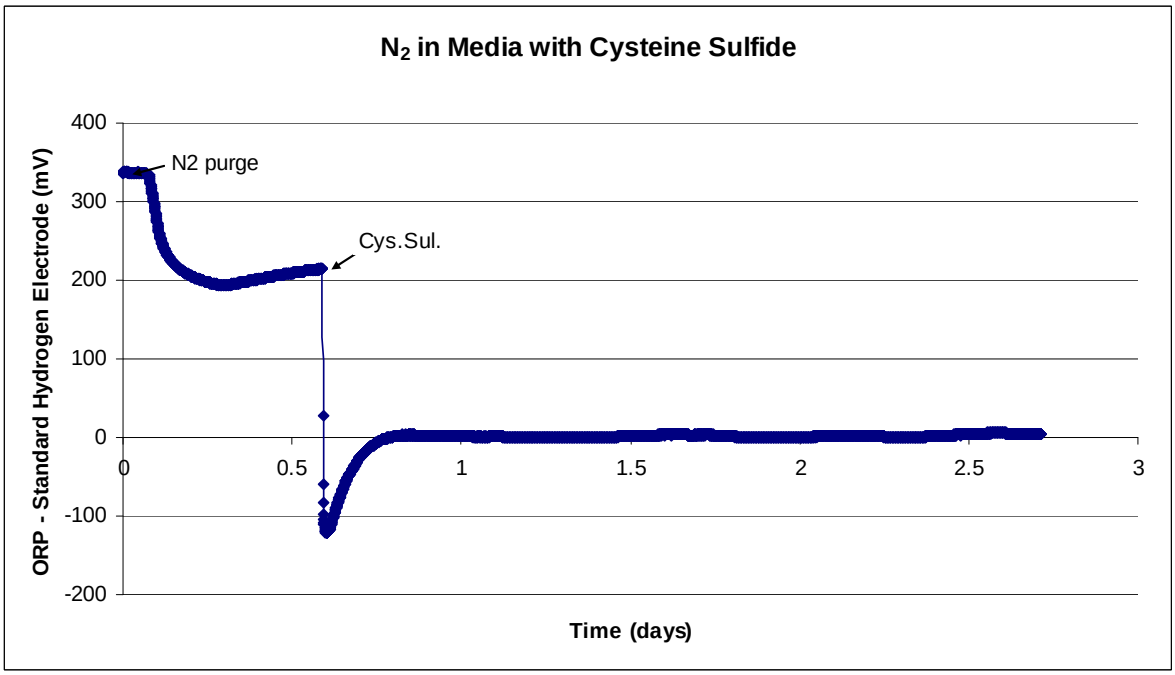

Figure 19. Redox potential (SHE) in cell-free media with nitrogen and cysteine sulfide.

Although there was ~ 100 mV difference in the redox level between the nitrogen solution and the syngas solution before the cysteine sulfide was added, after the addition of cysteine sulfide, both solutions leveled off to the same level. Since the effect of cysteine sulfide on the redox level outweighed the effect of the type of gas used (nitrogen vs. syngas), the results show that the redox level is dominated by cysteine sulfide, independent of the composition of the gas. Therefore, further analysis of the effects of gas composition on redox levels was considered not important when cysteine sulfide is present in the media. This is the case for the experiments performed in Objective #2. Therefore, the analysis of the redox level results in Objective #2 should not be a result of changing gas compositions during the experiments.

Although beyond the scope of this work, it should be noted that recent studies by another colleague (Peng Hu) at Brigham Young University have shown how both cysteine and sulfide contribute to the redox level. The rapid drop after adding cysteine sulfide is a result of both species lowering the redox level since they are both reducing agents. However, sulfide is stripped out of the solution with continuous gas purging, resulting in an increase of the redox level to a level associated with just cysteine. This is consistent with the trends shown in Figures 16 and 17 following the addition of cysteine sulfide. Although media purged with different gases (without cysteine sulfide) resulted in different redox levels, the change in the redox level to the same value in both experiments following the addition of cysteine sulfide again supports that cysteine sulfide dominates the redox level as compared to the gas composition.

Conclusions

It was determined that cysteine sulfide dominates the redox level of culture media (in the absence of cells), as compared to the gas composition. Therefore, a detailed assessment of the effect of gas composition on redox levels is not necessary. The assessment of redox levels in Objective #2 should be independent of the gas composition since the media used in Objective #2 contains cysteine sulfide. As a potential future application, the concentration of cysteine sulfide could be effective at controlling redox levels in bioreactors if redox control is desirable.

Chapter 4 – Optimum Redox Level for Production of Ethanol and Acetate

The hypothesis was that there will be a range of culture redox potentials at which P11 optimally produce ethanol (the desired end-product), and a range at which they optimally produce acetate (and therefore ATP, aiding in cell growth). To test this hypothesis, two 1-liter New Brunswick bioreactors were run with batch liquid and continuous gas flow (30% H_2, 30% CO_2 and 40% CO at 1 atm) at 37^{o}C. These experiments were labeled AFRED2-AFRED8 (AFRED standing for Allyson Frankman Redox Experiments). Redox, temperature and pH were monitored and recorded online. Daily liquid samples were taken to determine optical density, liquid acetic acid concentration and liquid ethanol concentration.

Methods

Microorganism

The bacterium P11 was kindly provided by Ralph Tanner, University of Oklahoma (Liou and Balkwill 2005). The bacterium was isolated in an agricultural lagoon and grown in a nutrient media. Because P11 is a strict anaerobe, all studies were performed in the absence of oxygen. A syngas composition of 30% H_2, 30% CO_2, and 40% CO was used as a standard for all experiments, a typical syngas composition when switchgrass is gasified in oxygen (McIlveen-Writght, Pinto et al. 2006).

1 liter bioreactor

Two BioFlo 110 Benchtop Fermentors (New Brunswick Scientific, Brunswick, NJ, USA) each with a 1-liter working volume (3 liter total volume) were used for the fermentation studies involving batch liquid feed and continuous gas feed (see Figure 20).

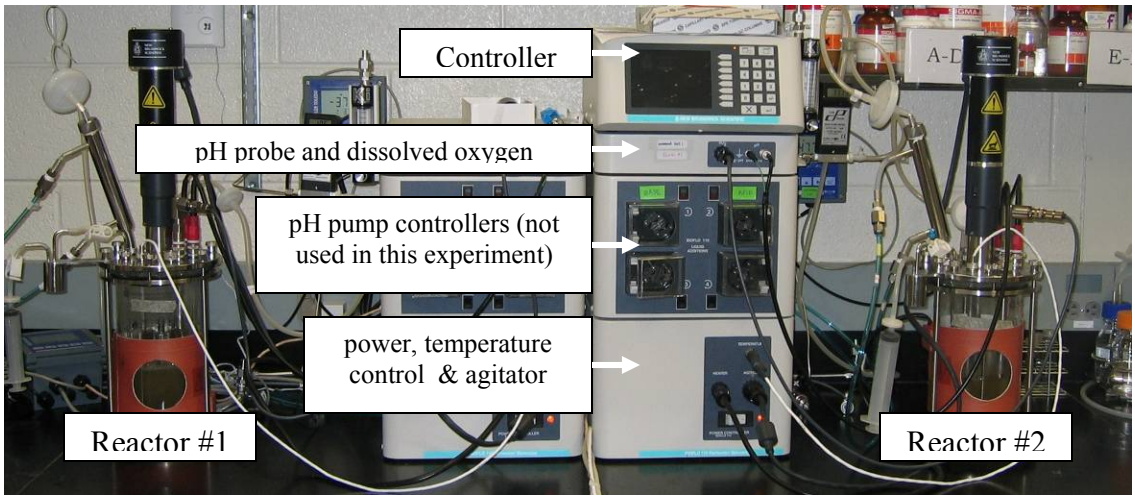

Figure 20. 1-Liter working volume BioFlo 110 Benchtop Fermentors used in redox experiments

The reactors included agitators, spargers, pH probes, dissolved oxygen probes, redox probes, and electrical jackets. The electrical jackets were used for temperature control at 37^{o}C. A septum port for liquid injections and a sterile sample removal port were also included in each reactor. The reactors were maintained at 175 rpm agitation and 100 sccm of gas feed. A close-up picture of the reactor is shown in Figure 21.

Before each run, a new septum was added to the liquid injection port. New 0.2 μm filters (for sterilizing the gas and preventing contamination) were added to the reactor on the gas inlet and gas outlet lines. If old filters are used, they may not allow the pressure to be relieved in the autoclave in addition to not allowing adequate gas flow in

the experiments. The hose on the liquid sample was clamped shut before the autoclave to prevent the liquid from leaking out.

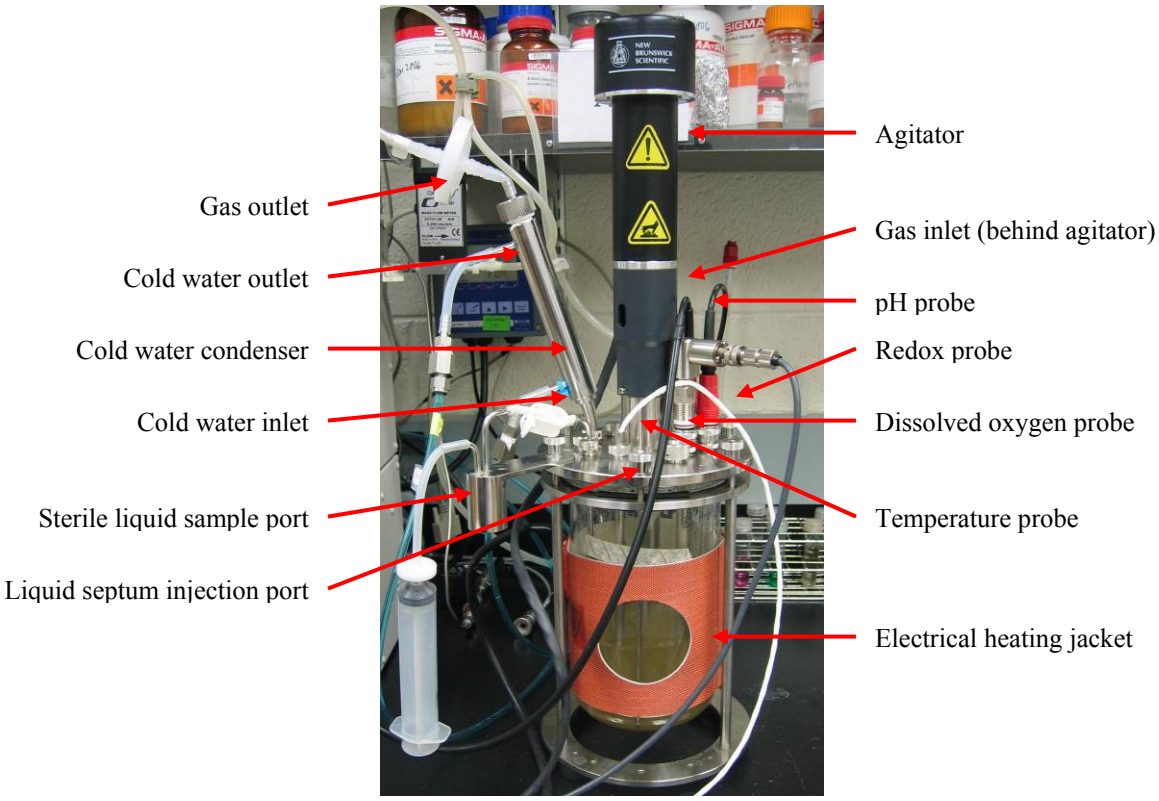

Figure 21. Close-up picture of 1 Liter bioreactor

The pH and redox probes were calibrated and then inserted in the reactor. The dissolved oxygen probe (previously calibrated by running a reactor of water with nitrogen purged 500 sccm overnight) was also inserted into the reactor. Equal amounts of media (1 Liter) were added to each reactor, the reactors were sealed and then autoclaved (20 minutes sterilization and 5 minutes dry time at 121^{o}C). After the reactors were cool enough to touch, they were hooked up to the controller (the two reactors share one controller, up to four reactors can be operated independently from one controller). The

controller provided data on reactor temperature, pH, agitation rate, and dissolved oxygen. However, only the temperature and agitation rate were controlled.

The cold water lines were also hooked up to the outlet gas condenser to condense any ethanol and water vapors existing in the outlet gas. It is important that the water be left on for the whole experiment to ensure that the media concentration doesn't change throughout the experiment from evaporation of the water. The reactors were then sparged with nitrogen overnight at 200 sccm. All fittings were checked to ensure there were no gas leaks. In the morning, the gas feed was switched from nitrogen to the syngas mixture noted above and allowed to run for a few hours to saturate the solution with syngas. Cysteine sulfide was then added and, after an hour, the reactor was inoculated with a 10% vol (100 mL) inoculum of P11 (see Inoculum section below).

Between reactor runs, the reactors were washed with Alconox, rinsed with purified water, and then soaked in an acid bath overnight. The acid bath was prepared by adding 5% Citrad to purified water and then adding sulfuric acid until the pH of the solution was ~2. The pH, redox and distilled oxygen probes were scrubbed with Alconox but were not soaked in the acid bath. The pH and redox probes were both stored in a 3M KCl solution. It is very important that the probes are not stored in water, as this can alter their accuracy.

Inoculum

All P11 bacteria were "passaged" three times before the beginning of an experiment to eliminate lag time at the beginning of an experiment and to make sure that the bacteria were strong and viable. Passaging was completed as follows: 10 vol % bacteria were inoculated into a serum bottle containing 50 mL of media and pressurized

34 psia with 30% H_2, 30% CO_2 and 40% CO. The cells were allowed to grow up to ~0.5 OD (660 nm). The bottle was then used to inoculate another serum bottle and allowed to grow up to a similar OD. This process was repeated one more time, and then the bacteria were inoculated into the experiment while still in the growth phase.

Analytical procedures

The optical density (OD), which is proportional to the cell concentration (~0.43 dry g l^{-1} per OD unit), was determined using a UV-Vis spectrophotometer. Cell samples were collected in 1.5 ml cuvettes and the OD was measured at 660 nm. Cell concentration was previously found to be linearly proportional to OD within a linear range of 0-0.4 OD units. Samples with an OD greater than 0.4 units were diluted to maintain the linear calibration.

The liquid samples were centrifuged at 12,100*g* for 14 minutes. The cell-free supernatant was collected and analyzed for ethanol and acetic acid using a Shimadzu Gas Chromatograph 2014 equipped with a flame ionization detector and an 8 ft Porapak QS 80/100 column (Restek, #80426-850). The supernatant samples were frozen in the time between sampling and analysis (Supelco 2 mL screwtop vial #27079, tan PTFE/white silicone septa #33213 and white propylene cap #507660) to maintain sample consistency between sample extraction and analysis.

Redox potential was measured using a Mettler Toledo ORP probe with an Ag/AgCl reference electrode (Pt4805-DPAS-SC-K8S/225) and a Mettler Toledo pH 2100e Controller. The redox reading was almost instantaneous (roughly 250 milliseconds to update the display). Labview was used with an NI USB DAQ (National

Instruments USB port data acquisition system) to convert the output from the ORP probe to mV so that it could be recorded on the computer.

All redox values were converted from the Ag/AgCl reference to the standard hydrogen electrode reference (SHE) (see Chapter 3 for details).

Results and Discussion

Redox levels

Seven experiments (AFRED 2-8) were completed using the 1-Liter bioreactors in which cell growth, redox level, pH, acetic acid concentration, and ethanol concentration were monitored with time during syngas fermentation. However, there were a few logistical difficulties with obtaining data for some of these runs. Although a backup tank of syngas was ideally on hand, AFRED3 & AFRED4 were cut short when the syngas tank ran out. AFRED5 was cut short when the controller quit working and the temperature spiked, killing the bacteria. However, data prior to the problems for these runs is presented. A representative pre-inoculation redox history is shown in Figure 22.

As shown in Figure 22 after the solution was saturated with the nitrogen, the redox level was approximately +200 mV SHE which is consistent with Figure 19. When the cysteine sulfide (0.4 gm/L) and syngas were added there was an immediate sharp reduction of ~260 mV SHE in the redox level. The gradual increase in the redox level was a result of the sulfide being stripped out of the solution by entering the gas phase in approximately 0.07 days (less than 2 hours).

However, the remaining cysteine kept the redox around -20 mV SHE, consistent with the studies shown in Chapter 3. When the reactor was inoculated, the redox level immediately dropped again. The drop in redox level following inoculation varied

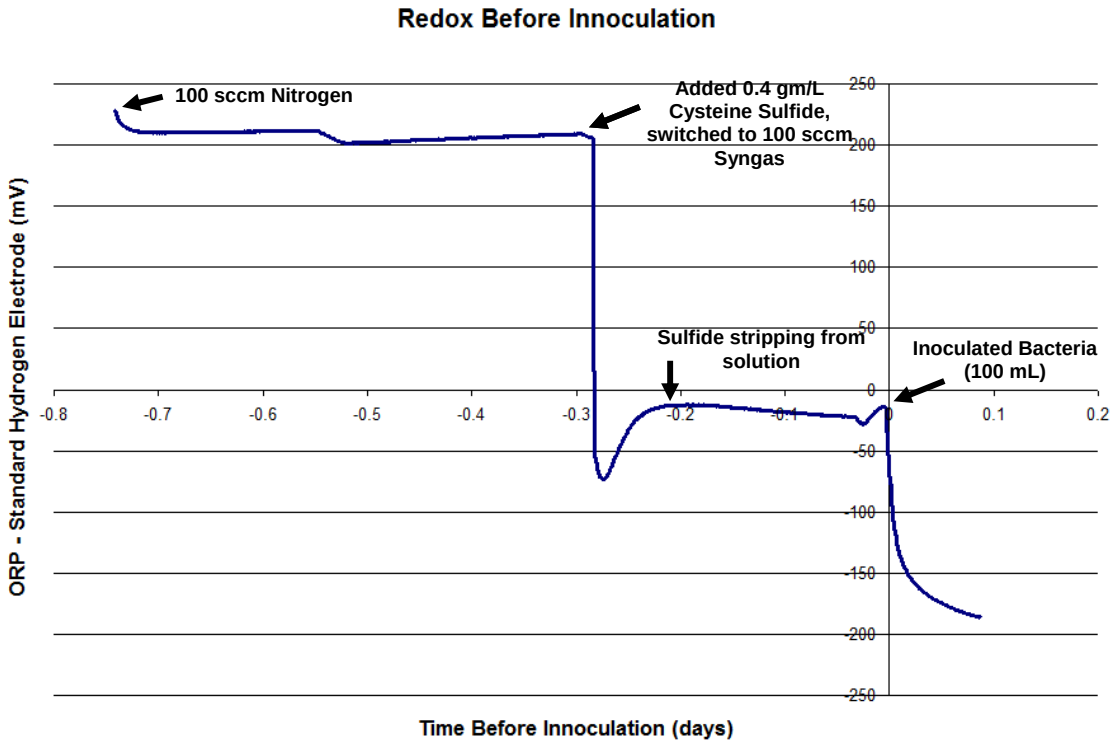

Figure 22. Representative pre-inoculation redox history (from AFRED 8).

depending on the inoculum as shown for all seven runs in Figure 26. The redox levels and their effect on growth, acetic acid and ethanol production is discussed further on in the chapter. The optical density data for these seven runs are shown in Figure 24.

The growth rate constant was calculated by first doing a material balance

$$\frac{dX}{dt} = \mu_m X \tag{5}$$

where t is time, X is the optical density (or cell mass) and μ_m is the maximum growth rate constant. Integrating both sides yields the following equation:

$$\ln(X) = \mu_m t + \ln(X_o) \tag{6}$$

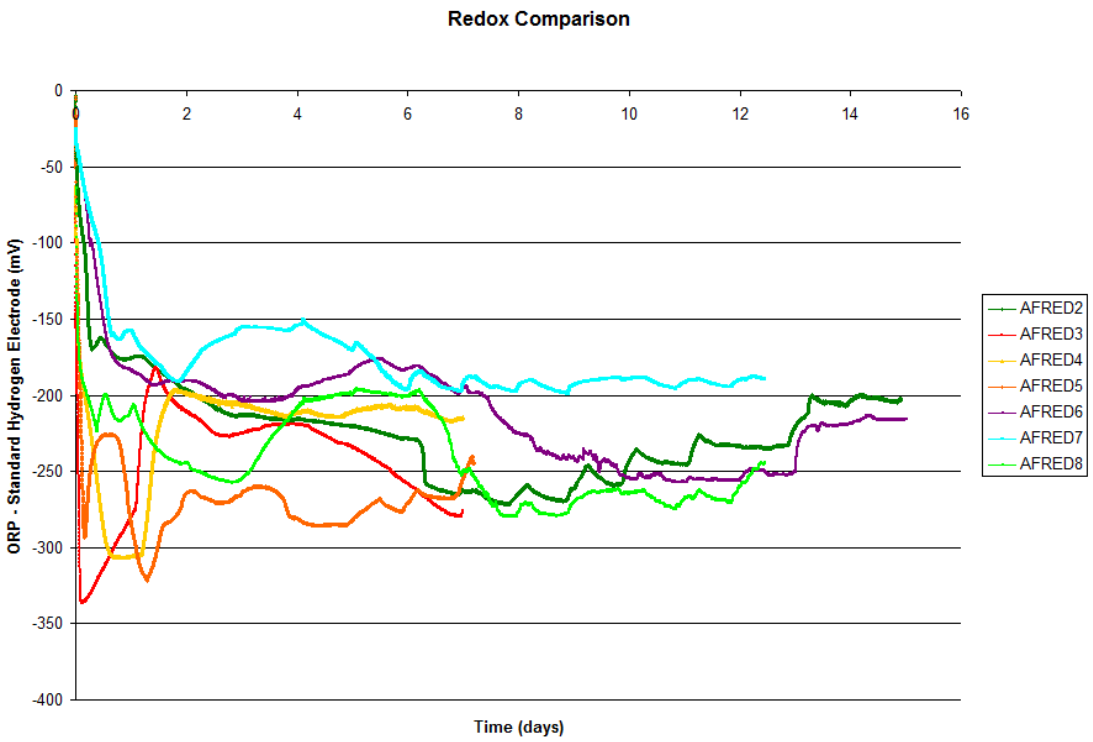

Figure 23. Redox levels for AFRED2, AFRED3, AFRED4, AFRED5, AFRED6, AFRED7 & AFRED8

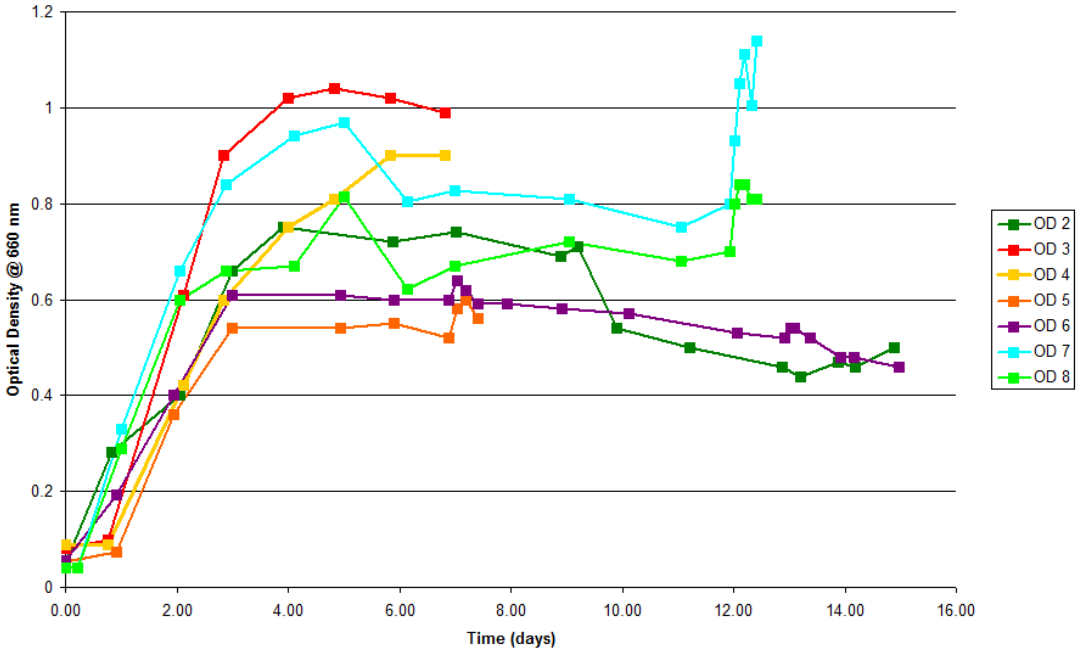

Figure 24. Optical Density profiles for AFRED experiments

By plotting the ln(X) or ln (OD) vs. time during the exponential growth phase, and fitting the data with a line, the slope is the growth rate constant. For example, AFRED3 does not begin growing until day 1, so data were graphed from day 1 to day 4, when it begins to level off. The growth rate constant for each run is shown in Table 3 below.

Table 3. Growth Rate Constants for experiments AFRED2-8

	Growth Rate Constant (day^{-1})
AFRED2	0.62
AFRED3	1.10
AFRED4	0.95
AFRED5	0.96
AFRED6	0.78
AFRED7	1.48
AFRED8	1.43

All experiments in the 1-liter reactor showed a growth rate constant that are of the same magnitude. It is difficult to directly compare growth rates since only a few data points were used in the analysis. However, it is important to note that the optical density leveled off at different values although there is not a clear connection to the redox data.

With regards to redox levels, an interesting observation is that AFRED3 and AFRED4 redox potentials continued dropping lower and then went back up to the same level (approximately -200 mV) as the other redox levels The drop coincided with a delay in the cell growth since the cells did not grow at all during the first day. When the cells started growing, the redox level went back up to approximately the same level as the redox levels of those with no lag time. AFRED5 dropped down as well, coinciding with delayed growth, and then started to return to the level of the other experiments when

growth began, but, instead of reaching -200 mV, AFRED5 dropped back down again. Perhaps the controller was acting up at time periods during the run such that the data is hard to fully understand. It is unclear why this behavior occurred, however, it is clear AFRED5 did not experience optimal growth and had the lowest peak OD level.

AFRED2, AFRED6, AFRED7 and AFRED8 experienced immediate growth, and their redox level did not drop nearly as low. On Day 2, it is noted that 5 of the 7 experiments (except AFRED 5 and 8) showed redox levels around -200 mV SHE. AFRED 8 eventually reached -200 mV SHE on Day 4. Therefore, cells appear to most optimally grow around -200 mV SHE. A representation of the above effects is shown for AFRED2 and AFRED 4 in Figure 25.

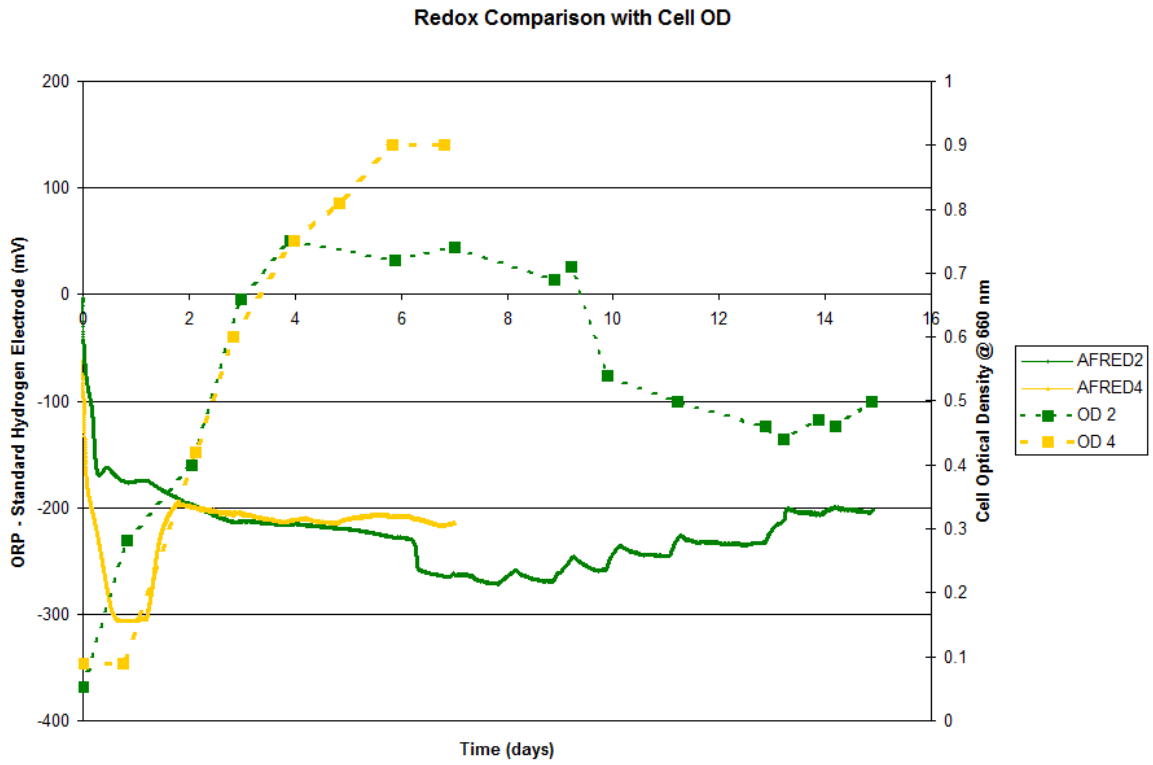

Figure 25. Redox comparison of a no lag-time run (AFRED 2) with that of a 1 day lag-time run (AFRED4)

Acetogenesis to solventogenesis switch

The acetic acid and ethanol concentrations in comparison to the redox level for all runs are shown in Figure 26 and Figure 27, respectively. It is interesting to note that there was a decrease in the redox level that coincided with the switch of acetic acid formation to ethanol formation. The peak of the acetic acid concentration coincided with a large drop of the redox level in the solution. After this point, the acetic acid concentration decreased (likely being converted back into ethanol). In addition the ethanol production ramped up as the redox level dropped. Perhaps this drop in redox level is a significant factor in the switch from acid to ethanol although the data cannot assess this question.

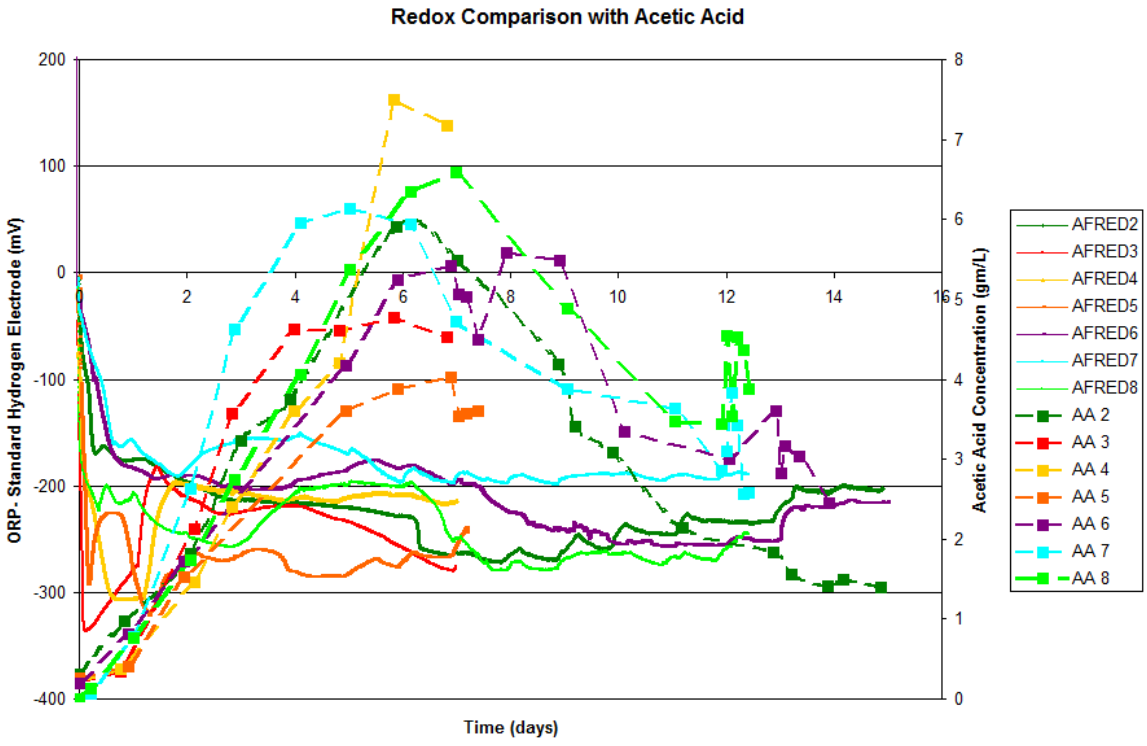

Figure 26. Acetic acid concentrations in comparison to the redox levels for all runs

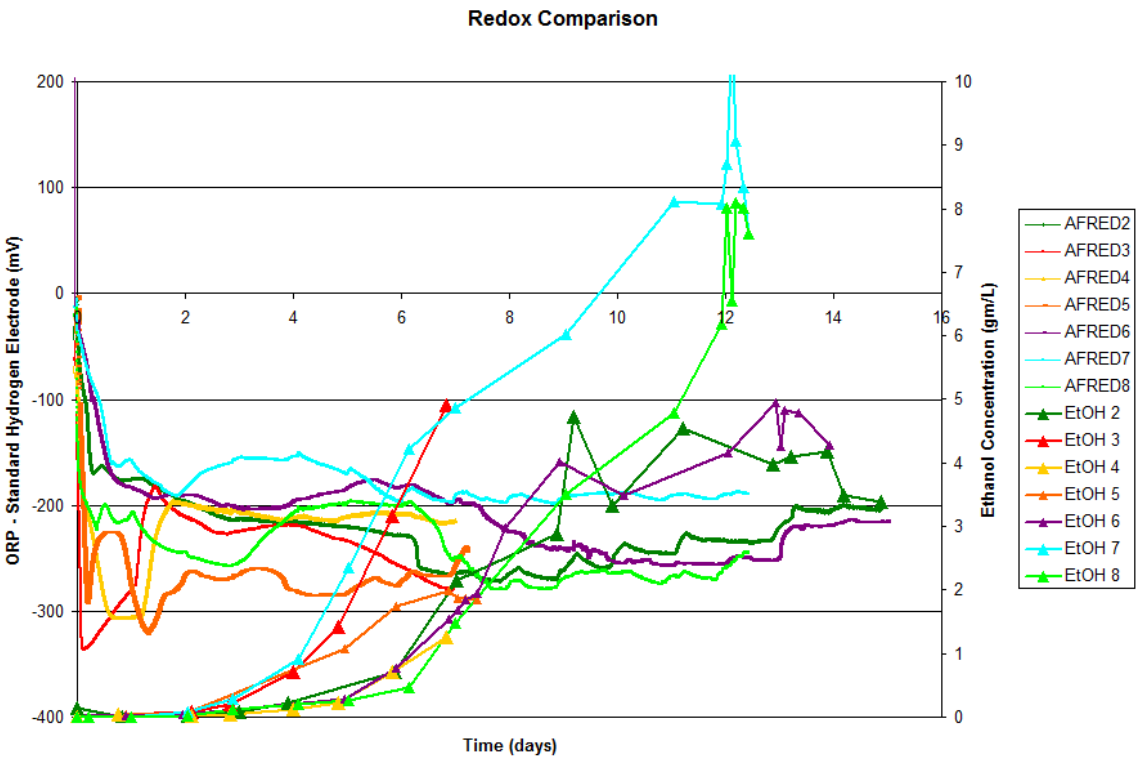

Figure 27. Ethanol concentrations in comparison to the redox levels for all runs

In three of the runs (AFRED 3, 5 & 7) the onset of ethanol production happened around day 4, almost 2 days earlier than other runs. For AFRED 3 and 7, the drop in redox level corresponded to the onset of ethanol production and the peak of acetic acid production as shown in Figure 28. AFRED5 showed a different behavior and will be discussed later.

The idea of the acetogenesis to solventogenesis switch coinciding with the drop in redox level is reaffirmed with a graph of the redox history vs. the pH. As shown in Figure 29, the pH level bottomed out right before the redox level began to drop.

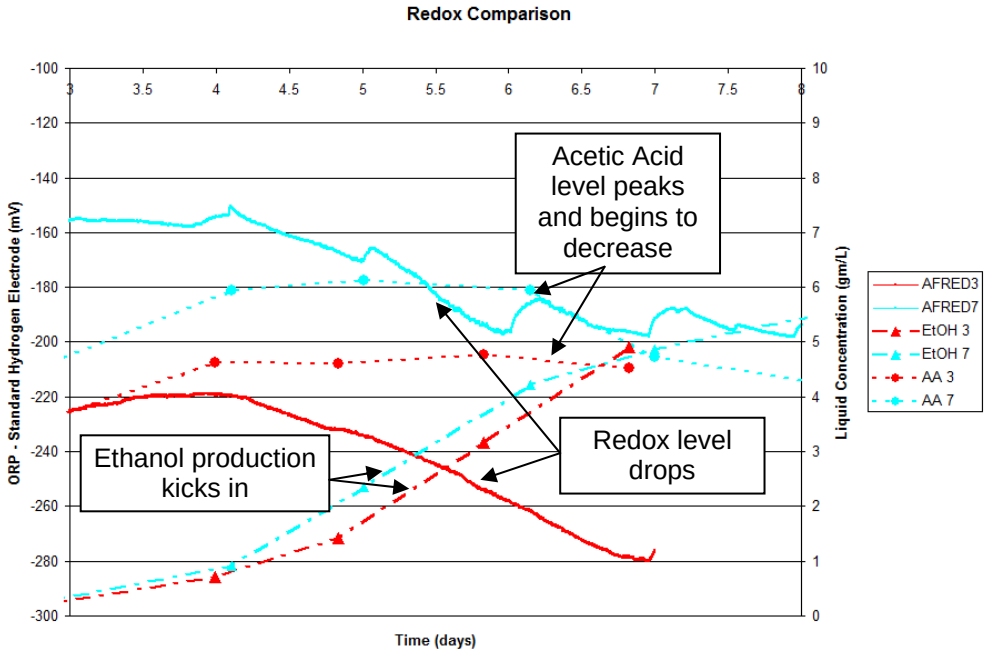

Figure 28. Redox comparison between the earlier onset of ethanol production profiles (AFRED3 and AFRED7) along with their acid and solvent concentrations

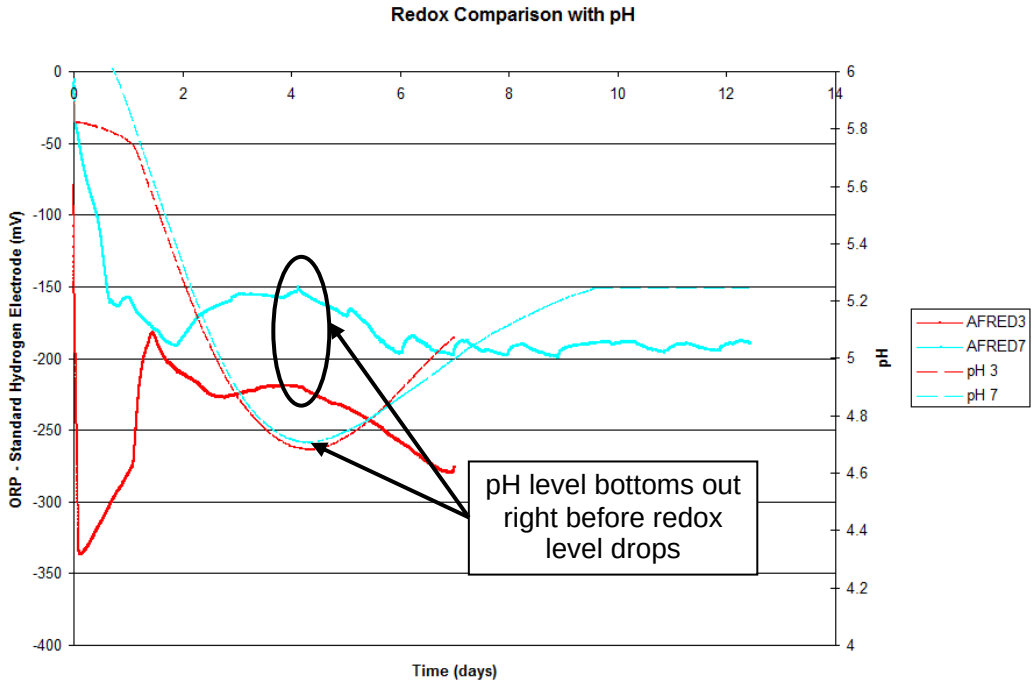

Figure 29. Redox comparison between the earlier onset of ethanol production profiles (AFRED3 and AFRED7) along with their pH

Although occurring around day 6 instead of day 4, the same drop in redox level corresponded to the onset of ethanol production and the peak of acetic acid production as seen for AFRED2, AFRED6 and AFRED8 (see Figure 30).

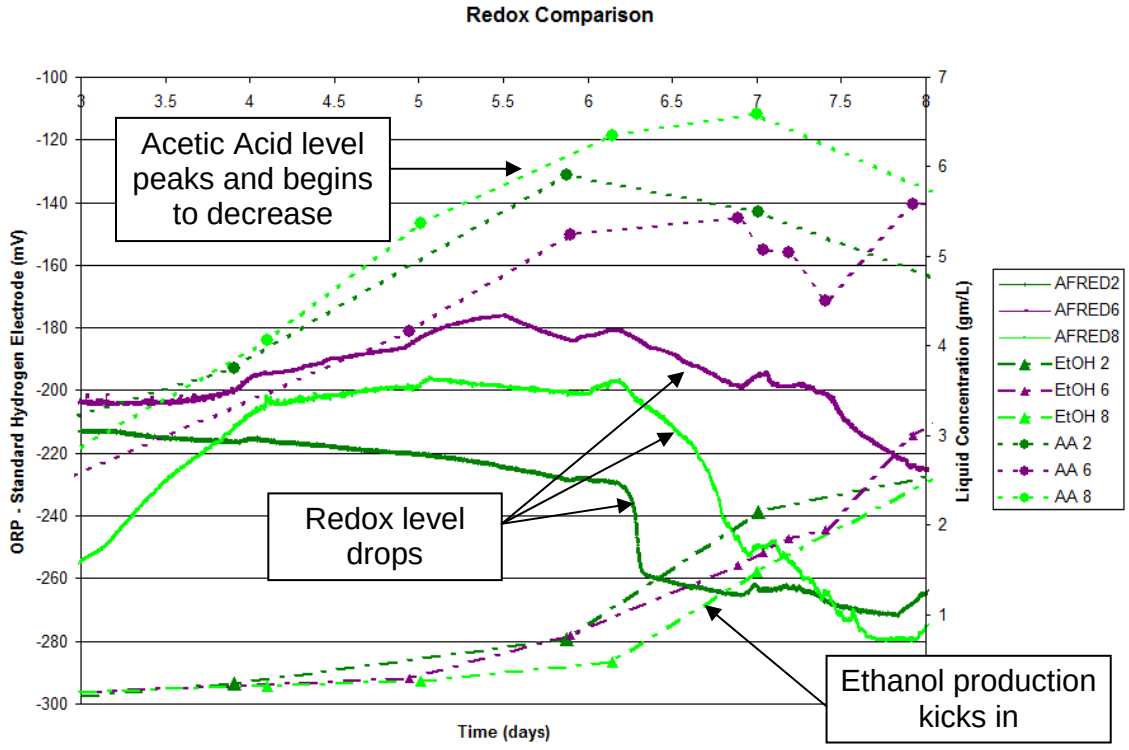

Figure 30. Redox comparison between the later onset of ethanol production profiles (AFRED2, AFRED6 and AFRED8) along with their acid and solvent concentrations

Once again, the acetogenesis to solventogenesis switch coinciding with a drop in the redox level was reaffirmed with a graph of the redox history vs. pH. As shown in Figure 31 below, the pH level bottomed out right before the redox level dropped.

In AFRED4, no large drop in redox level was observed and the ethanol production hadn't fully kicked in when the run was halted due to the syngas tank running out. Therefore, it is unclear if the redox would have dropped and ethanol production increased if allowed to run further (see Figure 32).

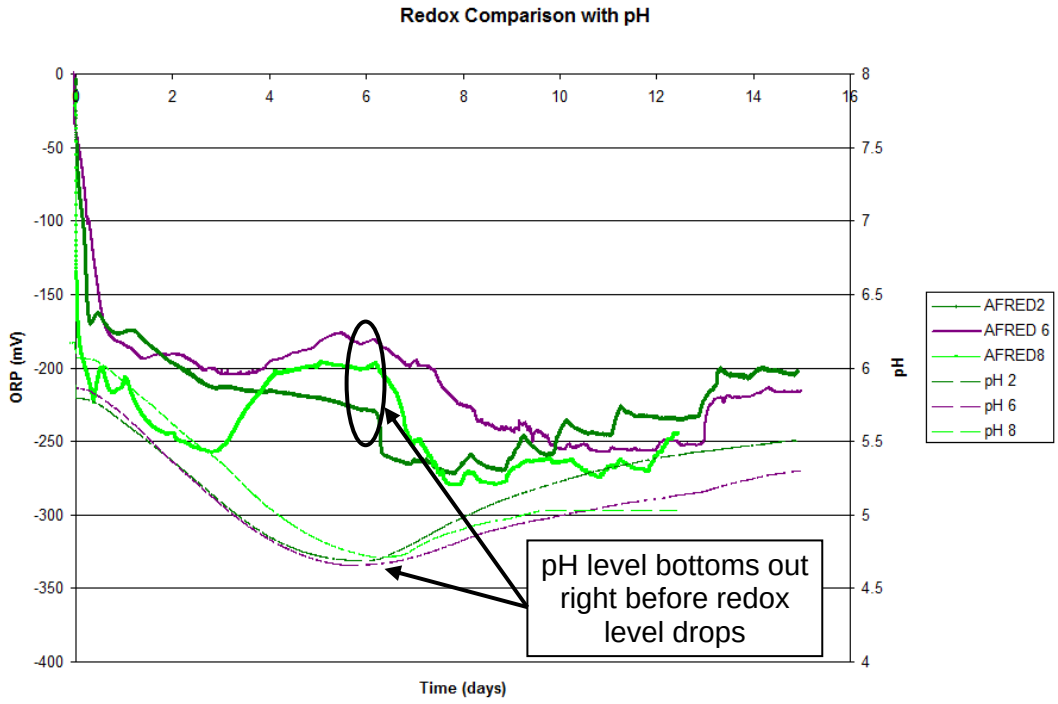

Figure 31. Redox comparison between the later onset of ethanol production profiles (AFRED2, AFRED6 and AFRED8) along with their pH

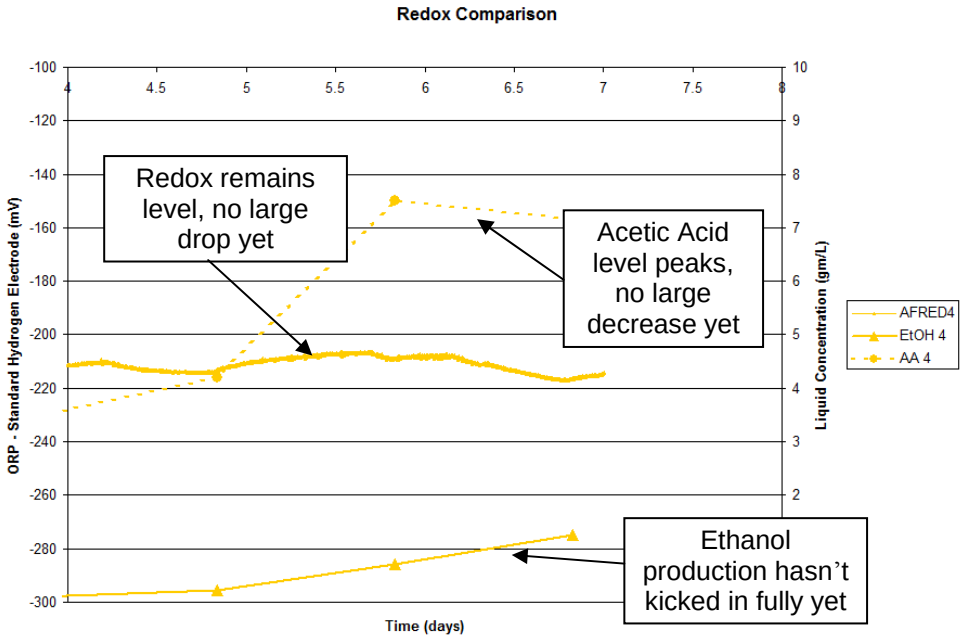

Figure 32. Redox for AFRED4 which exhibited no large redox level drop and ethanol production hadn't kicked in before run was stopped due to syngas tank running out

AFRED5's redox also remained level, with no large drop. However, the redox level was already low relative to the other experiments, and was in the optimal ethanol range (~-250 mV) observed in the other runs. Ethanol production did kick in, although still somewhat sluggish in comparison to the others (see Figure 33). It is unclear what would have happened if allowed to run to completion. However, the controller failed and the experiment was stopped.

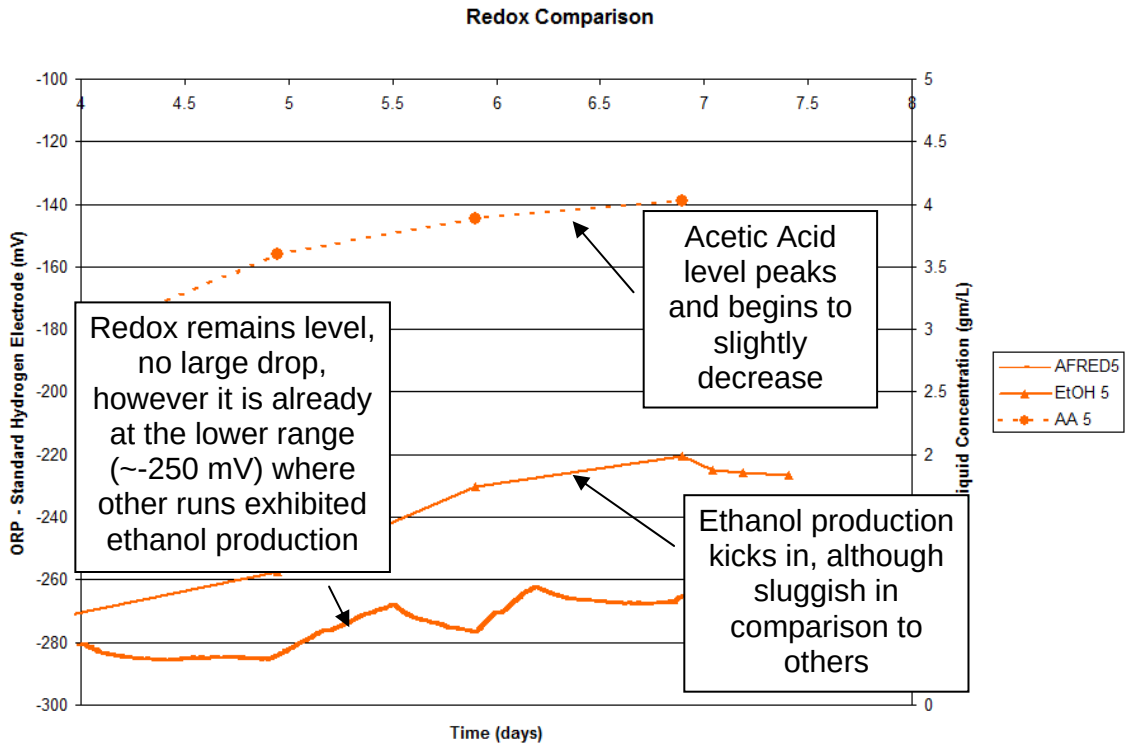

Figure 33. Redox for AFRED5 which exhibited no large redox level drop however, ethanol production did kick in, run was stopped due to technical failure of controller

To quantify the redox drop more accurately, the change in ethanol from the beginning of ethanol production, as well as the change in redox level from the beginning of ethanol production, was plotted in Figure 34 and Figure 35.

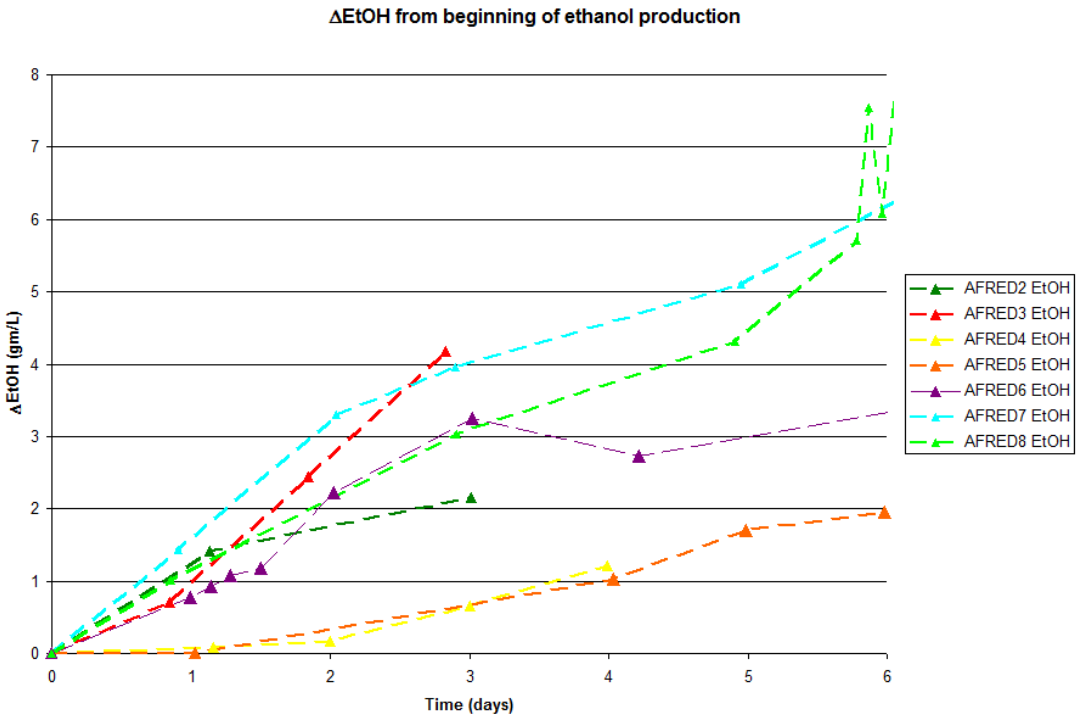

Figure 34. The change in ethanol from the beginning of ethanol production vs. time

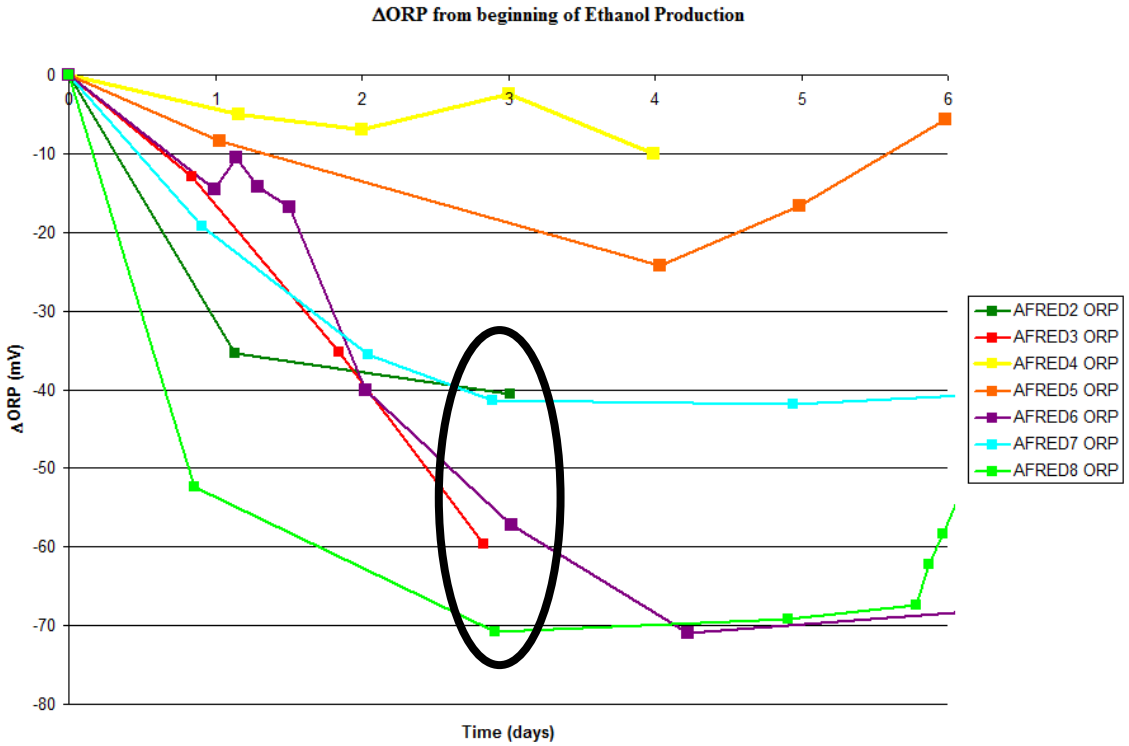

Figure 35. The change in redox level from the beginning of ethanol production vs. time

As shown in Figure 35 once ethanol production began, the redox level dropped anywhere from 40-70 mV. In AFRED 4 and AFRED5, where ethanol production was minimal, the redox level did not drop anywhere in the same range.

To verify that these relative redox levels were due to a phenomenon in the culture media and not only to the changing acetic acid and ethanol concentrations, an experiment (denoted additive experiment) was run in which media was autoclaved in the 1-liter reactor and then acetic acid and ethanol were added to the reactors to mimic the liquid concentrations observed in an actual run (AFRED2). For example, AFRED 2 had 0.01 g/L ethanol and 1.81 g/L acetic acid at time 2 days. Therefore, 0.01 g/L ethanol and 1.81 g/L acetic acid were added to the reactor and the redox level was recorded (denoted as $RL_{match,0}$). Ethanol and acetic acid concentrations were then added to the experimental reactor, at concentrations shown in Figure 36, to mimic similar increases in ethanol and acetic acid concentrations observed with AFRED2 from Day 2 until Day 6. The redox level at each of these additions was measured and $RL_{match,0}$ was subtracted from the measured redox level to show the net change in redox level relative to the initial ethanol and acetic acid concentrations. The net change in redox level was then compared to the net change in redox level observed with AFRED2 (relative to Day 2). The results are shown in Figure 36.

After the first addition, where the ethanol did not change much but the acetic acid increased, the additive experiment showed that the redox level substantially became more positive whereas the redox level became more negative for AFRED2. Following the 2nd addition, where the ethanol was increased slightly and the acetic acid was significantly increased, the additive experiment again showed the redox level substantially becoming

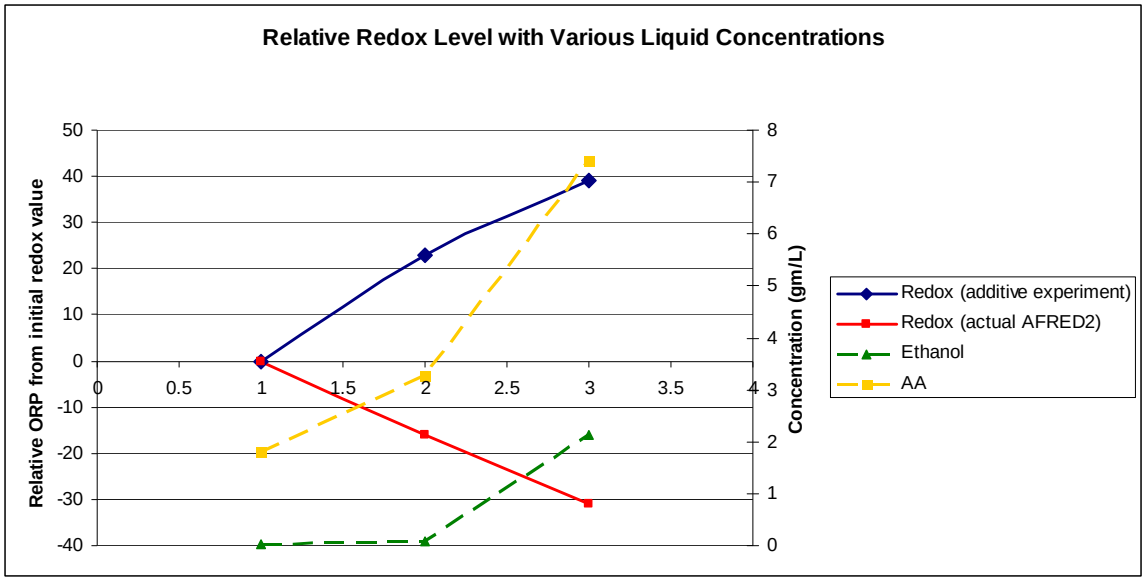

Figure 36. Relative redox levels with various liquid concentrations at the beginning of a run (increasing acetic acid, increasing ethanol)

more positive whereas the redox level became more negative with AFRED2. Since ethanol is a reduced form of acetic acid, the additive experiment is consistent with acetic acid making the redox level more positive. However, the redox level changes with the additive experiment were opposite the redox level changes observed with AFRED2. Therefore, it is clear that the observed changes in the redox levels are not merely a result in the change in acetic acid and ethanol concentrations being produced by the cells, but rather due to some other components generated or consumed in the cellular environment. As noted in Chapter 3, the partial pressures of gas constituents are likely not a contributor, especially since the gas partial pressures remained essentially constant during the process due to the continuous flow of gas.

Additional evidence that the observed changes in the redox level are not merely a result of the change in liquid concentration, is shown by observing the redox levels of

AFRED2 shown in Figure 23. Around day 6 there is a sharp decrease in the redox level of the experiment, but the corresponding change in ethanol concentration at that time was very minimal. Additionally, another experiment was run in which ethanol was increased by 2 g/L, while acetic acid was constant, which resulted in a redox decrease of 10 mV. However, in AFRED2 over the first four days after the onset of ethanol production (3 g/L produced) the redox showed a drop of approximately 50 mV. Furthermore, during the oscillations in the redox in the latter portion of the run, the redox level did not correspond with *large* overall concentration changes in acetic acid or ethanol.

On a final note, these oscillations that were observed in redox levels in the latter portions of many runs (see Figure 37) could indicate the cells are alternating production of acetic acid and ethanol. Oscillating behavior between acetogenesis and solventogenesis has been observed in another study involving *Clostridium acetobutylicum* on lactose (Kim, Bajapai et al. 1988). This oscillating behavior and its connection to the acetic acid and ethanol concentration need further exploration.

Conclusions & Future Work

When cells are first inoculated, the redox level begins dropping and for optimal growth, it levels off at ~ -200 mV, at which point, although still dropping, drops at a much slower rate. When cells have a lag phase where no growth is experienced, redox continues dropping until the growth begins, at which point, the redox will ideally return to the -200 mV level. When redox levels remain more negative than -200 mV, growth is experienced at a slower rate and the final optical density is lower. Therefore, it is clear that cells most optimally grow at approximately -200 mV.

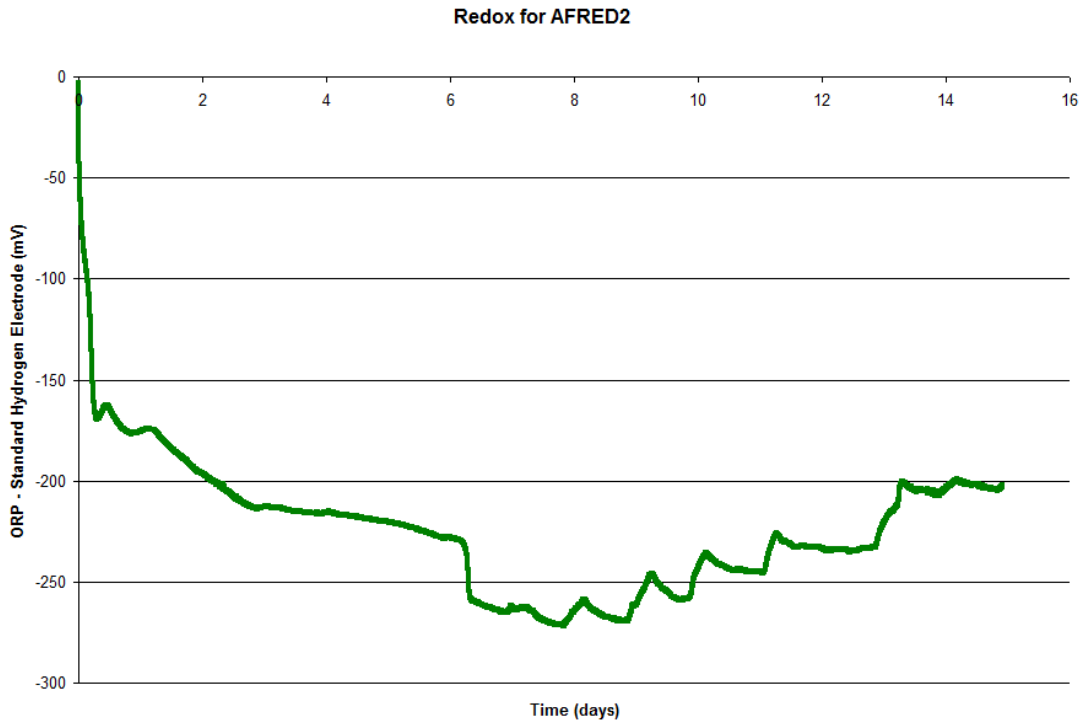

Figure 37. AFRED2 redox history

In addition, cells switch from acetic acid to ethanol production after a drop of ~40-70 mV in the redox level. Earlier work done on *Clostridium acetobutylicum* (Kim, Bajapai et al. 1988; Kim and Kim 1988) saw optimal acetogenesis between -225 and -275 mV, and optimal solventogenesis between -300 and -350 mV (a 75mV drop in redox level). Although the redox values are different than those observed in this study, the redox drop is similar. However, none of the studies above deal with the fermentation of syngas by the bacterium.

Now that a general redox history for the bacterial cells has been obtained, it is important to find out whether manipulating the redox levels can manipulate the production of acetic acid (and cell growth) and ethanol. In addition, whether cells are

oscillating production of acetic acid and ethanol is still unclear. Possible future experiments include:

- An experiment where liquid samples are taken more often than once daily to determine if the production of acetic acid and ethanol is really oscillating.
- If it is found that the production of acetic acid and ethanol is oscillating, the redox can be controlled at the level when ethanol is being produced to determine if controlling the redox level prevents the oscillations and maintains production of ethanol.
- An additional experiment to see if maintaining the redox level at -200 mV can induce cells to grow to higher optical density before leveling off.
- And finally, an experiment to determine if dropping the redox level by ~ -40-70mV earlier on in the experiment can induce ethanol production at an earlier time.

Chapter 5 – Pressure and Mass Transfer Effects

Syngas fermentations were carried out in three different reactor sizes. A 50 mL septum bottle (50 mL liquid, 200 mL gas), a 100 mL septum bottle (100 mL liquid, 150 mL gas), and a 1 liter reactor (1 liter liquid, 2 liters gas). Both the 50 mL bottle and the 100 mL bottle are purged with syngas (40% CO, 30% H_2, 30% CO_2) every other day (unless otherwise state) and pressurized to 20 psig. The 1 Liter reactor runs at atmospheric pressure, but has a continuous syngas feed.

Growth differences have been observed between the different liquid volumes of reactors. As shown in Figure 38 below, preliminary experiments showed that the 1 liter reactor and 50 mL bottle show a much higher growth rate than the 100 mL bottle growth rates with the same vol% of inoculum. The objective of this research was limited to focusing on the cell growth differences in the 50 mL and 100 mL bottles. The hypothesis was that partial pressure and/or mass transfer issues caused the observational differences in cell growth between 50 mL and 100 mL bottles. In addition, the CO partial pressure effect on ethanol production was explored.

This hypothesis was assessed using 50-mL septum bottles placed in a shaking incubator. Cell cultures were grown up on 30% H_2, 30% CO_2 and 40% CO (the standard syngas composition) with the temperature controlled at 37^{o}C inside the shaking incubator. Several experiments were run which compared three bottles of 50 mL liquid with three bottles of 100 mL liquid in bottles containing a total volume of 250 mL.

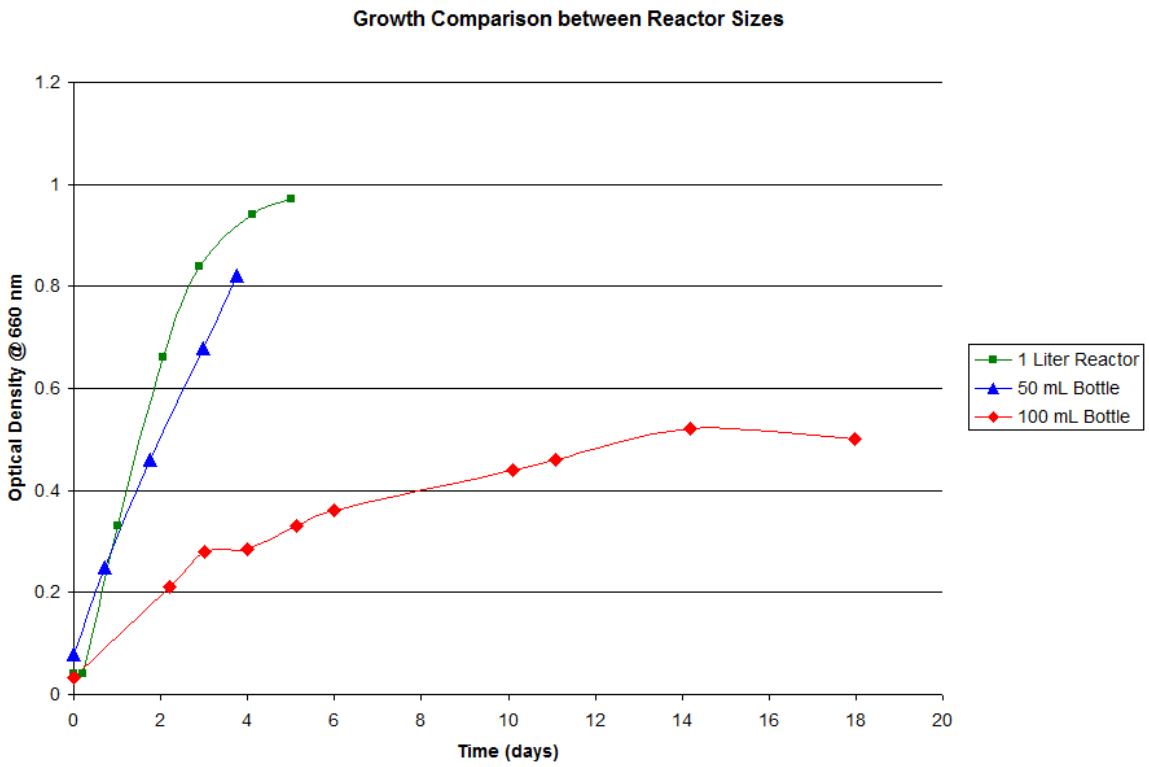

Figure 38. Growth comparison between 50 mL bottle, 100 mL bottle, and 1 Liter bioreactor

The mass transfer in the 50 mL bottles and in the 100 mL bottles was also measured using a micro dissolved oxygen probe to obtain an accurate mass transfer coefficient to determine if mass transfer was the reason for the differing growth rates observed in preliminary experiments.

Finally an experiment was run to determine if the partial pressure of CO had an effect on the production of ethanol. Nine 100 mL bottles were grown up (regassing every other day with standard 30% H_2, 30% CO_2 and 40% CO mixture, liquid samples every other day). Once ethanol production had begun and an ethanol production slope could be calculated from the data, three of the bottles were switched to a higher CO concentration (60% CO, 30% H_2, 10% CO_2) and three of the bottles were switched to a lower CO

concentration (20% CO, 30% H_2, and 50% CO_2) and the effect on ethanol production was determined.

Methods

Bottle studies

Bottle studies were performed in a 250 mL (total volume) septum bottle sealed with a #1 rubber stopper and a metal cap (Wheaton #224187-01) to ensure the rubber stopper stayed in place under pressure. Media were prepared (see Chapter 3 for details) and added to the bottle (media volume varied between 50 mL or 100 mL depending on the experiment). Bottles were boiled and sparged with nitrogen for 4 minutes. After they were sparged with nitrogen on the hotplate, the headspace was vacuumed and purged with nitrogen for three cycles (-20 psig to 20 psig). Cysteine sulfide was then added and the bottles were autoclaved (15 minute sterilization and 5 minute dry time at 121^{o}C). Bottles were then brought to 37^{o}C, pressurized up to ~20 psig with the appropriate syngas composition, and inoculated with a 10% vol innoculum of bacterium.

Gas composition

Gas samples were taken using a VICI precision sampling 1 mL gas-tight syringe. To determine the gas composition, the gas sample was then injected into a Shimadzu Gas Chromatograph 2014 equipped with a fused silica capillary column 30m x 0.53 (Shimadzu, #35136-02B) and a thermal conductivity detector. Argon was used as a carrier gas at 40 cm/s.

Gas pressure

The total pressure in the head space of each bottle was measured using a high accuracy digital pressure gauge (Cole Parmer #K-68920-34) connected to a needle. At specific times during the experiment, the needle (with the gauge) was inserted into the bottle to measure the pressure and then the needle and gauge were removed to minimize the potential loss of gas during the experiment. During each measurement, a new needle was used to ensure sterility and to minimize the breakage of the needle.

Results and Discussion

Growth in 50 mL vs. 100 mL bottles

An experiment was run in which three 50 mL bottles were compared to three 100 mL bottles. Cell cultures were grown up on 30% H_2, 30% CO_2 and 40% CO (the standard syngas composition) with the temperature controlled at 37^{o}C inside the shaking incubator rotating at 100 rpm. Liquid samples were taken every other day and the bottles were re-gassed after every liquid sample.

The optical density profile is shown in Figure 39. Initially, both the 50 mL and 100 mL grew up quite fast, and close to the same rate (although the 50 mL culture was growing at a faster rate). At day 2, the growth rates of both the 50 mL and the 100 mL cultures slowed down, however, the 100 mL culture slowed down to nearly half the rate of the 50 mL.

Between day 4 and 6, there was an observed decrease in the 50 mL optical density. Similarly, between day 8 and 10 this same decrease was observed in the 100 mL bottles. The cause of this observed decrease in the optical density is something that is

seen often in these bottle experiments and warrants further experimentation, although it is out of scope of the current research. Possibilities for the decrease include sporulation, nutrient consumption, pH changes, and product formation since the liquid is never replaced. However, this part of the work only assessed the first few days of growth.

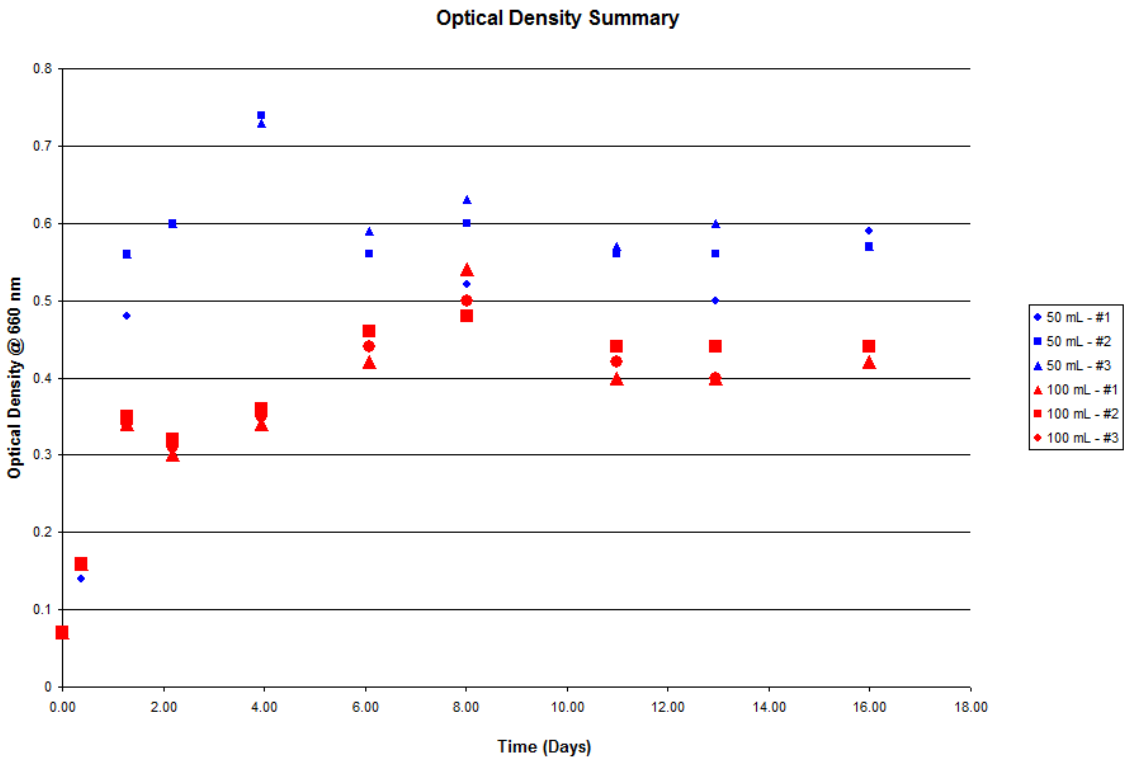

Figure 39. Optical Density summary for 50 mL vs. 100 mL bottles in a normal run

The growth rates are shown in Table 4 (calculations for growth rate are explained in Chapter 4 in detail). Growth rates were calculated during the exponential growth phase, days 0-4 for the 50 mL bottles and days 0-8 for the 100 mL bottles. The 50 mL bottles have nearly double the growth rate than the 100 mL bottles in the latter stages of growth. The liquid concentrations for these bottles are shown in Figure 40.

.

Table 4. Bacterial growth rate for 50 mL vs. 100 mL septum bottles

Run	50 mL (day 0-1)	50 mL (day 1-4)	100 mL (day 0-2)	100 mL (day 2-8)
1	1.59 day^{-1}	0.16 day^{-1}	1.17 day^{-1}	0.08 day^{-1}
2	1.48 day^{-1}	0.10 day^{-1}	1.17 day^{-1}	0.07 day^{-1}
3	1.59 day^{-1}	0.11 day^{-1}	1.19 day^{-1}	0.06 day^{-1}
Average	***1.55 day^{-1}***	***0.12 day^{-1}***	***1.18 day^{-1}***	***0.07 day^{-1}***

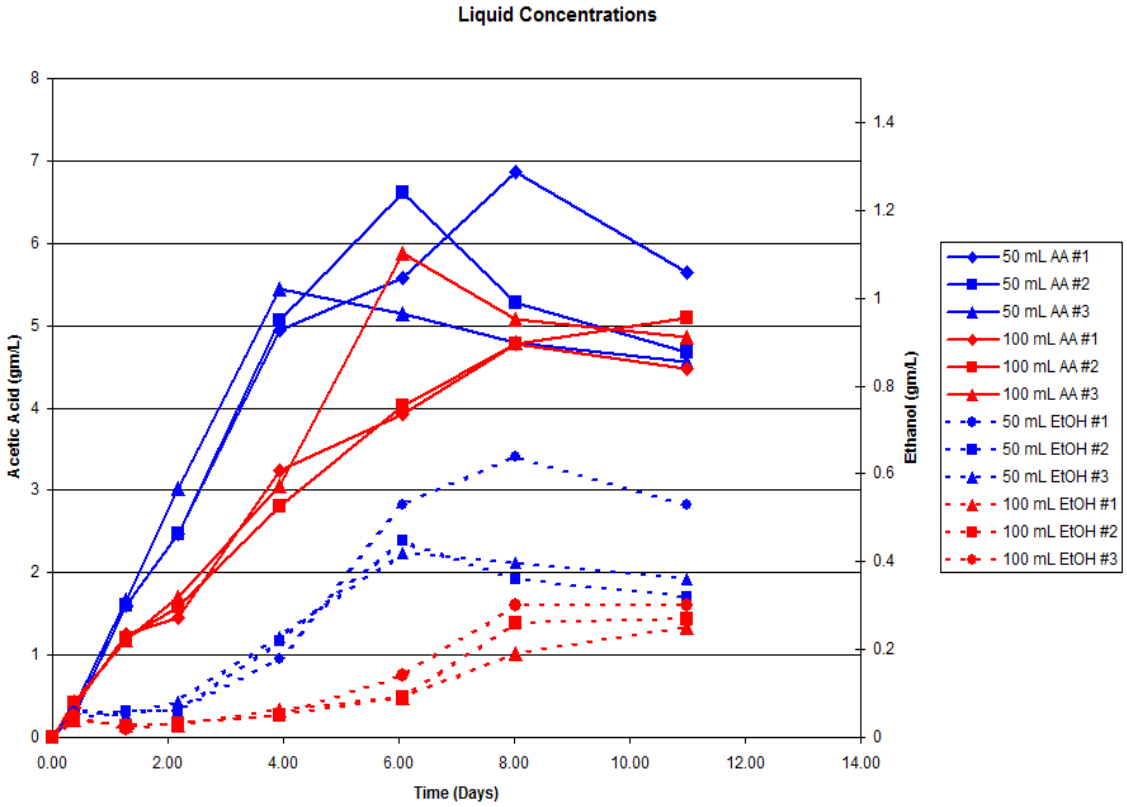

Figure 40. Liquid concentrations for 50 mL vs. 100 mL cultures

The acetic acid profile follows the same trend as the optical density (higher acetic acid formation rate in 50 mL cultures compared to 100 mL cultures) because acetic acid production is tightly linked to the growth of the cells. This is because the acetic acid pathway also produces ATP, the cells source of energy, which is necessary for cell

growth and division. It should be noted that although the rate was faster with the 50 ml cultures, the final acetic acid concentrations for both cultures were close to the same level.

The ethanol production began three days earlier in the 50 mL than in the 100 mL cultures. The beginning of the ethanol production is simultaneous to the peaking of the acetic acid production. Since the acetic acid peaked at slightly different concentration levels in the 100 mL (average of 5.3 gm/L) and the 50 mL bottles (average of 6.3 gm/L), the acetic acid concentration alone does not seem to cause the switch from acetogenesis to solventogenesis. Chapter 4 showed that the peak in acetic acid corresponded with a 40-70 mV drop in the solution redox level, which coincided with ethanol production.

Partial pressure

The next experiment was to assess the effects of partial pressure and gas uptake rates on 50 mL and 100 mL bottles. There were three bottles of 50 mL liquid and three bottles of 100 mL liquid grown up on the standard syngas composition (on 30% H_2, 30% CO_2 and 40% CO) and the headspace composition was monitored. Liquid and gas samples were taken once a day. The gas samples included overall pressure in the bottle, as well as the percentage of each gas in the bottle. The bottles were re-gassed every other day. This is the same experimental setup as used for the results shown above, except gas samples were also taken, whereas above, only liquid samples were taken. The optical density profile (growth) is shown in Figure 41.

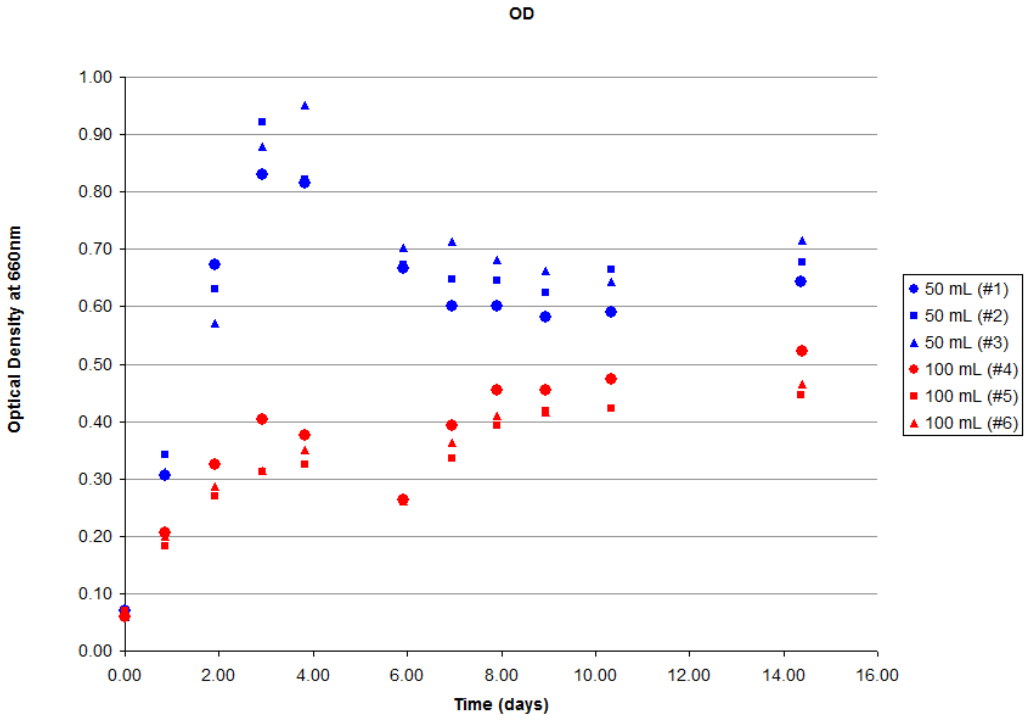

Figure 41. Growth profile for 50 mL vs. 100 mL experiment while monitoring headspace gas pressure and composition

It is interesting to note, that once again the 50 mL and the 100 mL cultures grew up faster in the first two days, although in this experiment the 50 mL was significantly faster than the 100 mL in both categories (see Table 5 and compare with Table 4). There is a large dip at day 6 where all three 100 mL bottles have nearly the exact same OD, this curious phenomenon is attributed to an experimental error, and most likely did not in actuality dip down so low.

Table 5. Growth rates for 50 mL vs. 100 mL experiment while monitoring gas pressure and composition

Run	50 mL (day 0-1)	50 mL (day 1-3)	100 mL (day 0-2)	100 mL (day 2-10)
1	1.7 day^{-1}	0.49 day^{-1}	0.69 day^{-1}	0.04 day^{-1}
2	2.0 day^{-1}	0.48 day^{-1}	0.86 day^{-1}	0.05 day^{-1}
3	1.9 day^{-1}	0.50 day^{-1}	0.72 day^{-1}	0.05 day^{-1}
Average	***1.87 day^{-1}***	***0.49 day^{-1}***	***0.76 day^{-1}***	***0.05 day^{-1}***

The acetic acid and ethanol profiles are also as to be expected (see Figure 42). The acetic acid in the 50 mL bottles goes up higher than in the 100 mL bottles (producing more ATP, feeding the higher growth observed in the 50 mL bottles). More acetic acid is consistent with more cell mass being able to produce the acetic acid. In addition, the onset of ethanol production happens earlier in the 50 mL than in the 100 mL.

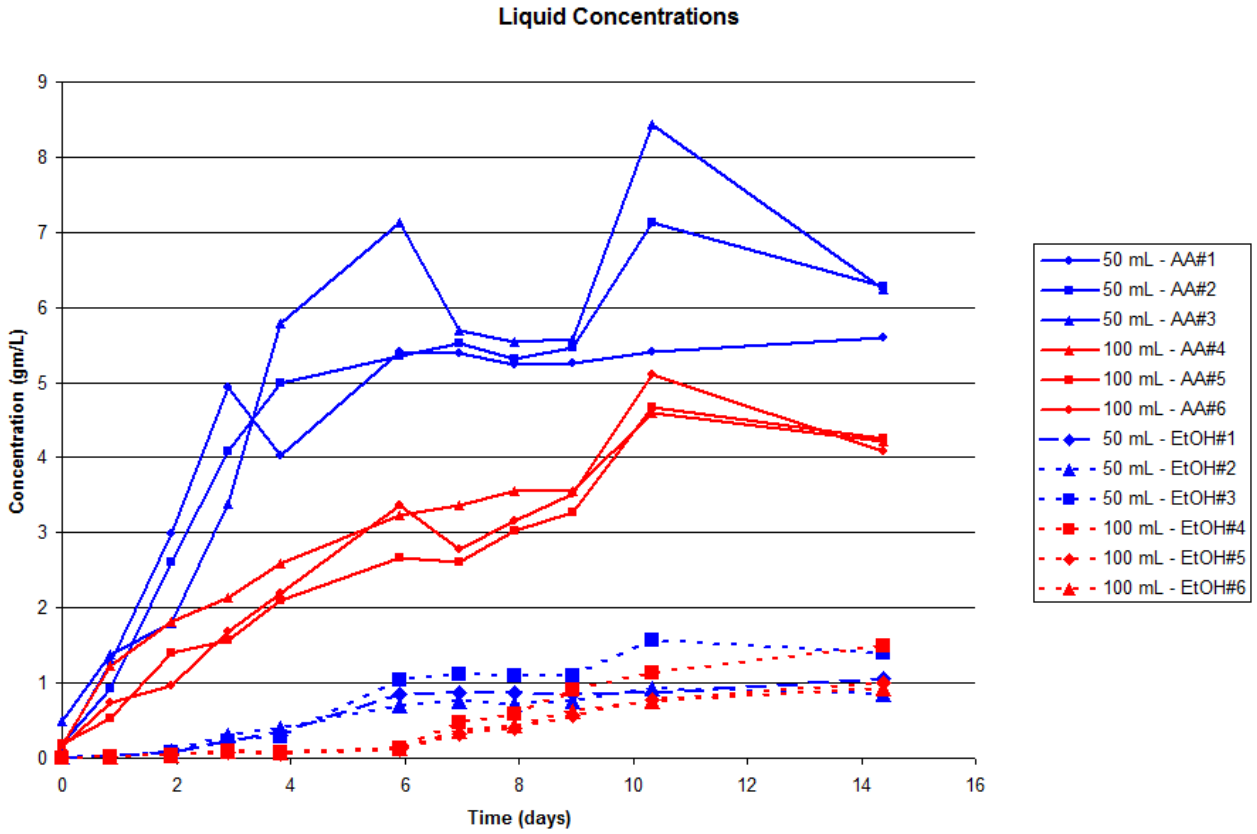

Figure 42. Liquid concentrations for 50 mL vs. 100 mL experiment while monitoring headspace gas pressure and composition

Similar trends in both the optical density profiles and liquid concentrations were observed in the earlier experiments shown in Figures 39 and 40. However, the pressure and gas composition throughout had never before been monitored. The pressure profiles

for the 50 mL vs. the 100 mL bottles are shown in Figure 43. The dotted lines simply help illustrate possible trends, and do not in any way demonstrate actual trends.

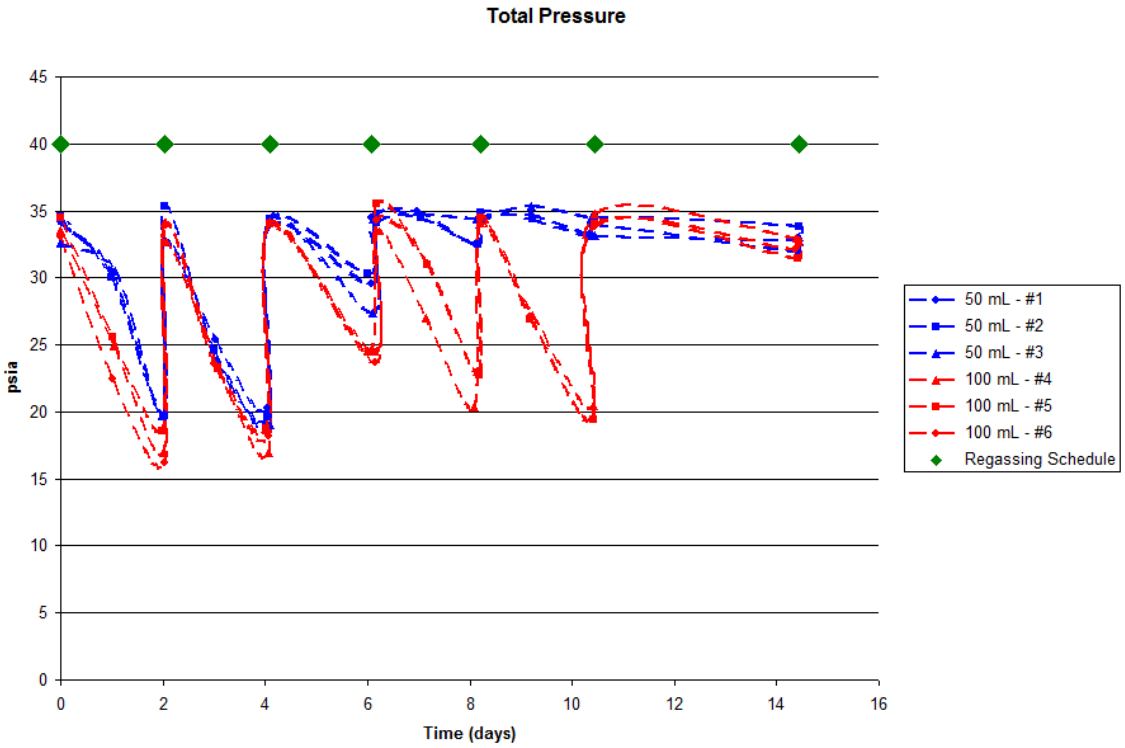

Figure 43. Total pressure profile for 50 mL vs. 100 mL experiment while monitoring headspace gas pressure and composition

The green diamonds represent when the bottles were re-gassed (approximately every two days). Initially, the pressure in both the 50 mL and the 100 mL bottles drop down around the same rate, although the 100 mL drops down to a slightly lower pressure (~17 psia) than the 50 mL bottles (19 psia). At about day 6, however, the pressure in the 50 mL drops less than in the 100 mL, while this trend is not seen in the 100 mL until much later (~day 11).

When pressure is plotted against acetic acid concentration (see Figure 44) the reason for this behavior becomes clear. The pressure decrease becomes less when the acetic acid begins to level off. At that point, the cells level off in their growth, and need

less carbon for cell building blocks, and in addition, the acetic acid level begins decreasing, indicating that the cells are using the acetic acid carbon to build ethanol.

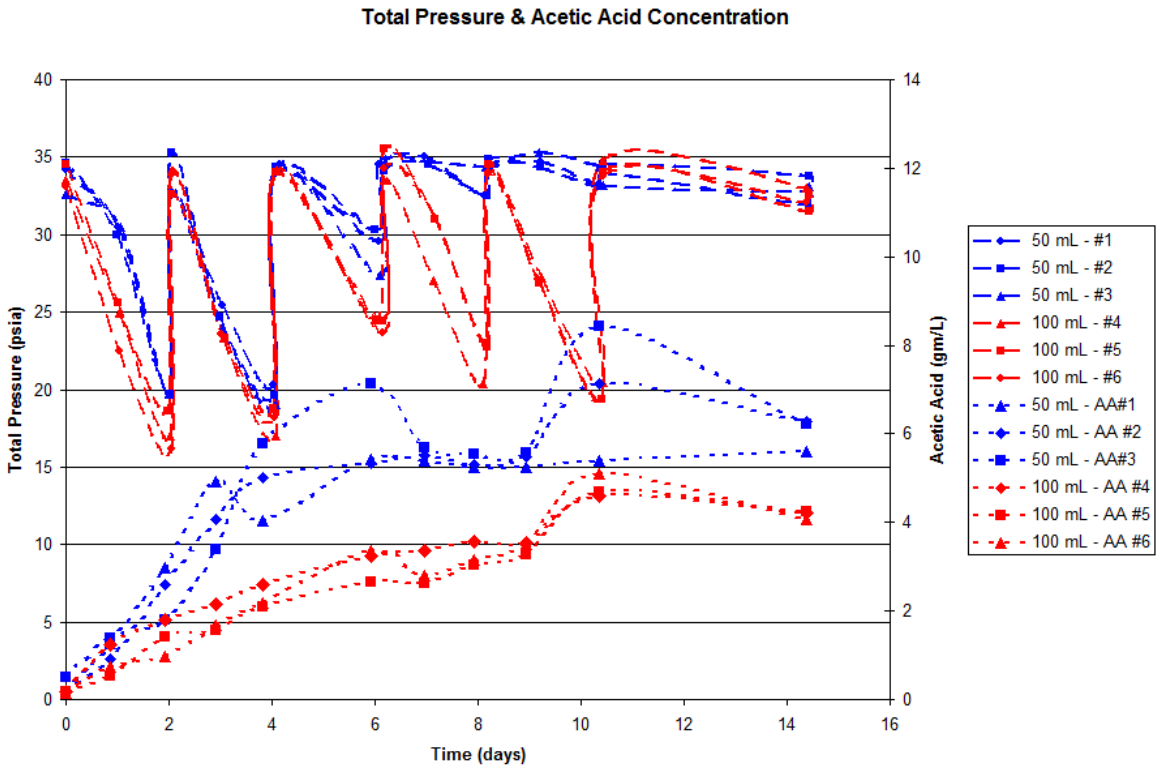

Figure 44. Total pressure and acetic acid concentrations for the 50 mL vs. 100 mL experiment while monitoring headspace gas pressure and composition

It was important to examine at what ratios the gasses were being consumed to help understand how the partial pressures were affecting the metabolism. The moles of the gas in reference to time were calculated using the ideal gas law (see Equation 8) the total pressure measured in the bottle and the gas composition from the gas sample according to:

$$n = \frac{PV}{RT}\%gas \tag{7}$$

where n is the number of moles, P is the total pressure measured in the bottle, V is the volume of gas in the bottle (changes as liquid samples are taken), R is the ideal gas constant (1206 psi mL K^{-1} mol^{-1}), T is the temperature, and %gas is the percentage of the gas in the sample. The moles of CO vs. time are shown in Figure 45.

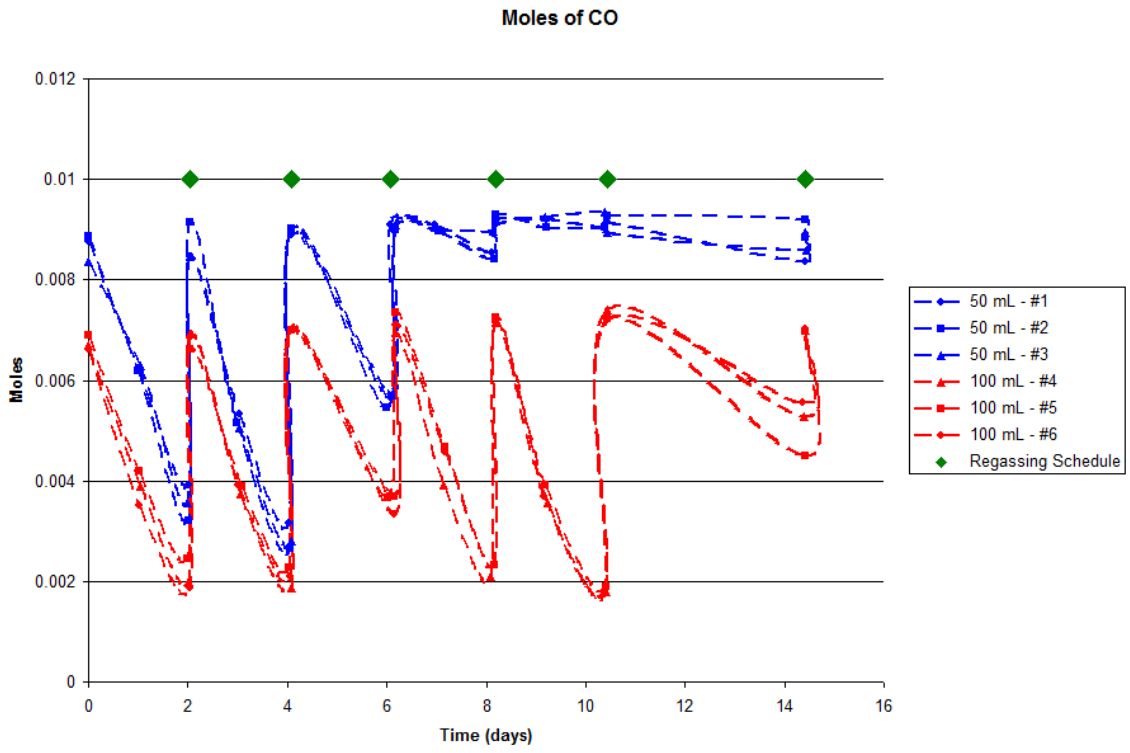

Figure 45. Moles of CO in the headspace for the 50 mL vs. 100 mL experiment while monitoring headspace gas pressure and composition

The moles of CO follow the same pattern as the total pressure shown in Figure 43. Although, the moles of CO in the 50 mL and the moles in the 100 mL drop down at the same rate, the moles of CO in the 50 mL start out higher and therefore become less depleted. The same pattern is seen for moles of H_2 in Figure 46.

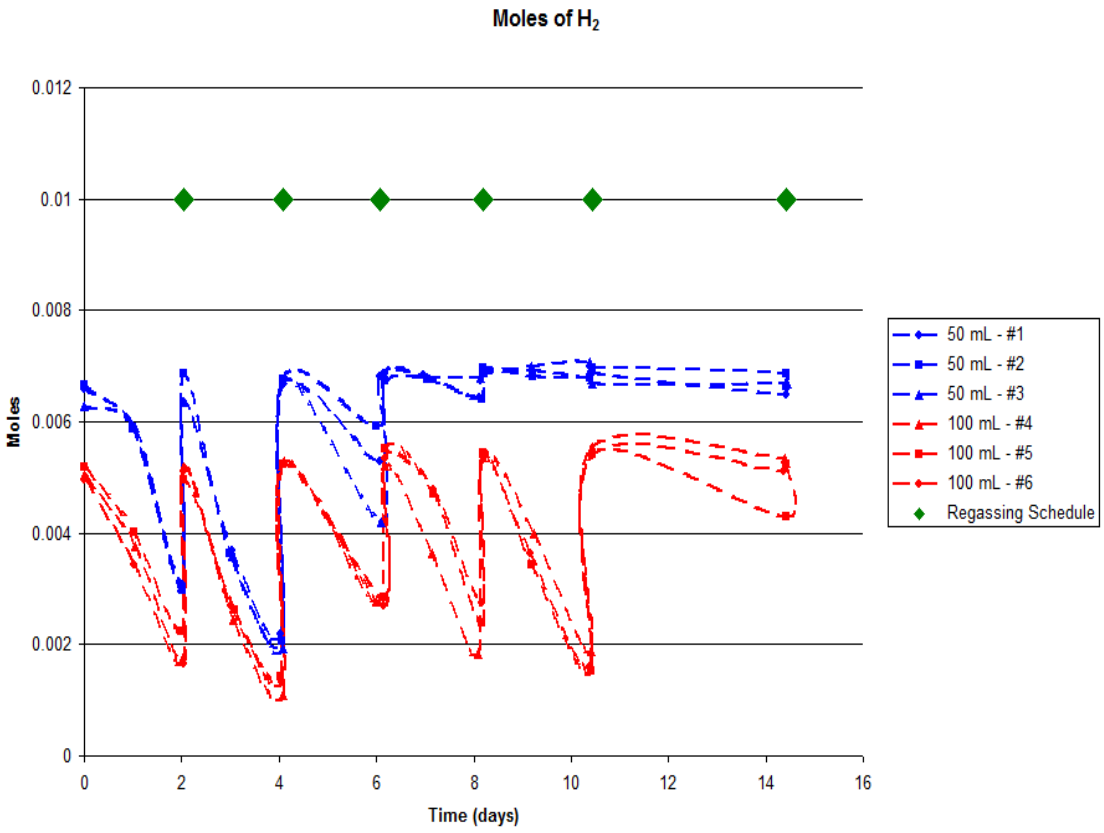

Figure 46. Moles of H_2 in the headspace for the 50 mL vs. 100 mL experiment while monitoring headspace gas pressure and composition

The CO_2 profile however is very different from CO or H_2, as shown in Figure 47. The net moles of CO_2 are initially consumed (although more CO_2 moles are consumed in the 100 mL than in the 50 mL), however, after day 2, net moles of CO_2 are *generated* instead of consumed. The CO_2 is generated from CO using the enzyme CODH (see Figure 4). One possibility for the observed differences in CO_2 is that the 50 mL bottles have more moles of CO available, thus the bacteria don't have to tap into the source of CO_2 as much as the bacteria in the 100 mL bottles.

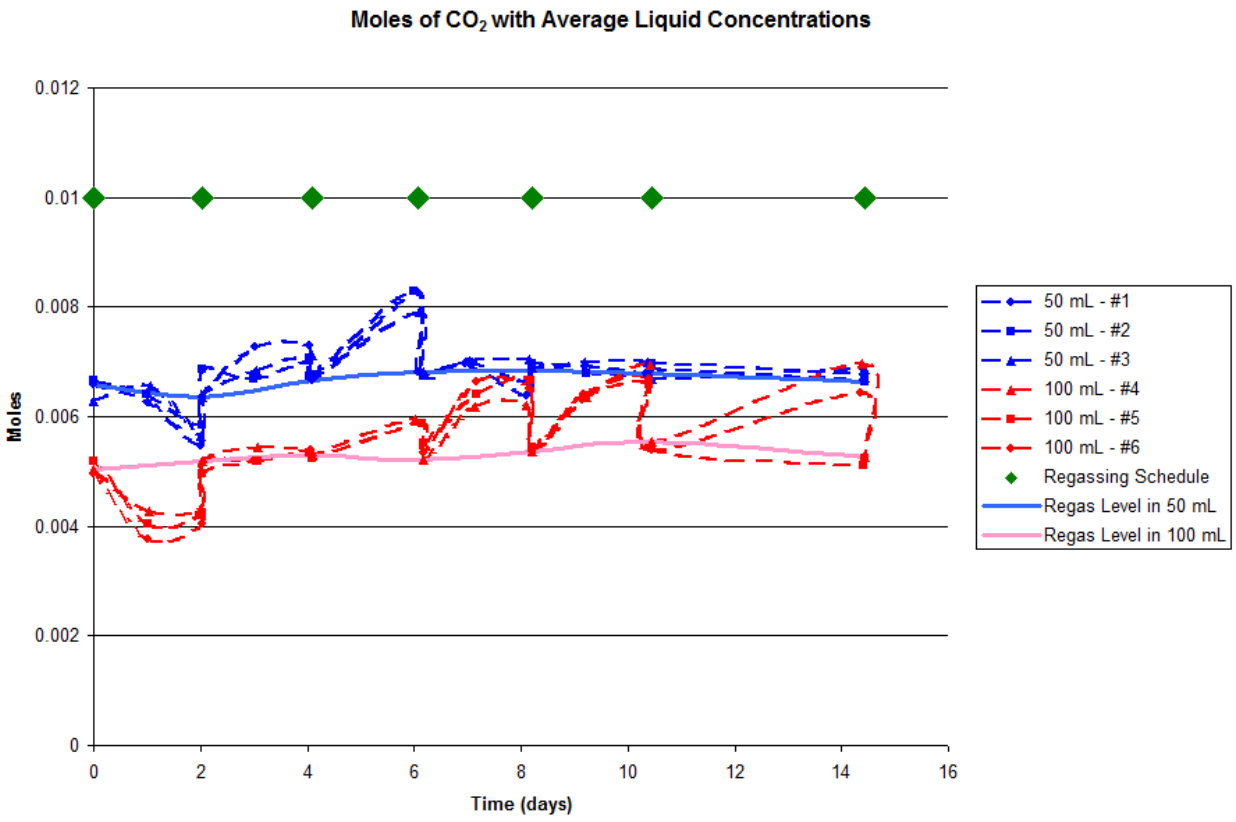

Figure 47. Moles of CO_2 in the headspace for the 50 mL vs. 100 mL experiment while monitoring headspace gas pressure and composition

To get a clearer picture, the moles of CO_2 are plotted on the same graph as average liquid concentrations (see Figure 48). Net moles of CO_2 are consumed initially, during growth. Once ethanol production begins, CO_2 is only produced, not consumed. However, this may not be the entire picture. Because the 50 mL and 100 mL bottles have not only different liquid volumes but also different optical densities, there is a different total amount of bacteria available to consume the moles of gas in the different bottles sizes. This was accounted for by dividing the moles of gas available by the total grams of bacteria in the liquid at that time (using liquid volume and optical density). The graph for moles of CO per gram of bacteria is shown in Figure 49.

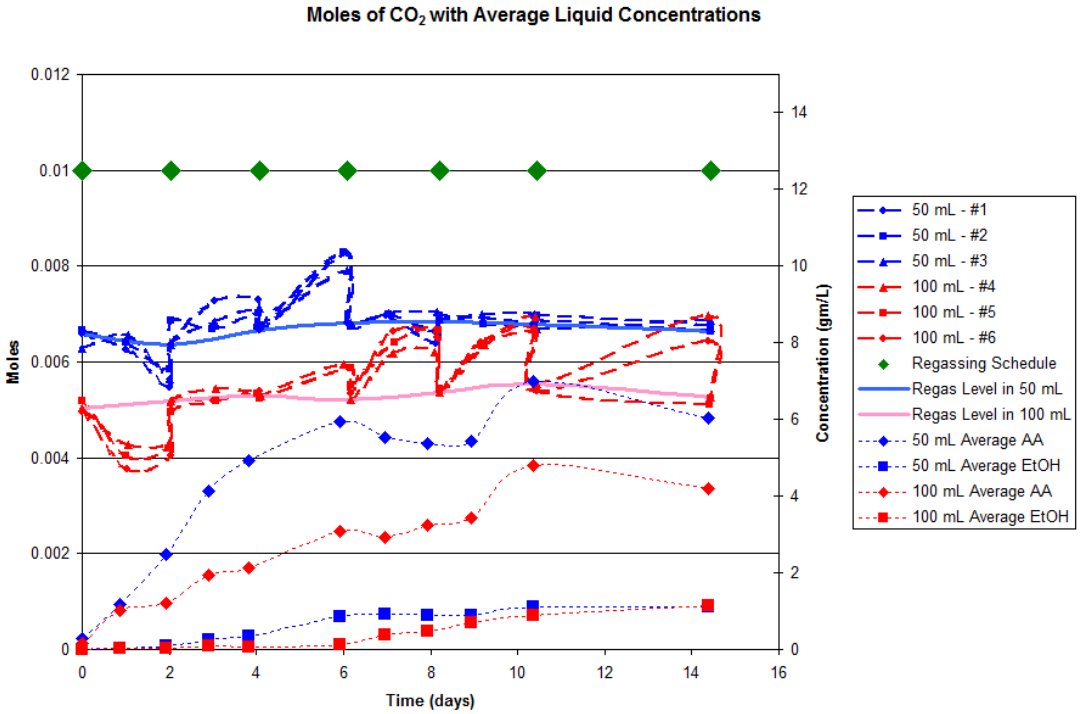

Figure 48. Moles of CO_2 with average liquid concentrations

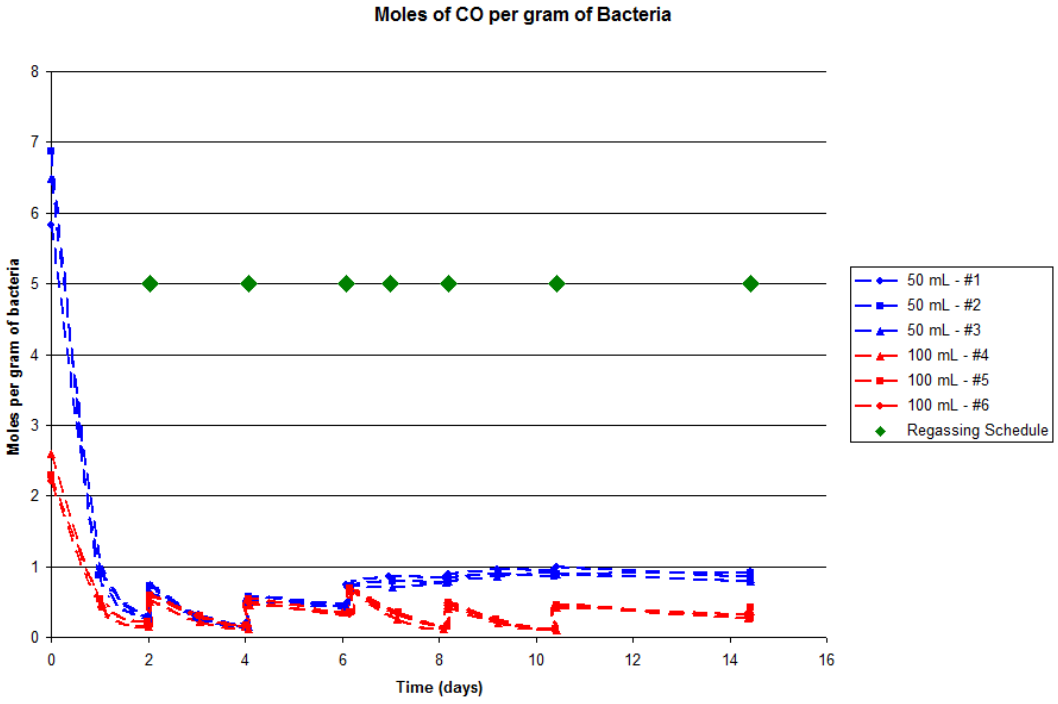

Figure 49. Moles of CO per gram of bacteria in the headspace for the 50 mL vs. 100 mL experiment while monitoring headspace gas pressure and composition

The biggest difference in moles of CO per gram of bacteria between the two different volumes is shown in the first two days. There are significantly more moles of CO per gram of bacteria in the 50 mL bottles than in the 100 mL bottles before day 2. After day 2, the levels remain the same for both the 50 mL bottles and the 100 mL bottles until day 6, when the 50 mL CO levels off (as seen in Figure 45 above) when the acetic acid level peaks and ethanol production begins, using the acetic acid as a carbon source.

The same trend is seen in the moles of H_2 per gram of bacteria, although the H_2 levels off a bit earlier than the CO did (see Figure 50).

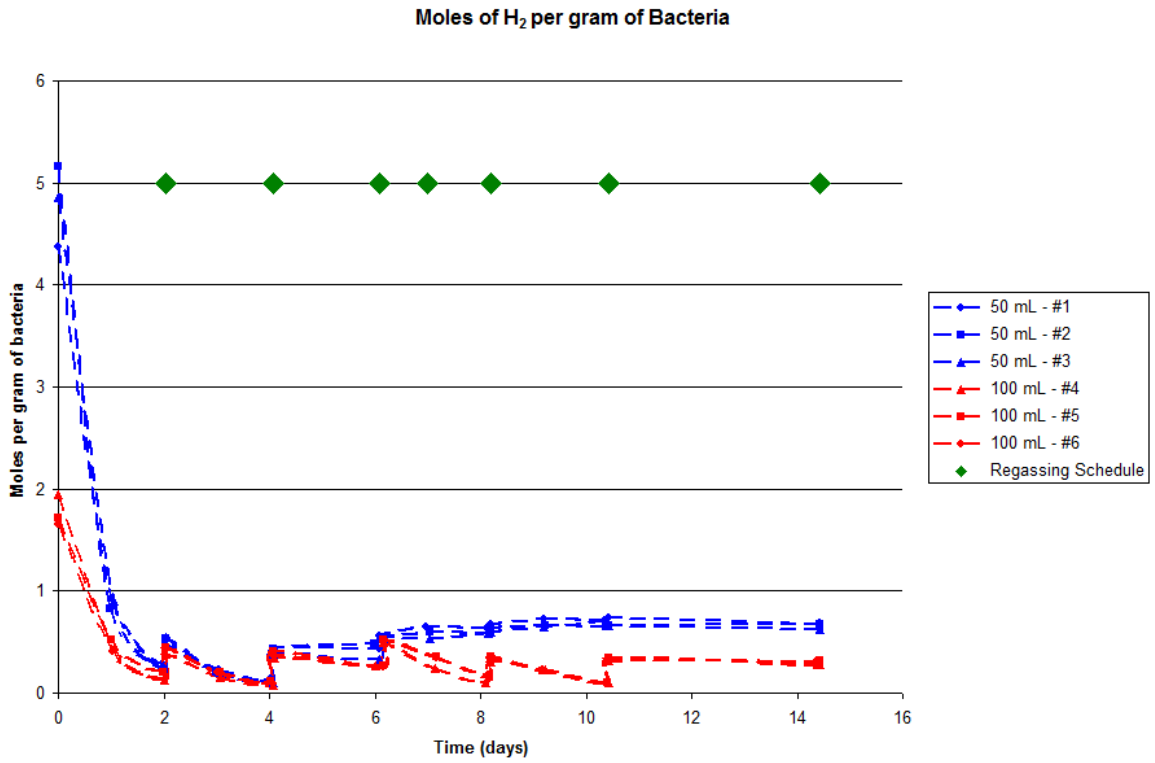

Figure 50. Moles of H_2 per gram of bacteria in the headspace for the 50 mL vs. 100 mL experiment while monitoring headspace gas pressure and composition

The moles of CO_2 per gram of bacteria are shown in Figure 51.

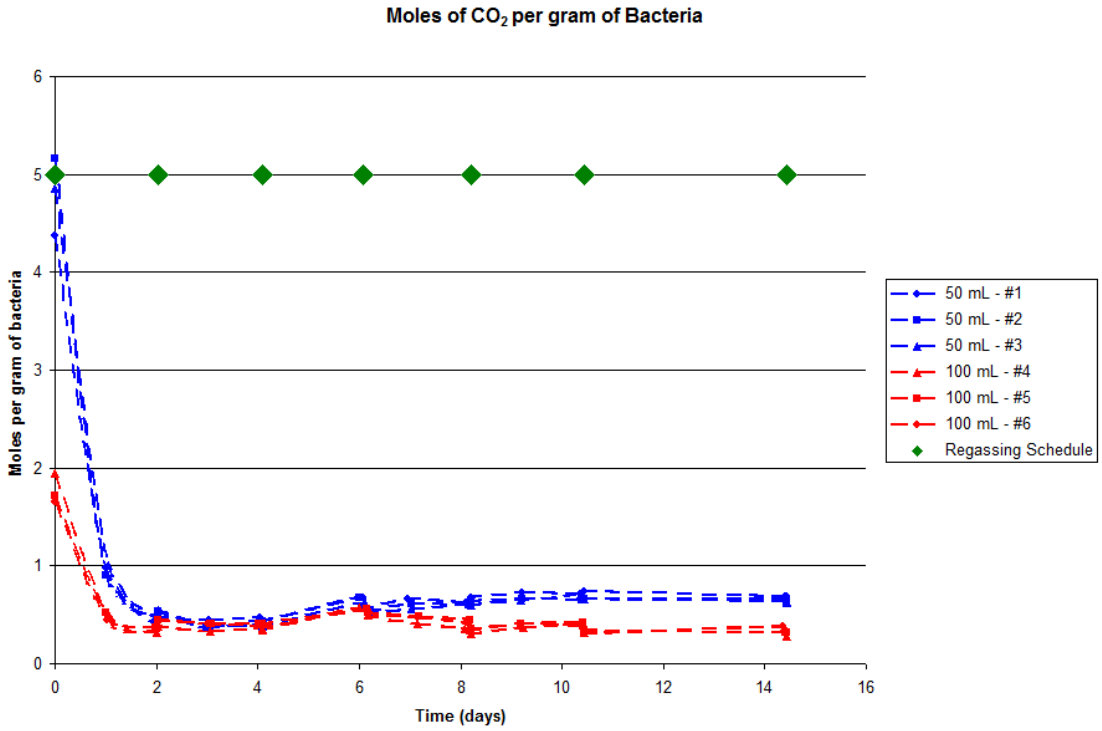

Figure 51. Moles of CO_2 per gram of bacteria in the headspace for the 50 mL vs. 100 mL experiment while monitoring headspace gas pressure and composition

Once again, the biggest difference in moles of CO_2 per gram of bacteria between the two different volumes is shown in the first two days. There are significantly more moles of CO_2 per gram of bacteria in the 50 mL bottles than in the 100 mL bottles before day 2. After day 2, the levels remain the same, both producing CO_2 at the same rate of moles of CO_2 per gram of bacteria.

From the graphs of moles of gas per gram of bacteria (Figure 49, Figure 50 and Figure 51) it is noted that the first two days seem to be the most important as to the effect the partial pressure (or the associated mass transfer) has on the growth. These findings led to an additional experiment in which the bottles were re-gassed more often (with the

same standard syngas composition), therefore keeping the partial pressures higher in the 100 mL bottles, to see if this had an effect on the growth rate.

Pressure experiment with regassing

The next experiment was run with three 50 mL bottles that were re-gassed every two days, three 100 mL bottles that were re-gassed every two days, and three 100 mL bottles that were re-gassed every 6 hours. Liquid samples were taken once a day, and total pressure in the bottles were measured every day for the all bottles, except for those bottles that were re-gassed every 6 hours, the pressure was measured every 6 hours before the re-gas. No gas compositions were measured in this experiment. The pressure history is shown in Figure 52 below. Once again, the data are connected by lines to show trends, but are not intended to infer values between the data points.

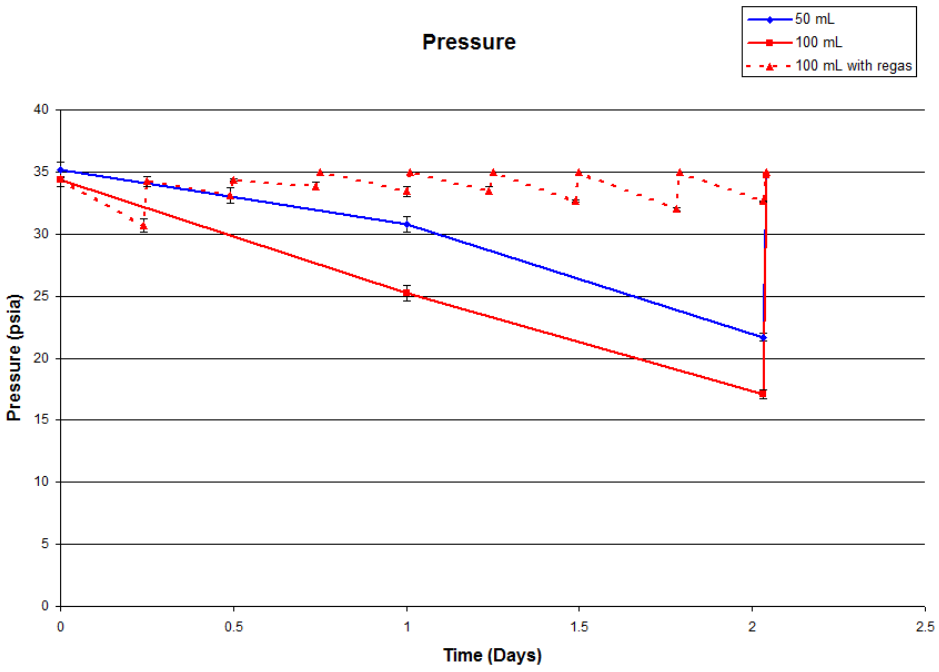

Figure 52. A plot of the pressure vs. time in the pressure re-gassing experiment with the error bars showing the standard deviation

With the re-gassing, the last set of 100 mL bottles followed a similar growth pattern to the 50 mL bottles. This trend is shown in Figure 53.

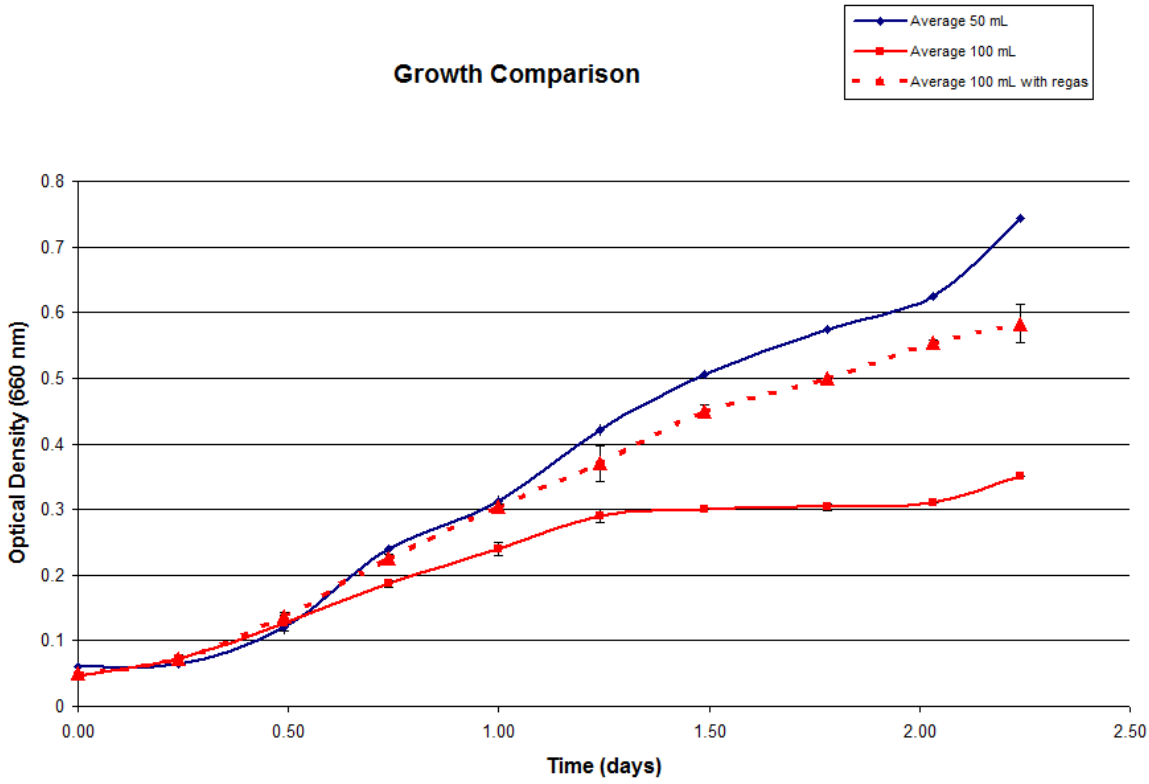

Figure 53. The growth comparison between the 50 mL bottle regassing every two days, the 100 mL bottle regassing every two days, and the 50 mL bottle regassing every six hours, error bars represent standard deviation

It is clear that re-gassing more often to keep the partial pressures of CO and H_2 higher makes a significant difference in the growth rate of the 100 mL bottles. All three follow a similar growth rate until 0.5 days, so it is probably only necessary to re-gas every 12 hours instead of every 6 hours.

As to why the 100 mL with re-gassing bottles do not follow the same or better growth than the 50 mL bottles, this could be because of the mass transfer. The 100 mL bottles (even with regassing) still don't have as much accumulated carbon available as

the 50 mL bottles. In addition, this difference could be due to the levels of sulfide in solution. Each time the bottle is re-gassed, some sulfide is stripped out of the solution and thus the redox levels may vary between the different studies. Although redox levels in the bottles were not monitored, this is a probable cause for the difference in growth rates of the 100 mL with regassing and the 50 mL bottles.

Effect of CO partial pressure on ethanol production

An experiment was run to determine the effect of the CO partial pressure on ethanol production after that ethanol production was already initiated. Nine 100 mL bottles were grown up (regassing every other day with standard 30% H_2, 30% CO_2 and 40% CO mixture, liquid samples every other day). Once ethanol production had begun and an ethanol production rate could be calculated from the data, three of the bottles were switched to a higher CO concentration (60% CO, 30% H_2, 10% CO_2) and three of the bottles were switched to a lower CO concentration (20% CO, 30% H_2, and 50% CO_2) and the effect on ethanol production was determined.

As shown in Figure 54, all bottles followed a similar growth pattern before the gasses were switched to different CO partial pressures. Because the cells had already leveled off in their growth, once the CO partial pressure was changed, there was no change in the level of the growth between the various CO gas compositions.

However, the ethanol production changed as a result of the regassing with a different CO partial pressure. As shown in Figure 55, the control produces ethanol at a continuous rate up to 40 days. When the gasses were initially switched (~day 20), both the High CO and Low CO experienced a lag phase where the cells adjusted to the

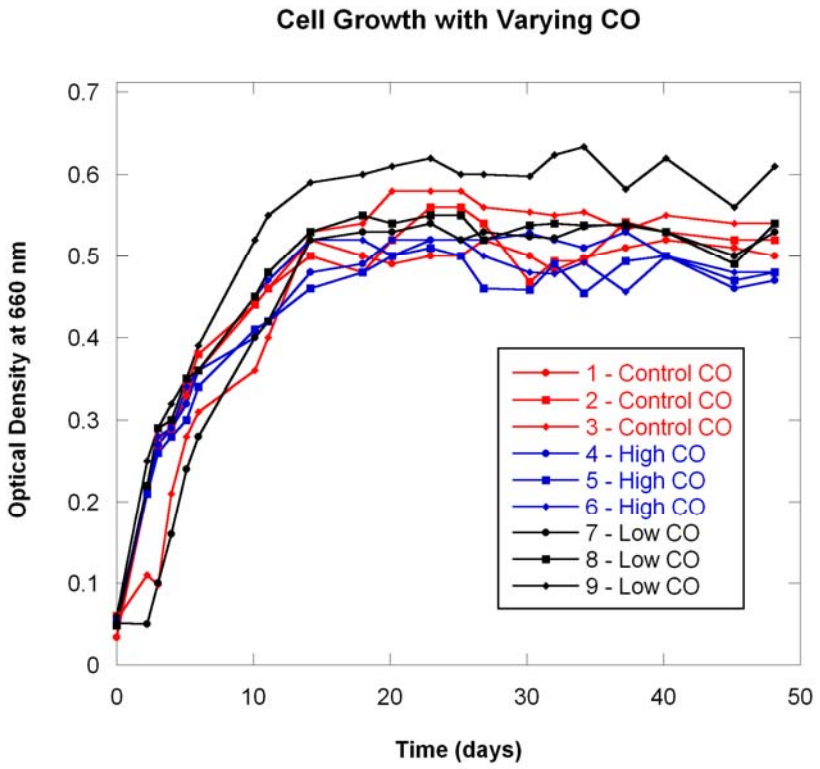

Figure 54. Cell growth (OD) data from CO experiment where bottles were switched to different CO levels halfway through the experiment

new gas they were being fed (for ~10 days). After that adjustment, ethanol production continued and the final ethanol concentration for the Low CO and the Control were around the same value (~4.8 gm/L), but the final ethanol concentration for the High CO as much higher (~6.5 gm/L). These values do not scale with the change in CO partial pressure, this indicates the possibility of mass transfer limitations from the liquid into the cell itself

With all of the above studies, it is clear that the partial pressure in the head space (or the associated mass transfer which is related to partial pressure) appears to have some affect on the growth and product formation. Thus, it is important to understand the mass transfer effects during the process.

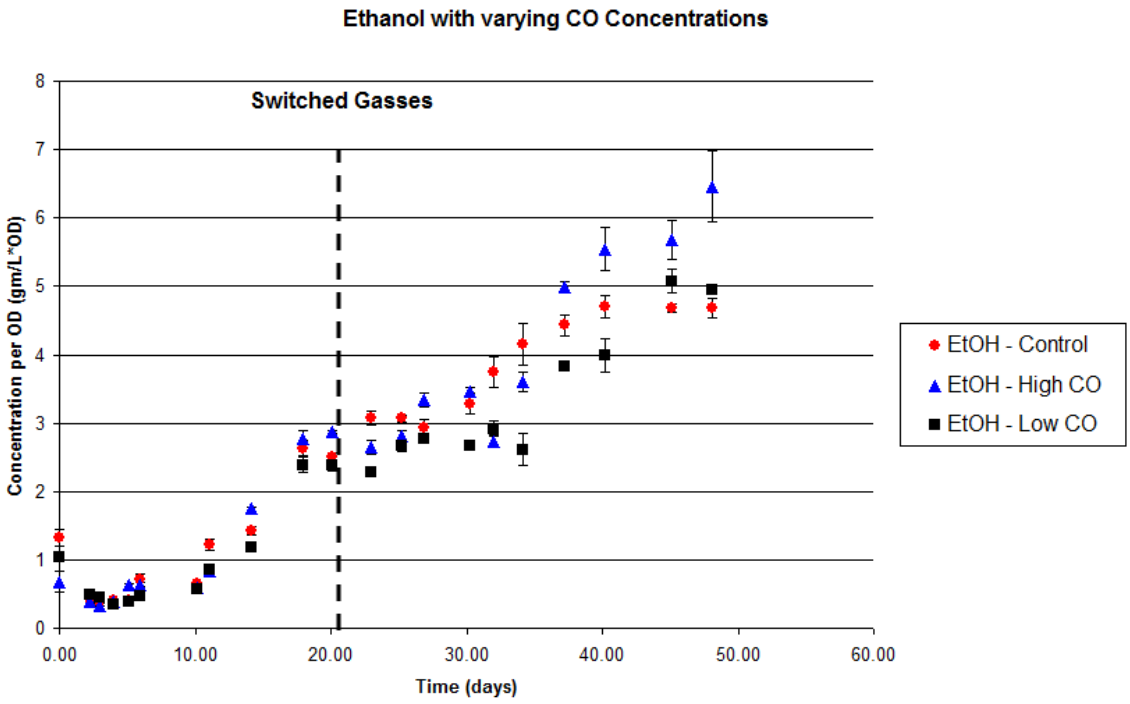

Figure 55. Ethanol production for CO experiment in which CO partial pressure was changed around day 20. High CO was 60% CO, 30% H_2, 10% CO_2, Regular CO was 30% H_2, 30% CO_2 and 40% CO and Low CO was 20% CO, 30% H_2, and 50% CO_2

Mass transfer

To assess whether or not mass transfer limitations were present during any of the bottle or 1-liter reactor studies, the volumetric mass transfer coefficient (k_La/V) for each reactor was obtained through experimentation. The reactor was filled with water to the appropriate volume and then purged with nitrogen until saturated. The gas feed was then switched to air and the dissolved oxygen was recorded with time. A representative run from the 1 liter reactor is shown in Figure 56a to illustrate how mass transfer coefficients were assessed for the different reactors. A mass balance yields Equation 8.

$$\frac{dC_L}{dt} = \frac{k_L a}{V}(C^* - C_L) \qquad (8)$$

Which when integrated, yields Equation 9.

$$\ln(C^* - C_L) = -\frac{k_L a}{V} t + C_o \tag{9}$$

The negative log of the concentration difference (saturated oxygen % represented as C* minus the dissolved oxygen % represented as C) shown in Figure 56b gives a straight line with a slope that is equivalent to (k_La/V).

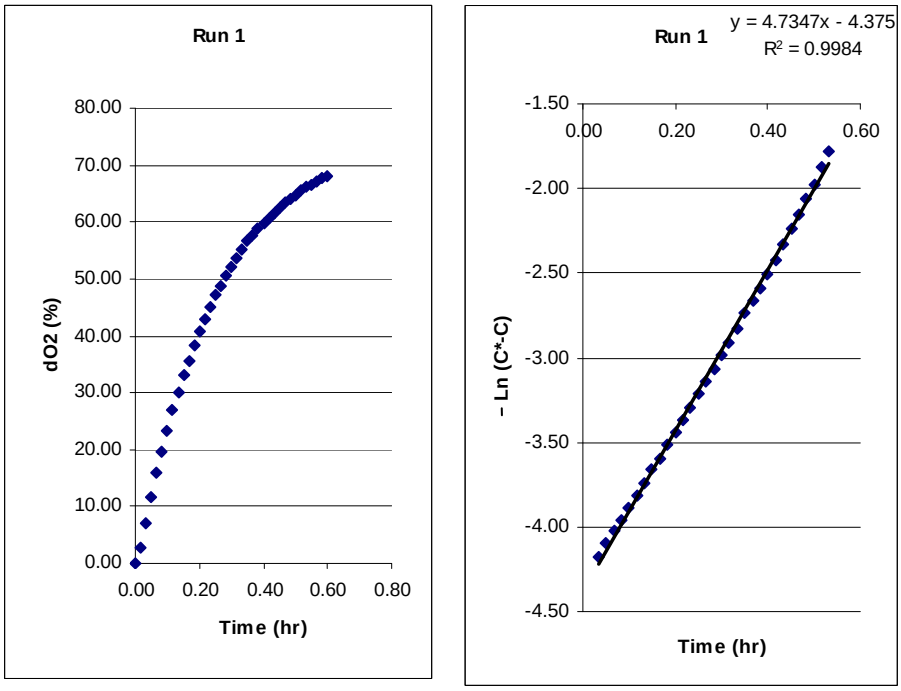

Figure 56. Mass transfer graphs for 175 rpm and 100 sccm. a). dissolved oxygen % as a function of time b). negative log of concentration difference where C* is saturated oxygen % and C is the dissolved oxygen %

To assess potential mass transfer limitations, the k_La values for oxygen were converted to k_La values for CO and CO_2. Boundary layer theory indicates a relationship between the aqueous diffusivities and k_La for different chemical species i and j under identical hydrodynamic conditions such that (Sherwood, Pigford et al. 1975):

$$\frac{(k_L a)_i}{(k_L a)_j} = \left(\frac{D_i}{D_j}\right)^{\frac{1}{2}} \tag{10}$$

where D is the diffusion coefficient. By rearranging this equation, the k_La for CO can be estimated by:

$$(k_L a)_{CO} = \left(\frac{D_{CO}}{D_{O_2}} \right)^{\frac{1}{2}} (k_L a)_{O_2} \qquad (11)$$

The same correlation can be used to find the k_La of CO_2 and H_2, with their respective diffusivities. Using diffusivities of 3.05 x 10^{-5} cm^2/s, 3.26 x 10^{-5} cm^2/s, and 2.74 x 10^{-5} cm^2/s, 6.48 x 10^{-5} cm^2/s for O_2, CO, CO_2 and H_2 at 37º C (Wise and Houghton 1968; Verhallen, Oomen et al. 1984; Tamimi and Rinker 1994) the k_La values for CO, CO_2 and H_2 were calculated.

Mass transfer in 1 liter reactor

One liter of water was placed in the reactor and nitrogen was purged through at a flow rate of 200 sccm until all the dissolved oxygen was out of solution (about 2 hours). Then air was bubbled into the reactor at the flow rates below. At least two runs were completed for agitation rates of 175 and 225 rpm and flow rates of 60, 100 and 150 sccm. The measured volumetric mass transfer coefficients (kLa/V), as well as the mass transfer coefficients (kLa) for oxygen, are shown in Table 6..

The volumetric mass transfer coefficients (k_La/V) were compared to a correlation for mass transfer coefficients found in "Fermentation and Enzyme Technology" to assess the accuracy of the measurements (Wang, Cooney et al. 1979).

Table 6. Summary of Mass Transfer Coefficients for oxygen in the 1 Liter Reactors

Agitation (rpm):	Flow Rate (sccm):	kLa/V (hr^{-1})	Average kLa/V (hr^{-1})	kLa (L/hr)
175	60	2.86 3.21	3.04	3.04
225	60	3.94 3.74	3.84	3.84
175	100	4.5 4.37 4.73	4.53	4.53
225	100	5.59 4.99	5.29	5.29
175	150	5.78 5.57	5.68	5.68
225	150	7.37 7.85	7.61	7.61

The correlation is:

$$\frac{k_L a}{V} = (\alpha + \delta N_i)(P_g / V_L)^{0.77} V_s^{\ 0.67} \tag{12}$$

where k_La/V is the volumetric mass transfer coefficient in mM hr^{-1} atm^{-1}, α and δ are the parameters for the correlation, N_i is the number of impellers, P_g/V_L is the gassed power (for the impeller) per unit volume in hp/1000 l, and V_s is the superficial gas velocity in cm/min. The superficial gas velocity is proportional to the volumetric flow rate (Q). Since the number of impellers, the impeller power (for runs with similar stirring rates), and the liquid volumes were the same for all 1-liter experiments, the ratio of Equation 6 for different runs gives:

$$\frac{(k_L a/V)_{run1}}{(k_L a/V)_{run2}} = \left(\frac{Q_{run1}}{Q_{run2}}\right)^{0.67} \tag{13}$$

Table 7 shows the kLa/V ratio and the corresponding $(\text{Q ratio})^{0.67}$ between two runs with similar stirring speeds. As noted, the percent difference between the k_La/V ratio and the corresponding $(\text{Q ratio})^{0.67}$ is very small, suggesting consistency between the measured data and representative correlations. Table 8 shows the estimated values for the k_La of CO and CO_2 at an agitation rate of 175 rpm and a flow rate of 100 sccm. This agitation rate and flow rate were the parameters used for the redox studies.

Table 7. Empirical ratio compared to a correlation for mass transfer coefficient ratio

RPM	Q (sccm)	k_La/V (hr^{-1})	Comparison		k_La/V Ratio	$(Q\ ratio)^{0.67}$	% Difference
			Q_{run1}	Q_{run2}			
175	60	3.04	60 sccm	150 sccm	0.53	0.54	1%
175	100	4.53	60 sccm	100 sccm	0.67	0.71	6%
175	150	5.68	100 sccm	150 sccm	0.80	0.76	5%
225	60	3.84	60 sccm	150 sccm	0.50	0.54	7%
225	100	5.29	60 sccm	100 sccm	0.73	0.71	2%
225	150	7.61	100 sccm	150 sccm	0.70	0.76	10%

Table 8. Summary of k_La (L/hr) at 175 rpm and 100 sccm for O_2, CO and CO_2 for 1 Liter reactor

$(k_La)_{CO}$	4.68
$(k_La)_{CO2}$	4.29

From a material balance standpoint, the maximum amount of carbon from CO that can enter the liquid phase (represented as T_{CO} in mass per time) is

$$T_{CO} = 12(k_L a)_{CO} P_{CO} / H_{CO} \tag{14}$$

where P_{CO} is the partial pressure of CO in the headspace and H_{CO} is the Henry's law constant for CO in water. The number "12" is for conversion from moles of CO to grams of carbon in CO since there are 12 grams of carbon per mole of CO. For the redox studies, P_{CO} was 0.40 atm. The value of H_{CO} is 1215 atm·L/mol at 37º C (Perry, Perry et al. 1963). Based on the value of $(k_La)_{CO}$ in Table 8, T_{CO} is 0.018 g C/hr or 0.44 g C/day. Similarly for CO_2, where P_{CO2} was 0.30 atm and H_{CO2} is 39.4 atm·L/mol at 37º C (Perry, Perry et al. 1963), T_{CO2} is 0.39 g C/hr or 9.44 g C/day.

The total cumulative carbon/liter converted to cells, ethanol, and acetic acid is shown in Figure 57 as a function of time for all redox runs. The data is compared to the maximum amount of carbon available from CO and CO_2. The amount of carbon in the cells was determined by calculating the dry weight of cells (1 OD = 0.43 gm dry weight/L of cells) and assuming 50 weight% of the dry weight of cells is carbon (Ahmed 2005). Of the mass of ethanol and acetic acid, 52% and 40% of the mass contains carbon, respectively.

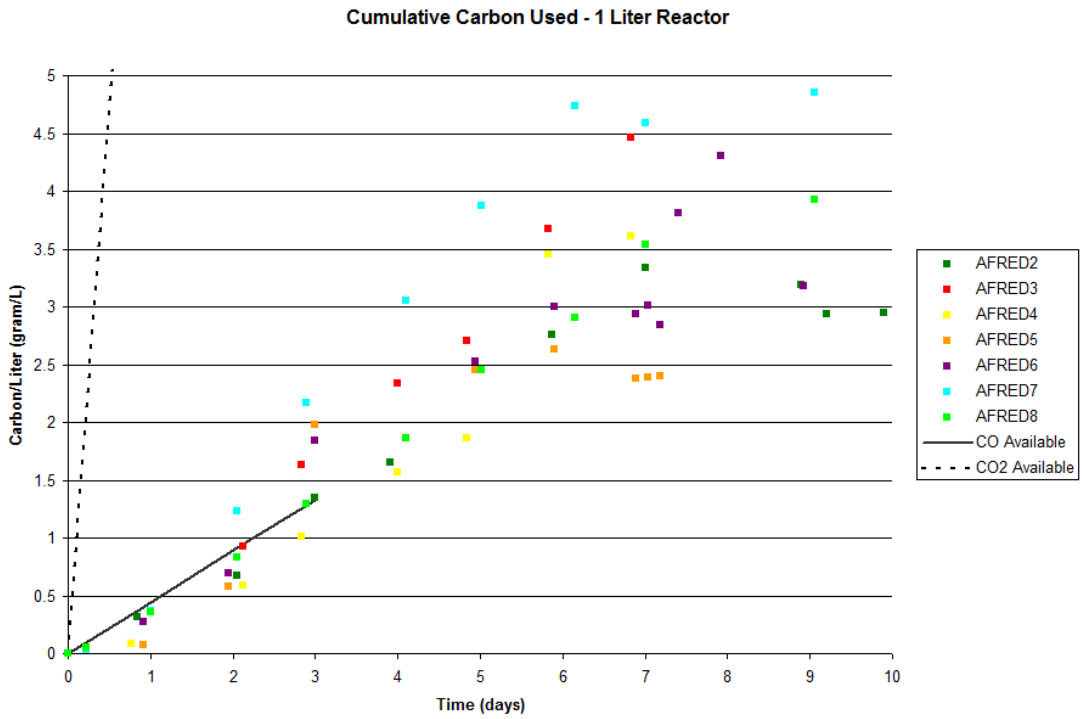

Figure 57. Cumulative carbon (grams/Liter) used in the reactor in the formation of cells, acetic acid and ethanol

All the AFRED runs follow the same cumulative carbon/liter increase, especially at the beginning. It is interesting to note, that if the cells are growing on CO alone, this means that CO could be limiting their growth. However, there is an abundance of CO_2 available. Although we know that cells can either generate or consume CO_2, the CO_2

generation and consumption was not measured for these experiments, so it is difficult to know if they are using CO_2 in these first few days or not. If cells are feeding off CO_2 in addition to CO, then they are not growth limited by CO alone. However, if they are not growing on CO_2, then the results show they are likely mass transfer limited during growth.

In the latter portion of the experiment after growth stopped, carbon use (through production of acetic acid and ethanol) was greater than the carbon available from CO alone. Thus CO_2 must have been used in the latter stages for product formation. Because there is so much CO_2 available, if the cells could be channeled to feed more off CO_2 than CO, then there is a possibility for much higher growth and ethanol production. CO will always be much more limiting than CO_2. However, CO has reducing potential to contribute to the reaction, whereas CO_2 does not, so additional reducing potential would need to come from somewhere. This warrants further investigation in future work.

Mass transfer in bottles

In order to rule out the possibility that mass transfer limitations of the 100 mL bottles result in the lower cell growth rates as compared to the 50 mL bottles, the mass transfer rate of oxygen in both liquid volumes was measured. A micro dissolved oxygen probe (#DO-166MT-1, Lazar Laboratories, Los Angeles, California) with 2 mm diameter tip, 6 mm diameter body, was placed in the liquid and a #1 stopper was placed over the bottle , with the cord for the probe coming up the side of the stopper. A hole was drilled through the stopper and a 1/8" stainless steel tube, used for continuously flowing air, was run through the stopper and into the gas head space. The tube end was crooked upward so that the gas flow would not disturb the water surface inside the sealed bottle. A needle

(18 gauge) was placed in the side of the stopper as an outlet for the air to prevent a buildup of pressure inside the bottle.

The mass transfer rate for O_2 was then measured using the same method as for the 1 Liter reactor, and then converted to a mass transfer rate for CO, CO_2 and H_2. A summary of the mass transfer coefficients for the different reactor sizes is shown in Table 9 below. Note that the 1-liter reactor mass transfer coefficient is shown for comparison.

Table 9. Mass transfer coefficients of O_2, CO, CO_2 and H_2 for 1 Liter reactor, 50 mL bottles and 100 mL bottles

Reactor Size	O_2		CO		CO_2		H_2	
	k_La/V (hr^{-1})	St. Dev.	k_La/V (hr^{-1})	k_La (L/hr)	k_La/V (hr^{-1})	k_La (L/hr)	k_La/V (hr^{-1})	k_La (L/hr)
1 Liter	4.53	0.18	4.69	4.69	4.30	4.30	6.61	6.61
50 mL	4.54	0.82	4.69	0.23	4.30	0.22	6.62	0.33
100 mL	2.55	0.17	2.64	0.26	2.42	0.24	3.72	0.37

A CO mass transfer coefficient of 0.23 L/hr for the 50 mL bottles and 0.26 L/hr for the 100 mL bottles is essentially the same. Similarly, the CO_2 mass transfer rates are also essentially the same. The similar coefficients are consistent with the same transport areas (a) and similar shaking leading to likely similar hydrodynamics (associated with k_L).

Next, an analysis on the experiments in which pressures and moles were measured with time in the bottles was performed. A mole balance in the gas phase of a fixed head space for a given species (CO for this example) gives:

$$\frac{dn_{CO}}{dt} = -(k_L a)_{CO}\left(C^*_{CO} - C_{CO}\right) \tag{15}$$

where n_{CO} is the moles of CO, $(kLa)_{CO}$ is the mass transfer coefficient for CO associated with the liquid volume, C^*_{CO} is the concentration of CO in the gas phase, and C_{CO} is the concentration of CO in the liquid. The fastest that the moles can change in the headspace would be if the bottles were mass transfer limited such that C_{CO} is 0 (i.e. as soon as a CO molecule enters the liquid it is consumed by the bacteria).) This would result in the following equation:

$$\frac{dn_{CO}}{dt} = -k_L a C^*_{CO} = -k_L a \frac{P_{CO}}{H_{CO}} = -k_L a \frac{\left(n_{CO} RT / V_G\right)}{H_{CO}} \tag{16}$$

Because all components, except n_{CO}, are essentially constant with time, integration yields

$$n_{CO} = n_{CO_i} \exp\left(\frac{-(k_L a)_{CO}\left(RT / V_G\right)}{H_{CO}}\right) t \tag{17}$$

This equation is applicable to all other species when using the appropriate H and $k_L a$ for each species. Figure 58 shows a plot of measured CO moles versus time in the various bottles (shown as solid diamonds). Using Equation 18, the predicted moles of CO with time (based on mass transfer limitations) were estimated following each data point (representing n_{COi}) and are shown by the dashed lines, with an open circle representing the final value that should be compared to the solid diamonds representing actual data.

In the first day, mass transfer limitations are not dominant in either the 50 mL nor the 100 mL bottles since the predicted moles on day 1 are lower than the measured moles on day 1. Over day 2 through 4, the CO mole predictions for the 50 mL bottles are similar to the measured moles, strongly suggesting mass transfer limitations. The 100 mL bottles over days 2-4 have slightly more CO than what was predicted if they were mass transfer limited, suggesting mass transfer limitations may not be as key of an issue

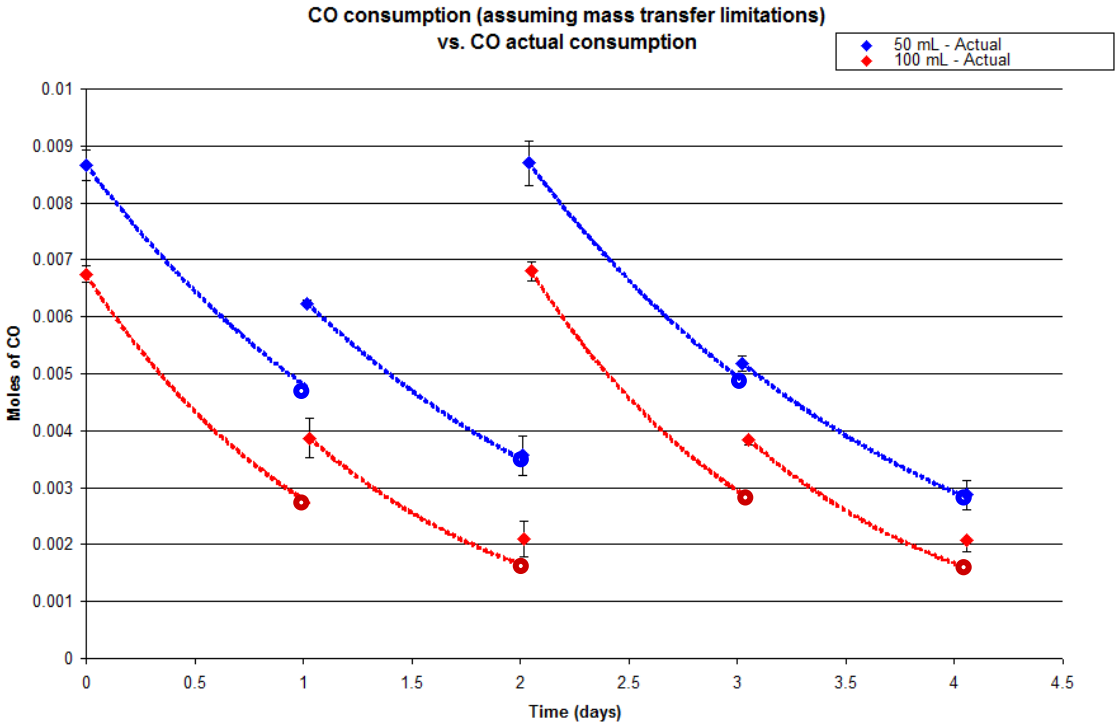

Figure 58. Average moles of CO consumption assuming mass transfer limited vs. actual moles of CO consumed, with error bars representing standard deviation between three bottles

as with the 100 mL bottles- although the predictions are close (especially if the standard deviation is propagated through) suggesting further analysis with regards to mass transfer limitations is needed. It's important to note that the available moles are higher for the 50

mL bottles, which is consistent with higher cell mass and product formation compared to the 100 mL bottles (see Figure 41 and Figure 42).

A similar graph for the moles of H_2 is shown in Figure 59. The dashed line represents predicted H_2 moles assuming mass transfer limitations with an open circle representing the final value, while the solid diamonds portray measured moles of H_2.

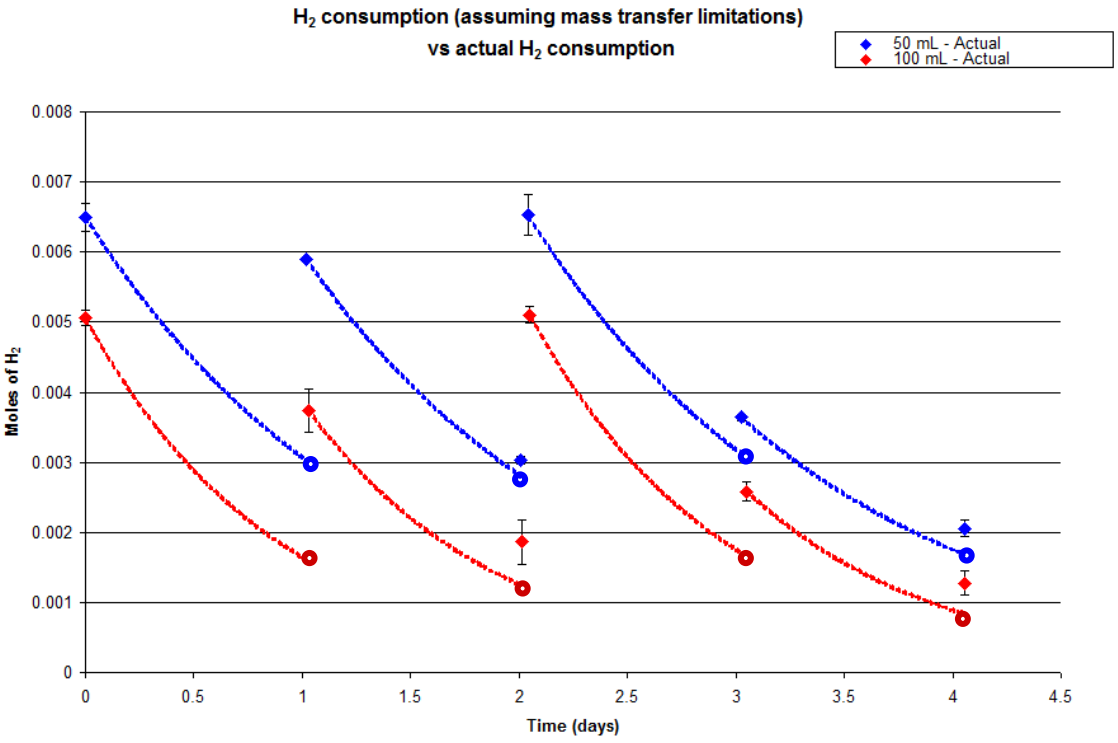

Figure 59. Average moles of H_2 consumption assuming mass transfer limitations vs. actual H_2 consumption, with error bars representing standard deviation

Once again, there are no mass transfer limitations on day 1 for either set of bottles. However, after one day mass transfer limitations appear to be present for the 50 mL bottles but not as much for the 100 mL bottles. This apparent lack of mass transfer limitations for the 100 mL bottles still resulted in a lower growth and product formation. The reason for this could be partial pressure related, i.e. enzymes required for growth and

production formation may have an optimal partial pressure of CO or H_2 to operate to their full capacity.

In addition to the above analysis, the amount of carbon available was calculated and compared to the amount of carbon used for cell growth and product formation, similar to the calculation done with the 1 Liter reactor. The maximum amount of carbon available was calculated by substituting P_{CO} with the ideal gas law in the equation for the maximum amount of carbon from CO that can enter into the liquid phase (equation 15).

$$T_{CO} = 12(k_L a)_{CO} \frac{n_{co} RT}{H_{CO} V_G} \tag{18}$$

Substituting equation 18 in for n_{CO} yields:

$$T_{CO} = 12(k_L a)_{CO} \frac{P_{coi}}{H_{CO}} \exp(\frac{-k_L aRT}{H_{CO} V_G} t) \tag{19}$$

Integrating Equation 20 with respect to time and dividing by the liquid volume gives

$$A_{CO} = 12 \frac{P_{COi}}{RT} \left(\frac{V_G}{V_L} \right) \left(1 - \exp^{\frac{-k_L aRT}{H_{CO} V_G} t} \right) \tag{20}$$

where A_{CO} represents the maximum accumulation of carbon (g/L) in the liquid, based on CO mass transfer limitations, beginning with a given initial CO partial pressure. Thus, following the injection of cells, A_{CO} can be calculated up to the time the head space is regassed. After regassing, A_{CO} can again be calculated from Equation 21 and added to

the accumulated amount at the time of regassing. This process can be repeated to obtain a profile of accumulated carbon with time.

From the 50 and 100 ml bottles studies in which pressure and composition was measured with time, the total accumulated carbon (cells, ethanol, and acetic acid) with time is shown as symbols in Figure 60. The predicted carbon accumulation (A_{CO}) relative to Day 1, based on CO mass transfer limitations, is also shown for both liquid volumes.

Figure 60 experimental data shows that the 50 mL bottles have more than double the carbon used (cell mass or liquid products) per liter as compared to the 100 mL bottles (at least for bottles #2 and #3). From the limited mass transfer analysis as shown during Days 2-6, both the 50 mL and the 100 mL bottles utilize about the same amount of carbon as predicted by CO mass transfer limitations (Equation 21). Thus, the above mass transfer analysis is in general agreement with the 50 mL and 100 mL bottles based on the headspace analysis (see Figure 58) which also shows likely CO and H_2 mass transfer limitations.

An additional important note of these studies is that more CO is available for the 50 mL bottles (on a per liter basis) as compared to the 100 mL bottles. Thus, this is the likely reason for the increases in cell mass and product formation observed in the 50 mL bottles as compared to the 100 mL bottles. One final thought is that it is important to note that the above analysis did not include CO_2 consumption leading to carbon-based products (i.e. carbon-based products were generated from both CO and CO_2) nor did it include CO_2 production (i.e. carbon accumulation did not include carbon going to a CO_2

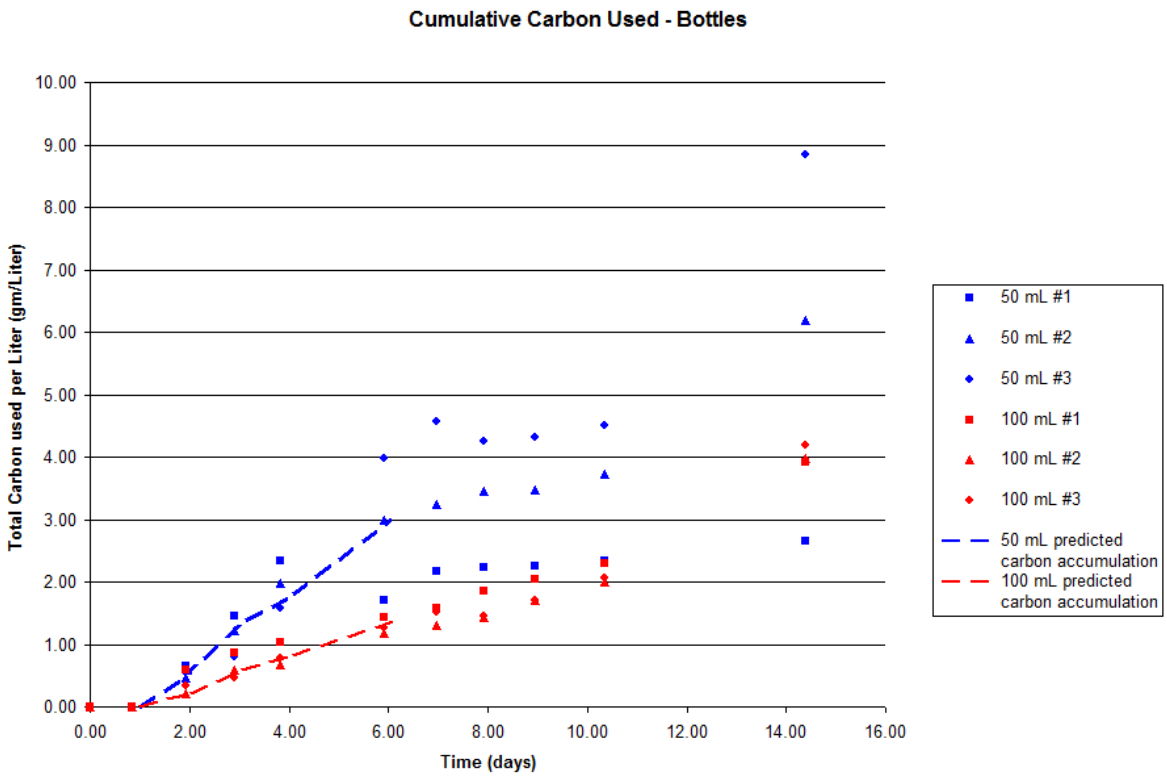

Figure 60. Cumulative carbon used (gram carbon) for 50 mL and 100 mL bottles

product). Thus, there is a possibility that mass transfer limitations may not be the complete story.

Conclusions and Future Work

The 50 mL bottles have more than double the growth rate than the 100 mL bottles (0.57 day^{-1} compared to 0.20 day^{-1}). The acetic acid goes up higher initially in the 50 mL bottles than in the 100 mL bottles (producing more ATP, feeding the higher growth observed in the 50 mL bottles). In addition, the onset of ethanol production happens earlier in the 50 mL than in the 100 mL.

When pressure and gas composition are monitored in an experiment, some interesting trends are observed. Initially, the pressure in both the 50 mL and the 100 mL bottles drop down around the same rate, although the 100 mL bottles drop down to a slightly lower level than the 50 mL bottles. At about day 6 however, the 50 mL bottles begin leveling off to a much higher pressure than the 100 mL bottles, while this trend is not seen in the 100 mL bottles until much later (~day 10).

When pressure is plotted against acetic acid concentration the reason for this behavior becomes clear. The pressure quits dropping off when the acetic acid reaches a peak. At that point, the cells level off in their growth, and need less carbon for cell building blocks, and in addition, the acetic acid level begins decreasing, indicating that the cells are using the acetic acid carbon to build ethanol preferentially over carbon in the syngas.

The biggest difference in moles of CO per gram of bacteria between the two different volumes is shown in the first two days. There are significantly more moles of CO per gram of bacteria in the 50 mL bottles than in the 100 mL bottles before day 2. After day 2, the levels remain the same for both the 50 mL bottles and the 100 mL bottles until day 6, when the 50 mL CO levels off when the acetic acid level peaks and ethanol production begins, using the acetic acid as a carbon source.

The same trend is seen in the moles of H_2 per gram of bacteria, (although the H_2 levels off a bit earlier than the CO did) and moles of CO_2 per gram of bacteria. It was found that CO_2 was consumed during the first few days of growth, however, once ethanol production set in, CO_2 was only produced and not consumed.

It is clear that re-gassing more often to keep the pressure higher in the 100 mL bottles makes a significant difference in the growth rate of the 100 mL bottles. All three (50 mL bottle, 100 mL bottle, and 100 mL bottle with re-gas every 6 hours) follow a similar growth rate until 0.5 days, so it is probably only necessary to re-gas every 12 hours instead of every 6 hours.

And finally, the effect of CO partial pressure on ethanol production was determined. When the CO partial pressure was raised after the onset of ethanol production, the high CO regassing had a higher ethanol final concentration (~6.5 gm/L) than the regular and low CO (~4.8 gm/L).

Both the 50 mL and 100 mL bottle were found to have essentially the same mass transfer rate, 0.227 L/hr for the 50 mL bottles and 0.255 L/hr for the 100 mL bottles. However, because of headspace differences, there is more CO available for the 50 mL bottles (on a per liter basis) as compared to the 100 mL bottles. Thus, this is the likely reason for the increases in cell mass and product formation observed in the 50 mL bottles as compared to the 100 mL bottles. Mass transfer limitation analysis proved useful in pointing out that both the 50 mL and 100 mL bottles are likely experiencing mass transfer limitations. This is an area that needs more research..

Although, much knowledge as to how partial pressure affects the cells has been obtained, future questions that have been left unanswered include:

- What is causing the decrease in optical density around day 6? Is something out of the liquid being depleted that is unable to sustain the higher cell density? Is it the gas partial pressure being too low?

- We observed that the gas consumption leveled off as the acetic acid peaks and ethanol production begins. The acetic acid level then decreases as the cells appear to use acetic acid as the carbon source to produce ethanol. Further research needs to be conducted as to what happens after the acetic acid level drops down low. Does gas consumption resume? In what ratios does it resume?
- CO_2 mass transfer limitations are less likely than CO. Can cells be engineered to feed off of CO_2 and H_2 more than CO? Can something be added to the solution to make the mass transfer of CO more effective?
- What systems can be employed to minimize mass transfer limitations?

Chapter 6 – Conclusions and Future Work

Conclusions

- Cysteine sulfide has a greater effect on the redox level of the solution, than does the gas composition. Therefore, the concentration of cysteine sulfide will be more effective at controlling redox levels in bioreactors and the syngas composition will not significantly affect the cell-free media once the cysteine sulfide has been added.
- When cells are first inoculated the redox level begins dropping and for optimal growth, it levels off at ~ -200 mV, at which point, although still dropping, drops at a much slower rate.
- When cells have a lag phase where no growth is experienced, redox continues dropping until the growth begins, at which point, the redox will ideally return to the -200 mV.
- When redox levels remain below -200 mV, growth is experienced at a slower rate and the final optical density is lower.
- In addition, cells switch from acetic acid to ethanol production after a drop of ~50 mV in the redox level.
- The 50 mL bottles have more than double the growth rate than the 100 mL bottles (0.57 day^{-1} compared to 0.20 day^{-1}). The acetic acid goes up higher

initially in the 50 mL bottles than in the 100 mL bottles (producing more ATP, feeding the higher growth observed in the 50 mL bottles). In addition, the onset of ethanol production happens earlier in the 50 mL than in the 100 mL.

- The pressure in the bottle experiments quits dropping off when the acetic acid reaches a peak. At that point, the cells level off in their growth, and need less carbon for cell building blocks, and in addition, the acetic acid level begins decreasing, indicating that the cells are using the acetic acid carbon to build ethanol preferentially over carbon in the syngas.
- The biggest difference in moles of CO per gram of bacteria between the two different volumes is shown in the first two days. There are significantly more moles of CO per gram of bacteria in the 50 mL bottles than in the 100 mL bottles before day 2. After day 2, the levels remain the same for both the 50 mL bottles and the 100 mL bottles until day 6, when the 50 mL CO levels off when the acetic acid level peaks and ethanol production begins, using the acetic acid as a carbon source.
- The same trend is seen in the moles of H_2 per gram of bacteria, (although the H_2 levels off a bit earlier than the CO did) and moles of CO_2 per gram of bacteria.
- It is clear that re-gassing more often to keep the pressure higher in the 100 mL bottles makes a significant difference in the growth rate of the 100 mL bottles. All three (50 mL bottle, 100 mL bottle, and 100 mL bottle with

re-gas every 6 hours) follow a similar growth rate until 0.5 days, so it is probably only necessary to re-gas every 12 hours instead of every 6 hours.

- The effect of CO partial pressure on ethanol production was determined. When the CO partial pressure was raised after the onset of ethanol production, the high CO regassing had a higher final ethanol concentration (~6.5 gm/L) than the regular CO and low CO (~4.8 gm/L). These values do not scale with the change in CO partial pressure, this indicates the possibility of mass transfer limitations from the liquid into the cell itself.
- Both the 50 mL and 100 mL bottle were found to have essentially the same mass transfer rate, 0.227 L/hr for the 50 mL bottles and 0.255 L/hr for the 100 mL bottles. However, because of headspace differences, there is more CO available for the 50 mL bottles (on a per liter basis) as compared to the 100 mL bottles. The lower liquid volume bottles (50 mL) can accumulate more mass per unit volume than the larger liquid volume bottles (100 mL). Mass transfer limitation analysis proved useful in pointing out that both the 50 mL and 100 mL bottles are likely experiencing mass transfer limitations.

Future Work

- Liquid samples can be taken more often than once daily while monitoring redox levels to determine if the production of acetic acid/ethanol is oscillating.

- If it is found that the production of acetic acid and ethanol is oscillating, the redox can be controlled at the level when ethanol is being produced to determine if controlling the redox level prevents the oscillations and maintains production of ethanol.
- The redox level can be controlled at -200 mV to determine if cells will grow to higher optical density before leveling off.
- Redox level can be dropped by ~ -50mV earlier on in the experiment to determine if ethanol production can be induced at an earlier time.
- Experiments can be run to determine the decrease in optical density around day 6, whether it be nutrient depletion in the liquids or gas partial pressure.
- We observed that the gas consumption leveled off as the acetic acid peaks and ethanol production begins. The acetic acid level then decreases as the cells use it as the carbon source to produce ethanol. Further research can be conducted as to what happens after the acetic acid level drops down after it's peak to determine if gas consumption resumes, and if so, in what ratio.
- CO_2 has far fewer mass transfer limitations than CO. Determine if cells can be engineered to feed off of CO_2 and H_2 more than CO, and what additional reducing potential would be required.
- Different systems can be explored that will minimize mass transfer limitations.

References

Abrini, H., H. Naveau, et al. (1994). "Clostridium autoethanogenum, sp. nov., an anaerobic bacterium that produces ethanol from carbon monoxide." Archives Microbiology **161**: 345-351.

Adler, H. and W. Crow (1987). "A Technique for Predicting the Solvent-Producing Ability of *Clostridium acetobutylicum*." Applied and Environmental Microbiology **53**(10): 2496-2499.

Ahmed, A. (2005). Effects of Biomass-Generated Syngas on Cell-growth, Product Distribution and Enzyme Activities of *Clostridium carboxidivorans* $P7^T$. Chemical Engineering. Stillwater, Oklahoma, Oklahoma State University. **Doctor of Philosophy:** 245.

Bredwell, M. D., P. Srivastava, et al. (1999). "Reactor design issues for synthesis-gas fermentations." Biotechnology progress **15**(5): 834-844.

Clarke, K. G., G. S. Hansford, et al. (1988). "Nature and significance of oscillatory behavior during solvent production by *Clostridium acetobutylicum* in continuous culture." Biotechnology and bioengineering **32**: 538-544.

Datar, R. P., R. M. Shenkman, et al. (2004). Fermentaiton of Biomass-Generated Producer Gas to Ethanol, Wiley Interscience.

Dayton, D. C. and P. L. Spath (2003). Preliminary Screening —Technical and Economic Assessment of Synthesis Gas to Fuels and Chemicals with Emphasis on the Potential for Biomass-Derived Syngas. N. R. E. Laboratory. Golden, Colorado 80401-3393.

Doctors, C. (2007). "Standard Electrode Potentials." Retrieved 8/13/2007, from http://www.corrosion-doctors.org/References/Standard.htm.

Doremus, M. G., J. C. Linden, et al. (1985). "Agitation and Pressure Effects on Acetone-Butanol Fermentation." Biotechnology and Bioengineering **27**: 852-860.

Drake, H. L. and S. L. Daniel (2004). "Physiology of the thermophilic acetogen *Moorella thermoacetica*." Research in Microbiology **155**(422-436).

Durre, P., R.-J. Fischer, et al. (1995). "Solventogenic enzymes of *Clostridium acetobutylicum*: catalytic properties, genetic organization, and transcriptional regulation." FEMS Microbiology Reviews **17**(3): 251-262.

Durre, P. and C. Hollergschwandner (2004). "Initiation of endospore formation in *Clostridium acetobutylicum*." Anaerobe **10**(2): 69-74.

Forsberg, C. W. (2005). "The hydrogen economy is coming, the question is where?" Chemical Engineering Progress: 20-22.

Girbal, L., C. Croux, et al. (1995). "Regulation of metabolic shifts in *Clostridium acetobutylicum* ATCC 824." FEMS Microbiology Reviews **17**(3): 287-297.

Girbal, L., I. Vasconcelos, et al. (1995). "How neutral red modified carbon and electron flow in *Clostridium acetobutylicum* grown in chemostat culture at neutral pH." FEMS Microbiology Reviews **16**(2-3): 151-162.

Gottschal, J. and J. Morris (1981). "The Induction of Acetone and Butanol Production in Cultures of *Clostridium-Acetobutylicum* by Elevated Concentrations of Acetate and Butyrate." FEMS Microbiology Reviews **12**(4): 385-389.

Guedon, E., S. Payot, et al. (1999). "Carbon and Electron Flow in *Clostridium cellulolyticum* Grown in Chemostat Culture on Synthetic Medium." Journal of Bacteriology **181**(10): 3262-3269.

Hurst, K. M. (2005). Effects of Carbon Monoxide and Yeast Extract on Growth, Hydrogenase Activiity and Product Formation of *Clostridium carboxidivorans* $P7^T$. Chemical Engineering. Stillwater, Oklahoma, Oklahoma State University. **Masters of Science:** 141.

Jee, H. S., N. Nishio, et al. (1987). "Influence of Redox Potential on Biomethanation of H_2 and CO_2 by *Methanobacterium thermoautotrophicum* in E_h-stat batch cultures." J. Gen. Appl. Microbiol. **33**: 401-408.

Kim, H. B., P. Bellows, et al. (1984). "Control of Carbon and Electron Flow in *Clostridium acetobutylicum* Fermentations: Utlilization of Carbon Monoxide to Inhibit Hydrogen Production and to Enhance Butanol Yields." Applied and Environmental Microbiology **48**(4): 764-770.

Kim, J., R. Bajapai, et al. (1988). "Redox Potential in Acetone-Butanol fermentations." Applied Biochemistry and Biotechnology **18**: 175-186.

Kim, T. S. and B. H. Kim (1988). "Electron flow shift in *Clostridium acetobutylicum* fermentation by electrochemically introduced reducing equivalent." Biotechnology Letters **10**(2): 123-128.

Kwong, S. C. W., L. Randers, et al. (1992). "On-line assessment of metabolic activities based on culture redox potential and dissolved oxygen profiles during aerobic fermentation." Biotechnology progress **8**: 576-579.

Liou, J. S.-C. and D. L. Balkwill (2005). "Clostridium carboxidivorans sp. nov., a solvent-producing clostridium isolated from an agricultural settling lagoon, and reclassification of the acetogen Clostridium scatologenes strain SL1 as Clostridium drakei sp. nov." Int J Syst Evol Microbiol **55**(5): 2085-2091.

McIlveen-Writght, D. R., F. Pinto, et al. (2006). "A comparison of ciculating fluidised bed combustion and gasification power plant technologies for processing mixtures of coal, biomass and plastic waste." Fuel Processing Technology **87**: 793-801.

McKendry, P. (2002). "Energy production from biomass (part 1): overview of biomass." Bioresource Technology **83**: 55-63.

Meyer, C. L., J. W. Roos, et al. (1986). "Carbon-Monoxide Gasing Leads to Alcohol Production and Butyrate Uptake without Acetone Formation in Continuous Cultures of *Clostridium acetobutylicum*." Applied Microbiology and Biotechnology **24**(2): 159-167.

Mollah, A. H. and D. C. Stuckey (1992). "The influence of H_2, CO_2 and dilution rate on the continuous fermentation of acetone-butanol." Applied Microbiology and Biotechnology **37**(5): 533-538.

Nakashimada, Y., M. A. Rachman, et al. (2002). "Hydrogen production of *Enterobacter aerogenes* altered by extracellular and intracellular redox states." International Journal of Hydrogen Energy **27**: 1399-1405.

Peguin, S., G. Goma, et al. (1994). "Metabolic flexibility of *Clostridium acetobutylicum* in response to methyl viologen addition." Applied Microbiology and Biotechnology **42**: 611-616.

Perry, J. H., R. H. Perry, et al. (1963). Chemical Engineers Handbook. New York McGraw-Hill.

Phillips, J. R., E. E. Clausen, et al. (1994). "Synthesis gas as substrate for the biological production of fuels and chemicals." Applied Biochemistry and Biotechnology **45-46**: 145-157.

Ragsdale, S. W. L. w. C. M. B. M. B.-. (2004). "Life Carbon Monoxide." Biochemistry & Molecular Biology **39**: 165-195.

Rao, G., P. J. Ward, et al. (1987). Manipulation of end-product distribution in strict anaerobes. Biochemical Engineering V., Henniker, NH, USA, New York Acad of Sciences, New York, NY, USA.

Sherwood, T. K., R. L. Pigford, et al. (1975). Mass Transfer. New York, McGraw-Hill.

Sridhar, J. and M. A. Eiteman (2001). "Metabolic flux analysis of Clostridium thermosuccinogenes: effects of pH and culture redox potential." Applied Biochemistry and Biotechnology **94**(1): 51-69.

Tamimi, A. and E. B. Rinker (1994). "Diffusion-coefficients for hydrogen-sulfide, carbon-dixoide, and nitrous-oxide in water over the temperature-range 293-368 K." Journal of Chemical and Engineering Data **39**(2): 330-332.

Verhallen, P., L. J. P. Oomen, et al. (1984). "The diffusion-coefficients of helium, hydrogen, oxygen and nitrogen in water determined from the permeability of a stagnant liquid layer in the quasi-steady state." Chemical Engineering Science **39**(11): 1535-1541.

Wang, D. I. C., C. L. Cooney, et al. (1979). Fermentation and Enzyme Technology. Stockholm, John Wiley & Sons.

Wang, M. (2005). Energy and Greenhouse Gas Emissions Impacts of Fuel Ethanol. NGCA Renewable Fuels Forum, The National Press Club.

Wikipedia. (2006). "Fermentation." Retrieved August 16, 2007, from www.wikipedia.org/wiki/anaerobic.

Wise, D. L. and G. Houghton (1968). "Diffusion coefficients of neon, krypton, xenon, carbon monoxide, and nitric oxide in water at 10-60.deg." Chemical Engineering Science **23**(10): 1211-16.

Yerushalmi, L., B. Volesky, et al. (1985). "Effect of increased hydrogen partial-pressure on the acetone-butanol fermentation by *Clostridium acetobutylicum*." Applied Microbiology and Biotechnology **22**(2): 103-107.